INFORMATION TO USERS

The most advanced technology has been used to photograph and reproduce this manuscript from the microfilm master. UMI films the original text directly from the copy submitted. Thus, some dissertation copies are in typewriter face, while others may be from a computer printer.

In the unlikely event that the author did not send UMI a complete manuscript and there are missing pages, these will be noted. Also, if unauthorized copyrighted material had to be removed, a note will indicate the deletion.

Oversize materials (e.g., maps, drawings, charts) are reproduced by sectioning the original, beginning at the upper left-hand corner and continuing from left to right in equal sections with small overlaps. Each oversize page is available as one exposure on a standard 35 mm slide or as a 17″ × 23″ black and white photographic print for an additional charge.

Photographs included in the original manuscript have been reproduced xerographically in this copy. 35 mm slides or 6″ × 9″ black and white photographic prints are available for any photographs or illustrations appearing in this copy for an additional charge. Contact UMI directly to order.

Accessing the World's Information since 1938

300 North Zeeb Road, Ann Arbor, MI 48106-1346 USA

Order Number 8801709

Epoxidation of trans-1,4-polyisoprene lamellas crystallized from solution

Elkayam, Abraham, Ph.D.

City University of New York, 1987

U·M·I
300 N. Zeeb Rd.
Ann Arbor, MI 48106

PLEASE NOTE:

In all cases this material has been filmed in the best possible way from the available copy. Problems encountered with this document have been identified here with a check mark __✓__.

1. Glossy photographs or pages _____
2. Colored illustrations, paper or print _____
3. Photographs with dark background _____
4. Illustrations are poor copy __✓__
5. Pages with black marks, not original copy __✓__
6. Print shows through as there is text on both sides of page _____
7. Indistinct, broken or small print on several pages __✓__
8. Print exceeds margin requirements _____
9. Tightly bound copy with print lost in spine _____
10. Computer printout pages with indistinct print _____
11. Page(s) __127__ lacking when material received, and not available from school or author.
12. Page(s) _____ seem to be missing in numbering only as text follows.
13. Two pages numbered __125__. Text follows.
14. Curling and wrinkled pages _____
15. Dissertation contains pages with print at a slant, filmed as received __✓__
16. Other _____

_____

_____

U·M·I

EPOXIDATION OF TRANS-1,4-POLYISOPRENE LAMELLAS CRYSTALLIZED FROM SOLUTION

by

ABRAHAM ELKAYAM

A dissertation submitted to the Graduate Faculty in Chemistry in partial fulfillment of the requirements for the degree of Doctor of Philosophy, The City University of New York

1987

This manuscript has been read and accepted for the Graduate Faculty in Chemistry in satisfaction of the dissertation requirements for the degree of Doctor of Phylosophy.

May 27, 1987
date

Arthur E. Woodward
Chairman of Examining Committee

May 27, 1987
date

A. M.
Executive Officer

D. M. for A. D. Baker

Kevin L. Kosanovich

Supervisory Committee

The City University of New York

ABSTRACT

EPOXIDATION OF TRANS-1,4-POLYISOPRENE

LAMELLAS CRYSTALLIZED FROM SOLUTION

by

Abraham Elkayam

Advisor: Professor Arthur E. Woodward

Selective epoxidation of double bonds in combination with C-13 NMR spectroscopy has been employed to explore the morphology of trans-poly-1,4 isoprene (TPI) folded chain lamellas from a hexane solution. The folded chain lamellas were suspended in 2-ethoxy ethanol (cellosolve) and reacted with m-chloroperbenzoic acid [MCPBA], a mild, quantitative, but highly selective reagent at O C, until the rate of reaction diminished to zero and leveled off. The reacted crystals were dissolved in $CDCl_3$ and the C-13 NMR spectra observed at 50.32 MHZ. It was expected that the surface folds would react completely and that the crystal stems would not react leading to a block structure. The fraction epoxidized, Fe, the average number of monomer units in the reacted blocks, ‹B›, and the average number of monomer units in the unreacted blocks, ‹A›, were obtained. The effect of molecular weight and crystallization temperature on the epoxidized fraction and the average block lengths for TPI lamellas was also studied. An

increase in the averages of ‹B› and Fe with decreasing molecular weight commences at an Mv value between 22,000 and 67,000 and is attributed to the importance of noncrystallizing chain ends at the lower molecular weights. The discrepancy between values of monomer units in the reacted blocks, ‹B›, for the noncrystalline fraction from density measurements on dry samples and from chemical reactions on lamellas kept in suspension, is found to decrease at low molecular weights. The average number of monomer units per fold for lamellas from hexane, as obtained from ‹B› at large molecular weights, is five, which is evidence for a predominance of adjacent reentry folding. From the molecular weight dependence of ‹B› and Fe the number of monomer units in the two noncrystallizing chain ends was calculated.

ACKNOWLEDGEMENT

I wish to warmly thank my advisor, Professor A.E.Woodward, for his excellent leadership, guidance and support during my graduate work.

I also want to thank the members of my advisory committee, Professors Rosano and Baker for their helpful suggestions and discussions.

Special thanks go to Professor M.Weiner, for letting me use his lab at the time I needed it the most. His stimulating conversations, keen knowledge and precise logic were invaluable to my work.

Thanks are extended to the faculty, staff and technicians of the Chemistry Department for being cooperative and considerate and for helping to create an enjoyable working atmosphere.

This brings me to my family. I never really knew how to show my appreciation for my father, mother, sisters and brother. I would have never achieved what I have without their encouragement and support. Their best reward is in my accomplishments. **THIS WORK IS DEDICATED TO THEM.**

My sincere gratitude is given to my daughter, Ingrid, for trying to be quiet at the time of study and to my dearest wife, Dr. Irene Bernard, whose love, understanding and encouragement sustained me through the dark days of self doubt.

There are two words, inadequate as they may be -**THANK YOU.**

TABLE OF CONTENTS

LIST OF TABLES

LIST OF FIGURES

I. INTRODUCTION

The modern concept of polymer crystals(folded chain lamellas) resulted from the careful work of Keller(1), Till(2) and Fischer(3), following an earlier lead by Jaccordine(4), who showed that polyethylene molecules could form single crystals from a dilute solution. This phenomenon has been reported for many polymers (5), including gutta-percha, polyethylene, polypropylene, polyoxymethylene, polyamides and cellulose derivatives. The preparation of macromolecular crystals from solution has been well summarized by Wunderlich (6) for work up to 1970.

Flexible chain polymers may be crystallized by cooling a dilute solution from a temperature above the crystalline melting point to its crystallization temperature (some degrees below). A wide variety of morphologies result, the exact nature of which seem to depend on polymer type, solvent, concentrations, temperature and growth rate. Single crystals appear in the electron microscope as thin, flat platelets or lamellae, 5-25 nm thick and several microns in lateral dimensions. An oval shaped folded chain lamells of 1,4 TPI, as shown in Figure 1 is used to illustrate the prominent features of polymer single crystals.

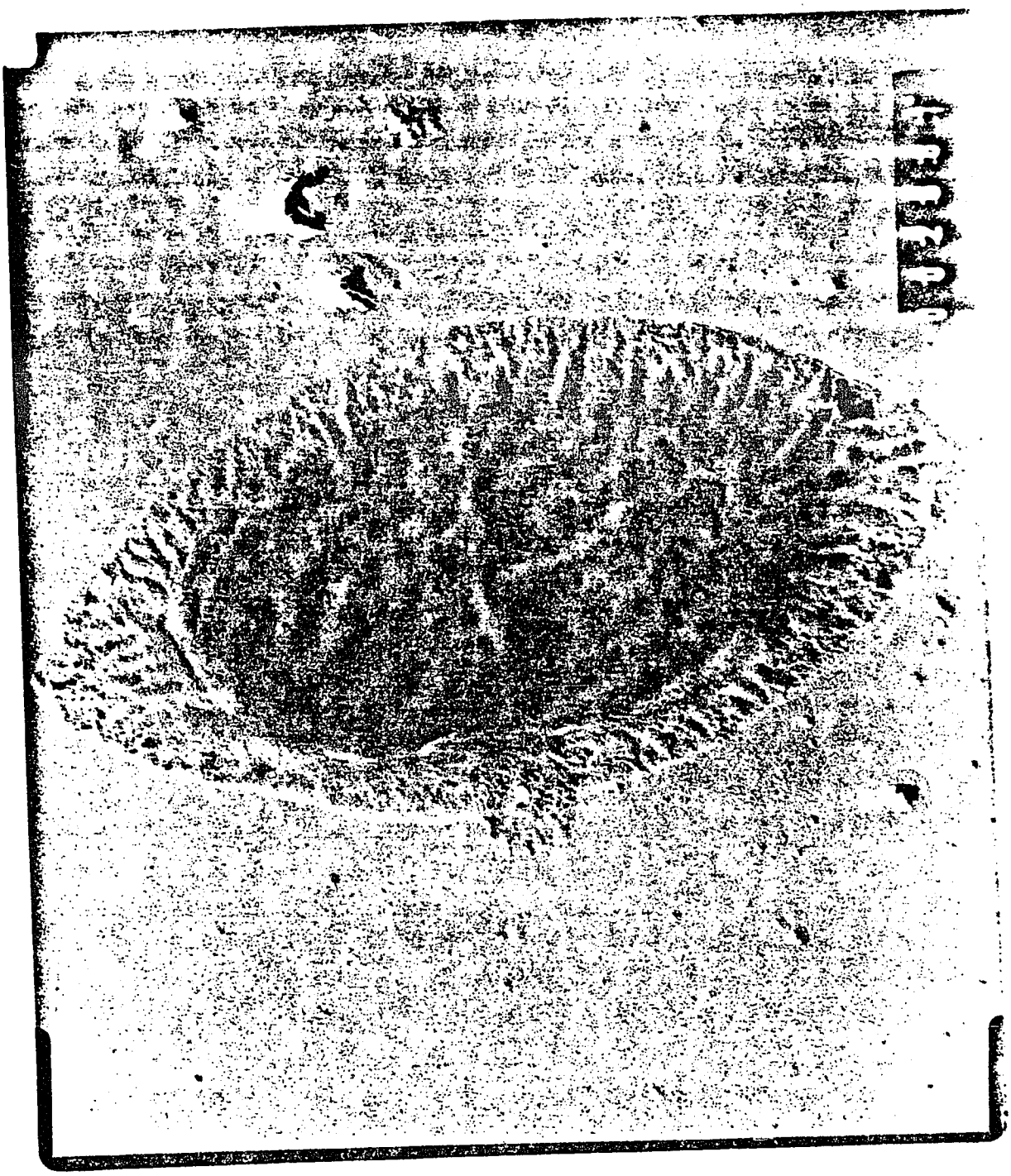

Fig.1. Electron micrograph of trans 1,4-polyisoprene, folded chain lamella grown from dilute hexane solution. Tr=34 C and Tc=20 C

In 1957 Keller (3) showed that polyethylene molecules could form single crystals from dilute solutions. Based on his studies of the properties of such crystals, he concluded that the polymer molecules in the crystals were folded back upon themselves. Keller's conclusions were supported by similar independent observations (2,4). From the work on the crystal structure of polyethylene by Bunn (7), electron diffraction experiments proved that the polymer chain axes in the body of the crystals were essentially perpendicular to the large, flat faces of the crystal. The lamellae thickness (5-20 nm) is much smaller than the other dimensions of the crystal ($10^3$to $2x10^4$nm) and the chain length (10^2 to 10^4 nm). The chains must, therefore, fold back and forth on themselves, forming chain folds on the upper and lower surfaces of the crystals. It is known that these lamellae contain a noncrystalline component, the most direct evidence to that being provided by X-Ray diffraction density, calorimetry, carbon-13 NMR, IR spectroscopy and proton magnetic resonance. These facts support the postulate that in addition to the chain traverses through the crystal core of the lamellae, chain folds exist which connect one crystalline chain traverse to another. Whether the traverses connected one to another are prodominantly adjacent or nonadjacent is still a matter of controversy (8-11). In either case, however, the polymer chain in a

lamellae is made up of alternating sections, one of which is part of a crystalline array and the other is part of the material at the crystal surfaces. A schematic two dimensional representation of models of the fold surface in polymer lamellae (9) is shown in Fig.2 indicating the different types of re-entry folding.

A dominant morphological entity formed when polymers crystallized from a more concentrated solution, is the spherulite (10). The spherulites consist of a radiating array of twisted lamellas, emanating radially outwards from the center, so that the overall structure is morphologically spherically symmetric, suggesting that the crystal organization within the spherulite, also possesses spherical symmetry. In addition, multilayer entities called hedrites (11-12) with many features of single lamellas have been also grown. According to Keith's theory (11), the transitional multilayered hedrite structures, structures which develop during the early stages in the growth of spherulites, and the spherulitic structures into which they ultimately evolve represent successive stages in the evolution of an initially formed lamellar chain-folded single crystal. The above studies have been extensively performed and reported by Woodward (13). In recent years a more detailed variety of morphological forms

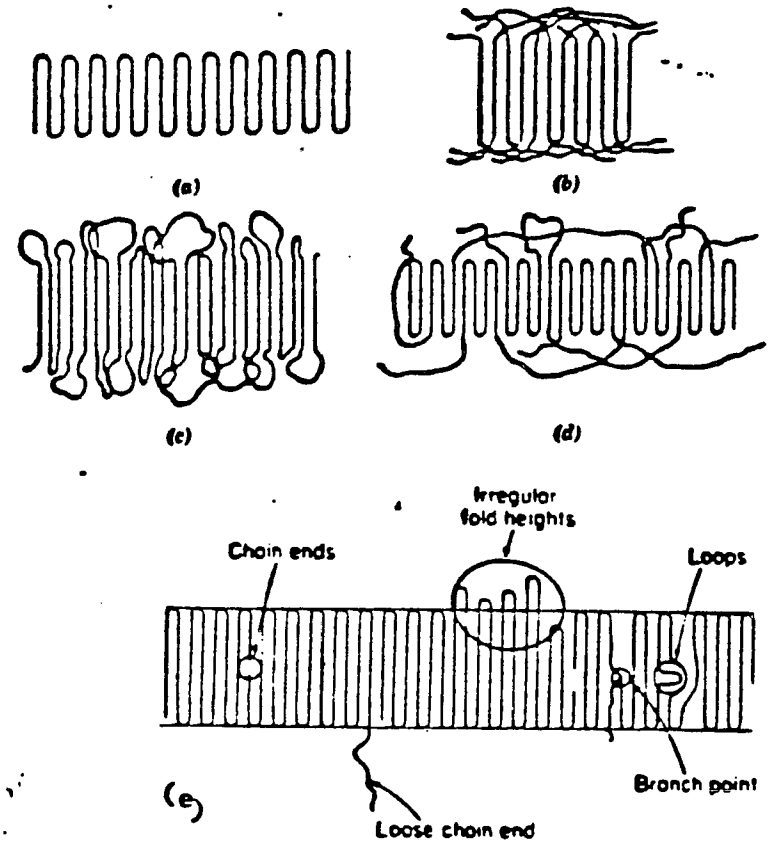

Fig.2. Schematic two dimensional representations of models of fold surface in polymers.
Proposed chain folding models in single crystal lamellae:
a) sharp folds- regular adjacent reentry (tight folds)
b) switchboard model- loose or irregular folds (random adjacent reentry)
c) loose loops with adjacent reentry (loose folds)
d, e) a combination of several features, illustrating chain with imperfections which may occur in structure

exhibited by lamellae crystals has developed, largely as a result of studies by Bassett and Hodge (14-19).

The nature of the noncrystalline material at the surface of the polymer has received considerable attention to date (20-21). Of particular concern are the length of the surface folds and the extent of the adjacent reentry. However, most physical methods used to evaluate the amorphous fraction of polymer samples, measure the total noncrystalline content and provide little datails as to the nature of the chains in the surface fold.They also do not provide direct evidencee as to how the chains are folded. Two different models have been advanced: one (3.22-26) which is backed by strong structural and kinetic evidence (27-29) favoring sharp, regular folding with immediate adjacent reentry of the chain into the crystal; another model (29-30) postulates that loose, loopy folds with considerable molecular disorder exist in the polymer single crystals. The extent of the disorder appears too great to be compatible with intercrystalline defects and to require some sort of amorphous region or layer at the fold surface. Such a region might involve loose or irregular folds or a more random "switchboard" model, as suggested by Flory(30).

Experimental evidence that adjacent reentry is the dominant feature on chain folded crystallization was derived(31)from

selective degradation of folded polyethylene chain crystals with nitric acid and by analysis of the IR absorption of mixed crystals of polyethylene and deuteropolyethylene. In this investigation, polyethylene crystals were exposed to fuming nitric acid. The latter attacks the polymer oxidatively by removing parts of the molecule and by cutting folds. It was found that there was a rapid reaction rate, followed by a markedly decrease in the rate. These kinetics were attributed to the attack first of easily accessible amorphous surface, followed by penetration into the crystalline interior, where, because of accumulation of degradation products blocking the reaction sites, the reaction rate diminished. Apparently, there was no reaction rate difference between amorphous and crystalline polyethylene with a reagent as powerful as fuming nitric acid.This chemical reaction resulted in the destruction of the crystals themselves, and therefore the results were difficult to interpret. They concluded that milder degradative techniques were necessary.

Using a chemical modification technique to characterize solution- grown single crystals and dendrites by oxidation behavior, Williams et al (32) analyzed melt crystallized polyethylene and found a high degree of adjacent reentry in the chain folding of polyethylene.

Keller et al (33) indicated that the crystal surface is rough and there is some disordered material at the surface. Keller and coworkers carried out another oxidation technique - digestion with strong oxidizing agents such as fuming nitric acid and destructive reaction with ozone, coupled with gel permeation chromatography to assess the regularity and distribution of folds length in polyethylene lamellas(34-36). They measured changes in molecular length single and double traverses of solution- grown polyethylene crystals after the oxidation with fuming nitric acid and ozone. The result of two peaks in a 2:1 ratio that dominated the chromatogram was attributed to molecular weight fractions corresponding to single chain and double chain traverse length that were degraded by the nitric acid. It was concluded that the surface consists of chains of various lengths, buried at different depths on either side of the lamella, confirming the model of adjacently reentrant folds of various lengths, which includes some chain ends (cilia) that are thought to protrude from the surface. Therefore, the lamella thickness L, includes the surface amorphous region consisting of chain folds and chain ends and the crystalline region with a crystalline thickness L_c, which is smaller than L.

Further evidence for adjacent reentry comes from the study

Bank and Krimm (37). The folded chain mixed crystals contain an isotopic nonequivalent species in the same relative crystal arrangement, which changes the symmetry and mass of the crystal at constant force field. Intermolecular interactions between the two different chains in the unit cell of pure polyethylene split the IR active interchain CH_2- bending mode into two components at 1463 and 1473 cm^{-1} ($\Delta\omega$ =10 cm^{-1}). The equivalent CD_2 mode at higher mass has the components 1084 and 1091 cm^{-1} ($\Delta\omega$ = 7 cm^{-1}). The magnitude of the splitting is known from the intermolecular force field and could thus be extended by Bank and Krimm to the related mixed crystals. For the paraffins $C_{36}H_{74}$ and $C_{36}D_{74}$ a continuous decrease in the splitting of the major component frequency was observed with increasing the minor component. The paraffin data were found to be in good agreement with calculated values assuming random arrangement of CH_2 and CD_2 chains. These results were explained qualitatively and quantitatively by Bank and Krim (37) on the basis of symmetry of regular 1:1 mixed crystals with adjacent like species (the species being arranged adjacently).

IR spectroscopy had been employed to study the nature of chain folding at the surface of crystals prepared from various polymers (37-40). In particular Koenig and coworkers (39-40) have identified bands due to unique fold

conformations in polyethylene terephthalate (33) and in polyhexamethylene adipamide (40). However, this work was carried out on specimens for which no independent method was used to determine the amount of chain folding. Such information could have been received by poly trans 1,4 butadiene - PTBD (41-42). For this polymer, the number of double bonds available for epoxidation was determined for crystals grown from various solvents. From the epoxidation data, the crystal thickness and the monomer repeat distance the average number of monomer units per fold have been estimated by Woodward et al (43). Information has also been obtained from IR spectra of TPBD crystal mats in the 1000-1400 cm^{-1} region, from dilute solutions of various solvents and solvent combinations. It was found that the increase in the ratio of the intensity of the 1350 cm^{-1} peak, an amorphous band, to that of the 1335 cm^{-1} peak, a regularity band, varies from 1.3 to 0.1 with the solvent used for crystal preparation, is believed to reflect a decrease in conformations associated with the crystalline region and an increase in the conformations taken up by the chains in the amorphous or disordered area.

Ng, Stellman and Woodward (26) studied TPBD crystals using DSC. Here H_t, the heat of transition for the conversion of the low temperature to high temperature modification, was assumed to be proportional to crystallinity. These results

were in agreement with those obtained by IR measurements. Tseng et al (44) extrapolated the straight line obtained by plotting the enthalpy of crystal-crystal transition versus specific volume to 100% crystallinity and obtained a value for the heat of fusion of TPBD, in agreement with the literature value.

Using long spacing X-ray results (34), Keller and Udagawa observed a disordered amorphous layer in the fold region which expands upon swelling polyethylene single crystals with a liquid. This increase in the long spacing depends mainly on the molecular weight of the polymer. Mandelkern (45) explained the dependence of the amount of swelling with molecular weight as a variation in size and distribution of amorphous loops connecting the crystalline sequence.

Attempts have been made to study the influence of block copolymerization on chain folding by carrying out chemical modifications at the fold surfaces of polymer lamellas. Methods such as substitution, elimination and addition reactions have been carried out on various polymer lamellas to date. The polymers used include polyethylene (46-49), poly (4 methylpentene -1) (50), polyvinyl alcohol (51), poly(vinylidine) chloride (52), TPI (53-56) and trans 1,4 polybutadiene (41-44, 57-60).

Three general requirements for the formation of such block

copolymers are necessary: the polymer must crystallize as folded chains; each repeat unit of the polymer must be quantitatively reactive towards a small molecule with a minimum of side reactions, particularly scission and depolymerization or must quantitatively eliminate a small molecule. If a liquid is necessary to disperse the nonpolymeric reactant, it should not penetrate the crystalline parts of the polymer lamellas.

The copolymer prepared will consist of blocks of unreacted polymer units alternating with blocks of reacted units. The number of repeated units in the unreacted blocks will depend on the crystal thickness along the chain direction, as determined by the crystallization temperature and solvent. The average size of the reacted blocks will be dictated by the average number of monomer units per fold. The average size will be smallest and the width of the size distribution sharpest for the reacted blocks if only adjacent reentry, using the minimum number of chain units, occurs.If fold looseness is present, then a distribution of fold lengths, ranging from tight to loose, is expected. The largest values for the average fold length and the broadest size distributions are expected if a significant amount of nonadjacent reentries occur. The number of blocks per molecule will decrease as the lamellar thickness increases and will increase with the molecular weight.

The block copolymers as first prepared could further be modified by reaction in solution involving either the reacted, the unreacted or both blocks. The most successful methods for the preparation of block copolymers from polymer lamellas to date are apparently those involving addition reactions. The reaction conditions are relatively mild and the reaction is specific. Complete conversion of the functional groups (double bonds) in the folds and noncrystallizing ends, apparently take place, whereas for substitution and elimination reactions, this has not been shown to be exclusively so.

Elimination reactions such as dehydrohalogenation of polyvinylidene chloride ($-CH_2-CH_2-$ lamellas) was carried out using pyridine at 45 C in benzyl and isopropyl alcohols (52).After an initial fast reaction, the percent of the removed HCl continued to increase linearly to 6-7% over the time period during which the reaction was studied.

Substitution of bromine atoms onto polyethylene lamellas using UV or visible light activation of the bromine in solution at room temperarure and above has been studied by various authors(46-49). Harrison and Baer (47) reported an initial fast reaction with changing rate corresponding to about 2-3% bromine by weight. Following that, the rate of bromine addition remains constant up to at least 7% bromine

by weight. Asuming tight reentry folding, it was estimated that 4.5% bromine by weight corresponds to one Br atom per fold. By using hydrogenated polyethylene, Equiluz, Ishida and Hiltner (48) found that the constant value of 3.5% by weight Br was reached at 40 C using Br_2 in bromobenzene under UV activation. This corresponds to about one bromine atom for every 50-60 ethylene units in the polymer. In a study of Harrison et al (49) , a polyethylene lamella sample with a bromine content of 14.3% was used to perform a Friedel Crafts substitution of toluene onto the chain. Substitution of chlorine atoms onto polyethylene lamellas using UV light activation of Cl_2 in solution at 7 C without apparent damage to the crystalline parts, as monitored by X-ray diffraction, was carried out for lamellas with four to thirty weight % chlorine added (61). A chlorine content of 26 weight % corresponds to one chlorine atom per each polyethylene unit in the folds for the crystals used. The ethylene blocks would contain about sixty units and the chlorinated blocks about fourteen units.

Schilling, Bovey, Tseng and Woodward (57) combined the technique of epoxidation at the crystal surface with NMR analysis to examine in a quantitative fashion the nature of the chain folds in solution α - grown crystals of

1,4 trans polybutadiene (TPBD). Values for average fold lengths uncorrected for the presence of cilia varied from 3.0 to 5.6 monomer units, suggesting that adjacent reentries predominate. In a subsequent study, using nondestructive chemical transformation of surface folds followed by high resolution C-13 NMR analysis, Schilling et al (54) were able to quantitatively measure the average length of the reacted blocks, the average length of unreacted blocks and the fraction crystallinity in solution- grown TPI crystals. Their results for one preparation was in excellent agreement with that reported previously (19), based on determinations of surface fraction by proton NMR, crystal and amorphous densities and the monomer repeat distance.

In a kinetic study, Wichacheewa and Woodward (59) carried out an epoxidation reaction of TPBD in suspension. The amount of MCPBA reacted relative to the MCPBA present was determined by an IR method in order to estimate the fraction of double bonds reacting with the epoxidizing agent (MCPBA). The number of monomer units per fold was calculated for heptane and toluene grown crystals. Comparing the above values with the theoretically estimated ones for possible tightest reentrants, it has been concluded that TPBD crystals grown from heptane principally contain regular reentrant folds and TPBD

crystals grown from toluene contain irregular adjacent reentrant folds. The results of that study can be compared with those of bromination (59) (with molecular bromine) at 0 C of TPBD crystals suspended in heptane or in CCl_4, where a close agreement in surface fractions by the two methods on a similar preparation is obtained.

The agreement between the brominated and the epoxidized amount for TPBD lamellas suggest that block copolymers of the dibromodiene and the diene units are also formed. It seems that in the bromination of TPI lamellas, some substitution as well as addition may take place (56). This work, however, is unconclusive and needs further work to prove or disprove that point.

The formation of $-CH_2-\overset{\overset{CH_2Br}{|}}{\underset{\underset{Br}{|}}{C}}-CHBr-CH_2-$ units when TPI is brominated in solution had been postulated by Tutorskii et al (66). When bromination is carried out in solution, cyclization also takes place. However, this is not expected to occur if the chains are under sufficient restraints, such as is in a chain fold, although it can take place in a chain end. However, an increase in crystallization led to a decrease in the number of monomer units per fold. As the lamellar thickness of the single crystal is increased by increasing Tc, a larger number of double bonds per fold are

brominated, since a larger number of repeat units become accessible to the bromine. This is consistent with an increase in the thickness of disordered surface layers with an increase in the crystallization temperature.

A-B block copolymers of crystallizable poly(ethyleneoxyde) (A) and atactic noncrystallizable polystyrene (B) were studied by Lotz et al (67). On crystallization from dilute solution, lamellar crystals resulted. It has been found that the morphology of the crystals is in every detail equivalent to poly(ethylene oxide) homopolymer crystals.The poly(ethylene oxide) portion must be folded in a regular adjacent fashion, while the polystyrene portion is rejected from the crystal and lies as a thick amorphous layer, about 25A thick, on top of the surface fold. As mentioned before, the fold length is influenced by the crystallization temperature. Polyethylene oxide crystals grown at 15 C were thinner (115A) than those grown at 25 C (150A). A structure analysis of cyclic $C_{34}H_{68}$ by Kay (68) proved that crystals of this substance collapsed with the triclinic polyethylene subunit cell with a top and bottom fold, corresponding closely to the shortest path between adjacent zigzag chains on a diamond lattice. Experiments on melt crystallized poly(ethylene terephthalate) etched hydrolytically by water were carried out by Miyagi

et al (69) showed weight loss and change in lamellar thickness of polyethylene and polyethylene terephthalate as a function of reaction time (etching at 190 C under H_2O pressure by hydrolysis. The major portion of the initial weight loss correlates well with the total noncrystalline material in the starting polymer. The crystallinity of the remaining etched sample after the initial rapid weight decrease is close to that of a completely crystalline polymer.

Measurements of density and heat of fusion of folded chain crystals reveal that melt-grown, as well as solution-grown folded chain crystals did not have a high enough crystallinity to agree with a model of crystallographically perfect folds and crystal interior (70) . Typical crystallinities of solution - grown polyethylene ranged between 0.80 and 0.95, the variation being caused by the crystallization temperature, the molecular weight and by the molecular weight distribution. The absolute value of the density is less than predicted from the unit cell dimensions, perfection is favored (other conditions being constant) by high crystallization temperature, lower molecular weight and narrower molecular distribution.

The perfection of the interior of folded chain crystals of polyethylene grown from melt and solution was assessed by Davis et al (71) and Kitamaru and Mandelkern (72) through the determination of variation of the unit cell size by X-ray diffraction. The a and b dimensions of the unit cell were found to be larger for solution-grown crystals grown at larger supercooling.The changes in the density resulting from this unit cell changes are not enough to account for the total density defect, i.e. the density of polyethylene grown at 70 C from a dilute xylene solution is 0.978 g/cm^3, while the unit cell density is 0.997 g/cm^3. This deviation from a perfect crystal can be accounted for as a disorder that must be located at the crystal surface.

Direct experimental evidence of lower enthalpy and higher density of the amorphous portion of polyethylene was shown by Peterlin and Meinel (81) and Glenz et al (82). Illers and Haberborn (83) could show by careful analysis of Nylon 6, 6.6, and 8, that the density of the amorphous portion is influenced by the structure of the crystalline portion.

The total noncrystalline fraction calculated from density measurements, assumes that the crystals for the unit cell obtained by X-ray diffraction and a component which is completely amorphous, as found in the melt, but with an extrapolation to room temperature. Total noncrystalline

values from densities for 1,4 polybutadiene and for TPI crystals have been obtained by Woodward et al (44, 58) with only two exceptions out of eighteen TPDB samples. Surface fractions from epoxidation (F_s) are less than $1-W_c$, the total noncrystalline amount from density. In one case it varies by 40% ($M_n=1.7x10^4$, $F_s=0.16$, $1-W_c=0.26$). Two possible explanations for Fs being lower than $1-W_c$ (44) are:
1) The crystallinity is underestimated by the density method due to the assumption that the surface component has the same density as in the melt corrected for temperature.
2)The surface fraction is underestimated by the penetration technique due to the inability of the penetrant to reach all portions. This is, however, inconclusive and further work is necessary to determine which of these, if either, is correct.

Another experiment showing the disordered material on the crystal surface comes from the density difference of sedimented single crystal mats before and after annealing to larger fold length by the measurement of the absolute value of the X-Ray scattering intensity of lamellas in the low angle region, as carried out by Fischer et al (73). The mean square fluctuation of the electron density distribution $\langle \Delta\eta^2 \rangle$ can be determined from diffraction data

$$\langle \Delta\eta^2 \rangle = k \int_0 J(\theta)\, d\theta$$

where k is a proportionality constant, J - the intensity of

the incident beam, and $J(\theta)$ - the intensity scattered at the angle θ. The density difference $\Delta\rho$ between the crystalline cores and the intercrystalline surface layer can be calculated assuming a model of alternating crystalline and disordered layers. The final equation is

$$\Delta\rho = \frac{(M_o/\Sigma z_i^2)\langle\Delta\eta^2\rangle + (\rho_c - \rho)^2}{\rho - \rho_c}$$

with M_o, the molecular weight of the repeating unit; z_i, the sum of atomic numbers (electrons); ρ the density of the overall sample and ρ_c, the density of an ideal crystal. The density difference evaluated for a sedimented single crystal mat before and after annealing to a larger fold length were between 0.158 and 0.171 g/cm^3, close to a crystalline -amorphous density difference.

The density of solution- grown crystals has been a matter of debate for many years. The difference between dry mat crystals and suspension crystals is not resolved at present, but may have to do with the detailed surface structure which is associated with slight roughness or irregularity of the chain folded surface. Experiments which aided in the elucidation of the chain fold and crystalline stem length were carried out by Woodward and coworkers

in experiments such as X-ray techniques, proton NMR (53, 58, 74), density measurements (53, 74), differential scanning calorimetry (DSC) (41, 42), C-13 NMR (54, 55, 57), solid state NMR (65), electron microscopy (53, 55, 74, 84), IR analysis(43) and chemical modifications (26, 42, 44, 53-59).

It has been established that variation of the molecular weight and crystallization temperature have a considerable effect on all the physical properties of bulk crystallized polymers. In here the crystal habits and shape offers a rough means of distinguishing between samples of different molecular weights. The crystal structure is not expected to change with the molecular weight. For equilibrium crystals, only the crystal thickness in the molecular chain direction would increase linearly with the chain length. As it was evident for both TPDB and TPI (42, 44, 58-59), the increase in lamellae thickness that occurred with increasing the crystallization temperature was accompanied by a density increase. This suggests an increase in the crystallinity due to a decrease in the noncrystalline fraction present at the crystal surface. For both and . Similar results were reported for polyethylene (75-76) and for various polyethylene oxides crystallized

from the melt (77-80). However, at molecular weights below 10^4, a decrease in crystallinity occurs for a number of these polymers, including polyethylene(76), polyethylene oxide (79) and polyhexamethylene oxide (78). Also a decrease in crystallinity with decreasing molecular weight in the 5,000-30,000 range was reported for TPBD (44,58). There is a broad range of molecular weights where the effects on fold length are negligible. The higher molecular weight samples do not display any well defined morphology under any crystallization temperature conditions.However, as the molecular weights get lower, changes , of course, occurred. The lower molecular weight isothermally crystallized samples developed well defined shapes.Detailed studies of linear TPI fractions by Kuo and Woodward (13) have shown that in fact a variety of crystalline morphological forms can be obtained by varying systematically the molecular weight and crystallization temperature. For TPI, the crystal shape varied from ellipsoidal to hexagonal, depending on M_n and T_c. TPI crystals have been found to exist most commonly in two crystalline modifications, α and β. The β form can be described by an orthorhombic unit cell with angles $\alpha = \beta = \gamma =$ 90 , with a=7.78A , b=11.78A and c=4.72 from X-rays

diffraction (104) or with a=7.83A , b=11.87A and c=4.75A from electron diffraction (105). The structural parameters of the form are a matter of dispute. Two different monoclinic unit cells have been proposed by Fischer (105) and by Takahashi et al (96). The three molecular models are shown in appendix I in comparison with structure.

There in not enough independent information for the complete studies of TPI. The majority of studies on crystallization have been performed with linear polyethylene. It is of interest to perform such an investigation on an easily crystallizable polymer such as TPI (trans 1,4 poly 2-methylbutadiene), which contain chemically reactive double bonds in the polymer chain. Since epoxidation is a good chemical method for determining crystallinity of block copolymer samples and since C-13 NMR analysis has been proven to be particularly well suited for addressing structural problems concerning such block copolymers, it was felt that it might provide insight into differences in surface and internal structure of crystals, grown from hexane and subjected to thermal treatment.

In the work to be presented here, TPI crystallizes from solution in the form as folded chain lamellas depending

on the crystallization conditions(53, 74, 84).Determination of the crystallization by density (53, 74) and by solid state NMR measurements (85) show that a sizeable noncrystalline component is present in dried crystal mats.A large portion of this noncrystalline component is expected to be at the lamellas surface as chain folds and noncrystallizing chain ends; this can be quantitatively investigated by chemical reactions in suspension of the double bonds at the lamellar surfaces. Use of chemical reactions to study the fold surfaces assumes that the lateral surfaces are negligibly small in the total area and that penetration of the crystalline core of the lamellas does not occur. In an earlier work, some α-TPI preparation, crystallized from amyl acetate, were reacted in an amyl acetate suspension at O C with metachloroperbenzoic acid (MCPBA) to form an epoxide (53, 74).In those studies, proton NMR was employed to determine the fraction of the double bond reacted and this quantity was combined with the lamellar thickness from electron microscopy to calculate the number of monomer units per fold. More recently, a C-13 NMR method was developed to directly measure the average fold size and the crystalline stem length (54). Electron microscopic examination of lamellas epoxidized in amyl acetate, showed errosion at the edges and holes in the

internal portions, the amount of which increased with reaction time and amount of MCPBA present and decreased with the crystallization temperature (53). These results suggested that the double bonds on additional lateral surfaces were becoming available for epoxidation during the reaction period. Also in some cases it was found that the total epoxidized fraction exceeded the noncrystalline fraction from density measurements (53,74), suggesting penetration of the lamellas. Therefore, in addition to using the newly developed C-13 NMR method to analyse the products of the reaction, it was considered improtant to explore the use of other liquids in which to carry out the epoxidation, in order to minimize the effect of the medium on the partially epoxidized lamellas.

In the work carried out recently by J.Xu in this laboratory unfractionated synthetic TPI crystallized from solution in the β form was epoxidized at O C in fourteen different liquids, for one or more period of time. Using C-13 NMR, the resulting products were analysed in solution in terms of an average reacted block length, ‹B›, and an average unreacted block length ‹A›. In the study reported here, an investigation was carried out on the effect of molecular weight and crystallization temperature on the ‹A› and ‹B› values obtained by epoxidation of α-TPI lmellas at O C in

2-ethoxyethanol, a poor solvent for both the reacted and the unreacted blocks. Also, the effects of the epoxidation reaction in 2-ethoxyethanol on the morphology of TPI lamellas were studied using electron microscopy. The experimental work to be described next involves a quantitative chemical assay of the surface of TPI single crystals and is part of an attempt to provide more definitive understanding of the structure of TPI crystals.

THE OBJECTIVE OF THE PROPOSED RESEARCH

In the investigation to follow TPI single lamellas in the α form were used. The crystals were epoxidized in suspension to various degrees of completion at a temperature of 0 C. The resulting segmented block copolymers were dissolved and subjected to ^{13}C NMR analysis as the main investigative tool. That has proven to be particularly well suited for addressing structural problems concerning block copolymers such as sequence distribution, extent of blockiness and purity.

The purpose of this investigation is the determination of the surface fraction and the average number of monomer units in TPI block copolymers, as a function of:

a) molecular weight.

b) crystallization temperature

To meet these goals, the following were carried out:

1) preparations of crystals from dilute solutions using TPI with molecular weights in the range of 0.05 to 5.8×10^5

2) a systematic study of the density of TPI single crystals obtained from solution over a 10-30 C range of crystallization temperatures

3) NMR analysis of the copolymer that provided a measure of the fold length, stem length and fraction crystallinity of the polymer samples as a function of molecular weight.

II.EXPERIMENTAL

1.Preparation of samples.

Synthetic TPI was obtained from Polyscience; Metachloroperbenzoic acid (MCPBA) and deuterated chloroform from Aldrich Chemical Company; hexane and amyl acetate from Amend Chemical and Drug Company; toluene from J.T.Parker Chemical Company; methanol, ether and 2-ethoxy ethanol were obtained from Fisher Co. The trans 1,4 content has previously been determined to be 99% for sample crystallized from amyl acetate solutions at a polymer weight fraction of 5.7×10^{-4} (86). These determinations were made by F.A.Bovey and F.C.Schilling by C-13 NMR, using a Varian XL 200 (54,87).

The molecular weight distribution of unfractionated synthetic TPI has been determined by Anandakumaran (87) using a Waters 200 analytical gel permeation chromatograph with toluene at 85 C as the solvent. The M_n and M_w/M_n values of the unfractionated samples are 3.5×10^4 and 4.8 respectively.

2.FRACTIONATION

Liquid-liquid phase separation methods were originally proposed by Maffroy-Biget (89) and Meyerhoff (90) involved a triangular scheme which was a combination of successive precipitation and extraction. In the first step, the

polymer is separated into two fractions. The next step comprises further separation of either fraction into two portions.

Ten grams of unfractionated TPI were dissolved in one liter of toluene along with 0.1g of 2,2'-methylene bis[4-methyl-6-tertiary butyl] phenol as an antioxidant with methanol as the nonsolvent. Nitrogen gas was passed through the toluene in the flask before the solution was made. The solution was placed in a 28 C bath and agitated, while adding methanol and heating till it became turbid at 50 C. Then the turbid solution was heated till it cleared at 53 C. Approximately 4-5 liters of methanol as a nonsolvent were used to collect each fraction. The separation involved two liquid phases as required. By increasing the amount of solvent, different fractions were collected. The concentrated phase was precipitated by the addition of methanol [the top phase was removed by suction into another flask for further fractionation (91-92)], then it was filtered, washed several times with methanol and dried in vacuum at room temperature. Samples were stored in the refrigerator to reduce the possibility of degradation and/or oxidation. Viscosity measurements and molecular weight determinations were obtained only for the final collection of each fraction.

3.MOLECULAR WEIGHT DETERMINATION

Viscosity measurements of the fractions: the viscosity

weight average was calculated using an Ubbelohde capillary viscometer (93), see Fig.3, and toluene as solvent at 30 C. The polymer solution viscosities were measured, in order to determine the molecular weight using the following relation:

$$(\eta) = k\ M_v^{\ a}$$

$[\eta]$ = intrinsic viscosity; a value at infinite dilution was obtained by using least squares analysis after correcting for the kinetic energy. $[M_v]$= average viscosity molecular weight. [k,a]= constants, characteristic of the solvent-solute system. The values used here were obtained by Xu (88) and are comparable with other literature values. By using known M_v and MWD samples predetermined by GPC and by plotting $\log[\eta]$ vs. $\log M_v$, values of $k=3.34\times10^{-2}$ and a=0.686 were obtained. The M_v is an average molecular weight, somewhere between the number average and the weight average values, but close enough to the latter to furnish a useful approximation.

4.CRYSTAL GROWTH TECHNIQUES

A series of 0.1%(w/v) TPI solutions in amyl acetate and in hexane were made by dissolving fractionated and unfractionated polymers and filtering them. The technique used involves dissolution (T_d), precipitation at O C and heating to a temperature T_r that caused the precipitate to disappear. The solutions were held at 66 C for one hour, then quenched in ice water or a dry acetone mixture (T_p),

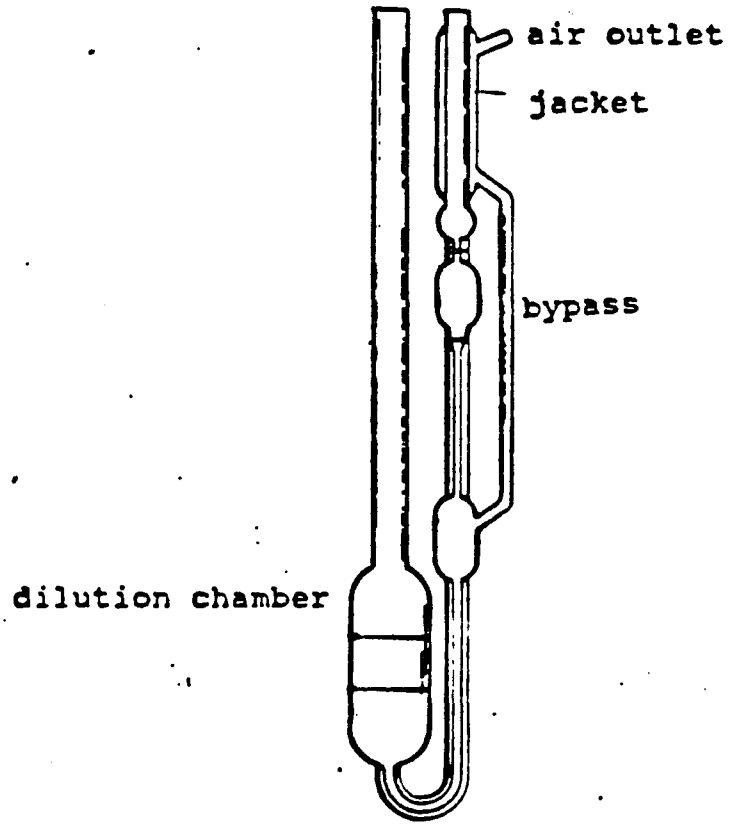

Fig. 3. Ubbelohde dilution viscometer
Capillary viscometers commonly used for measurements of polymer solution viscosities

redisolved by increasing the temperature at a rate of 0.2 C/min, approximately to the redissolution temperature (T_r) and finally it was quickly transferred to a constant temperature water bath at the desired crystallization temperature (0.1 C) in the range of 10 C to 30 C (0.1 C). The crystallization overnight appeared complete. The precipitated polymer was separated from the mother liquor by filtration. The precipitate was washed with fresh solvent at the same temperature and then either resuspended in 2 ethoxyethanol at 0 C for epoxidation, or dried at room temperature for density measurements and X-ray diffraction studies.

5.REDISSOLUTION TEMPERATURE MEASUREMENTS

Redissolution temperatures of α-TPI grown from hexane were measured at the temperature of disappearance of the last portion of the precipitate and were found to be 34 C for the lower molecular weight($0.05-0.67\times10^5$), and 37 C for the higher molecular weight($2.3-5.8\times10^5$).

6.GROWTH OF β FORM

In order to choose a proper suspending liquid for epoxidation, samples in the β modifications have been grown by J.Xu (55) from a 1% amyl acetate solution heated to 90-95 C for an hour and then cooled to 0 C and left undisturbed for 24 hours. The resulting suspension was

heated to 30 C at a rate of 0.06 C/min, left at that temperature for 40 hours and then washed with fresh amyl acetate, followed by drying (for X-ray analysis or for density measuerments), or by suspension in another liquid in preparation for epoxidation.

7.DENSITY

A density column gradient was used to measure the density. By this method the density is determined by matching the buoyancy of the unknown solid and the surrounding liquid, so that the solid floats freely for an extended period of time. The apparatus is shown in Fig.4 and it consists of two Erlenmeyer flasks, connected by a glass tubing to a vertical glass column. A density gradient is set up by mixing various proportions of a high density liquid, water and a less dense liquid, ethanol(95% purity), so that the density in the glass column increases linearly from the top to the bottom. Either end of the vertical column was controlled by the density of the original liquids in the reservoirs. Calibration curves as shown in Fig.5 are calculated each time by a linear regression. All samples were pressed at 3.4×10^7 Pa to eliminate air, cut in small pieces and dropped into the column. The densities were measured from the flotation level.

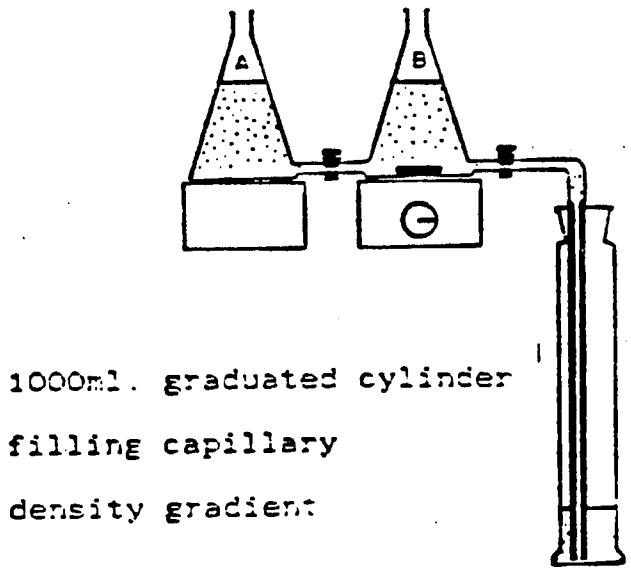

Fig.4 Density gradient column. Flask A contains the heavy liquid which is continuously diluted with the light liquid from flask B. The stirring keeps the contents of flask B homogeneous at all times.

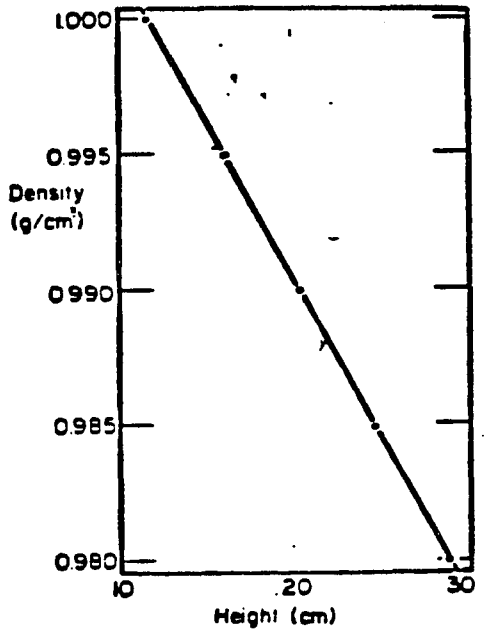

Fig.5 Typical calibration curve of a density gradient column. The marked points are the positions of the calibrated floats.

The weight fraction of the noncrystalline component $1-W_c$ was calculated (eq 1) assuming a two phase system using an amorphous density (95) ρ_a of 0.905 g/cm^3 and a crystalline density (96) ρ_c of 1.05 g/cm^3

$$Wc = \frac{\rho_c(\rho_s-\rho_a)}{\rho_s(\rho_c-\rho_a)}$$

where ρ_s = the density of the sample.

8.OPTICAL MICROSCOPY

As soon as the lateral dimensions of the folded chain crystals exceed 1 μm it becomes possible to observe directly the lamellas, under the optical microscope. The crystals grown by the self seeding technique were washed with a lot of crystallization solvent at the same temperature at T_c to remove material remaining in the solution. Then the crystals were deposited on a microscope glass slide and kept in the refrigerator till it dry. The morphology was studied in suspension under the optical microscope, using both the interference contrast and crossed nicols (to observe the birefringence in order to establish the orientation of the chain). A photomicroscope (Zeiss) with a magnification from 500 to 800 was used.The crystals were also observed on a precooled glass slide, while floating in 2 ethoxy ethanol or in hexane. Photographs of these crystals were recorded with a 35 mm camera connected to the instrument on a Kodak technical pan film 2415 with an ESTAR

AH base. When the reflecting system is in the exposure position, the object is imaged in the film plane and on the focusing reticle. The image will be sharply focused on the film if it is sharply defined on the focusing reticle. The image scale on the film depends on the position of the projective (3.2x and 6.3x). It is computed as the product of

$$\begin{pmatrix}\text{Image scale}\\ \text{on the film}\end{pmatrix} = \begin{pmatrix}\text{scale factor}\\ \text{optovar*}\end{pmatrix} \times \begin{pmatrix}\text{objective factor}\\ \text{(magnification changer)}\end{pmatrix}$$

*a cylindrical extension is in the optical system and gives a further magnification of 1.25x, 1.6x or 2x.

9.ELECTRON MICROSCOPY

The usual technique of heavy metal shadowing is used. The direct observation of thin specimens, such as polymer single crystals, is possible and allows the observation of the electron diffraction pattern of the same specimen area, invaluable for determining crystallographic directions and relating them to morphology. The 0.5g crystals obtained each time by the precooling method were washed with 500cc of crystallization solvent at T_c. The drop of the suspension was deposited on a copper grid, which was coated with carbon. The grid was then shadowed with Pt/Pd or Au/Pd vapor in vacuum ($10x^{-6}$ mm Hg) to increase the image contrast at a shadowing angle of $\alpha = \tan^{-1} 1/3$ and observed in the transmission mode with a Phillips EM 300 electron

microscope at 60KV. Usually, the magnification was in the range of 5,000 to 25,000 times. Pictures of crystals were taken directly with a plate camera attached to the electron microscope. Epoxidized crystals were also observed under the electron microscope, in order to monitor possible changes in the surface morphology.

10.WIDE ANGLE X-RAY DIFFRACTION

Wide angle x-ray diagrams were obtained with a cylindrical camera of 57.3 mm diameter, for crystal mats, which were pressed to 10-20 mm thick sheets in order to disorient the system. Exposures were made with nickel - filtered (Cu-K) radiation, using an accelerated potential of 35 KV and a filament current of 15 mA for one and a half hours.Black paper was commonly used to prevent light from exposing the film. For a random poly-crystalline sample, diffraction from all the crystals in the sample having (hkl) planes making the proper Bragg angle with an incident beam, produces a cone of radiation with semiapex angle 2 , which intersects the film of the camera. The most accurate measurements are made along the equator. The measured 2Z (the diameter of the diffraction ring) equatorial values may be converted into 2θ values by the equation

$$2\theta = 180\ (2Z)/nD$$

where D is the diameter of the camera. These 2θ values may be converted to d spacing for the diffracting planes by the

equation

$$d = 1/2\mathrm{Sin}\ (180)z/nD)$$

11.DIFFERENTIAL SCANNING CALORIMETRY (DSC)

Measurements were made with a Dupont 990 thermal analyzer with TPI single crystals grown from hexane, at weights of approximately 2 mg. All scans were made using the maximum sensitivity that kept the peak on the recorder paper and at the scanning speed of 10 C/min. This speed was high enough to avoid recrystallization phenomena during heating and to maximize the size of the peak. All scans were made using the routine procedures described in the operating manual. The temperature indicated by the analyser was checked by comparing the melting point of pure Indium to its literature value. The melting points of reacted and unreacted TPI single crystals were taken as the endothermal temperatures of these crystals, after the zero correction for each run. These measuerments were made by I.Zemel.

12.EPOXIDATION

A reaction of the double bonds at the crystal surfaces was carried out in a 2 ethoxy ethanol suspension at O C with enough MCPBA [a ratio of 1.6:1 MCPBA/DB] to react with the total double bonds in the polymer samples initially

crystallized . The crystals were separated from hexane - the crystallization liquid (a few perparations were made with amyl acetate as the crystallization liquid) by filtration and washed with fresh distilled 2 ethoxyethanol. The crystals always remained in suspension and were not allowed to dry out or mat together. The mixture was then resuspended in 2 ethoxyethanol at 0 C and MCPBA was added at once at the beginning of the reaction. Using a molar ratio of MCPBA to TPI repeat units of 1.6:1 . For a few runs, this ratio was set at 0.78 or 4.8. The progress of the reaction was followed with time and was permitted to proceed well beyond the point at which the rate diminished to zero. After reacting for a particular period, the epoxidized crystals were filtered and washed with 2 - ethoxyethanol and then with ether, to remove the unreacted MCPBA and the by-product MCPBA that may have been trapped in the polymer or in the solvent. Failure resulted in cross-linking of the epoxidized TPI. The polymer was dried at 0 C in vacuum and dissolved in a 10% (w/v) solution of deuterated chloroform and subjected to C-13 NMR analysis.

13. ^{1}H NMR

Epoxidized and unreacted TPI crystals were freeze dried, dissolved in deuterated chloroform containing tetramethylsilane (TMS) as solvent and was subjected to ^{1}H NMR analysis, using a 60 MHz Varian NMR, a 100MHz Jealco NMR and a 200 MHz WP- 200sy Bruker IBM NMR spectrometer.The epoxidized fraction was generally determined using the areas under both the CH and CH_3 resonance peaks and by weighing a photocopied paper cut of the spectral peaks or using the computer's integrated curves. The extent of epoxidation and the percent crystallinity could thus be obtained. The CH, CH_2, and CH_3 resonances for TPI are found at 5.1, 2.0 and 1.6 ppm and for epoxidized units they are at 2.7, 1.6 and 1.3 ppm. In this method ^{1}H NMR was used to determine the epoxidation of TPI.

14.C-13 NMR

The 50.32 MHz C-13 NMR spectrum of each preparation was obtained with an IBM WP 200-SY NMR system on an about 10% (w/v) solution in $DCCl_3$ using TMS as an internal standard with 32k memory, a special width of 8333 Hz and a 20 second delay time. Gated broad-band proton decoupling, both with and without NOE was used. The number of scans collected in the gated experiments was 612-2600 with NOE

and 2,000-10,000 without. The C-13 NMR results were used quantitatively to obtain the fraction reacted and the average reacted and unreacted block lengths, resulting from the epoxidation of the α-TPI preparation. All quantitative measurements were made by computer integration.

III. RESULTS

1. MOLECULAR WEIGHT DETERMINATION (VISCOSITY MEASUREMENTS)

Solution viscosity is used here as a measure of the molecular weight of TPI. The simplicity of the measurement, and usefulness of the viscosity measurement, constitutes a valuable tool for the molecular weight characterization of TPI. The results for various molecular weight fractions are listed in table I. The flow diagram for TPI fractionation is shown in Fig. 6. The pure solvent (toluene) flow time is 95.4 sec.

Viscosity measurements were obtained for unfractionated synthetic TPI and for TPI lamellas grown at different crystallization temperatures at T_c=10, 20 and 30 C (table II). An increase in the molecular weight is observed with increasing T_c, suggesting an elimination of the lower molecular weight chains as the temperature is increased.

2. GROWTH OF α - CRYSTAL FORM

Overgrown lamellas can be obtained from solution by the precooling method. Analysis of solution- grown crystals is considerably easier since the crystal can be separated from the surrounding solvent without difficulty and maximum information can be obtained by microscopic examination of the structures being formed, while they are still in the suspension liquid. The method involves (97)

first the preparation of the crystal suspension by fully dissolving the polymer in solution at a dissolution temperature (T_d), followed by quenching to a precipitation temperature (T_p) to crystallize. The suspension is then warmed up to a redissolution temperature (T_r), where the population of the nuclei can be controlled efficiently between large limits by heating at a slow rate.It has been found(97) that within a limited range above this clearing point, the solution retains a memory of previous crystallization when crystallizing at constant temperature(T_c). This method yielded only one crystal form, the α form, as evidenced by the appearance of a single, sharp DSC endotherm(Fig. 12) in a region where it has previously been identified(98, 99) with α TPI. TPI crystalisation tends to result in highly overgrown lamellas, probably through dislocation growth. Many layers can be seen on these lamellas (Figs. 7-9). An increase in the lamellar thickness is seen with increase in the crystallization temperature, as has been shown previously(13). In all cases, this is closely related to the fold length, since the molecular chain axis is always at right angles or at relatively steep angles with respect to the lamellar surface. An important feature is the fact that shape changes are not taking place with respect to either molecular weight or temperature. From the flat-on view, the structure of the single crystals of various molecular

Fig. 6\. Flow Diagram for TPI Fractionation

Solvent- Toluene
Nonsolvent- MeOH
T - Toluene
M - MeOH

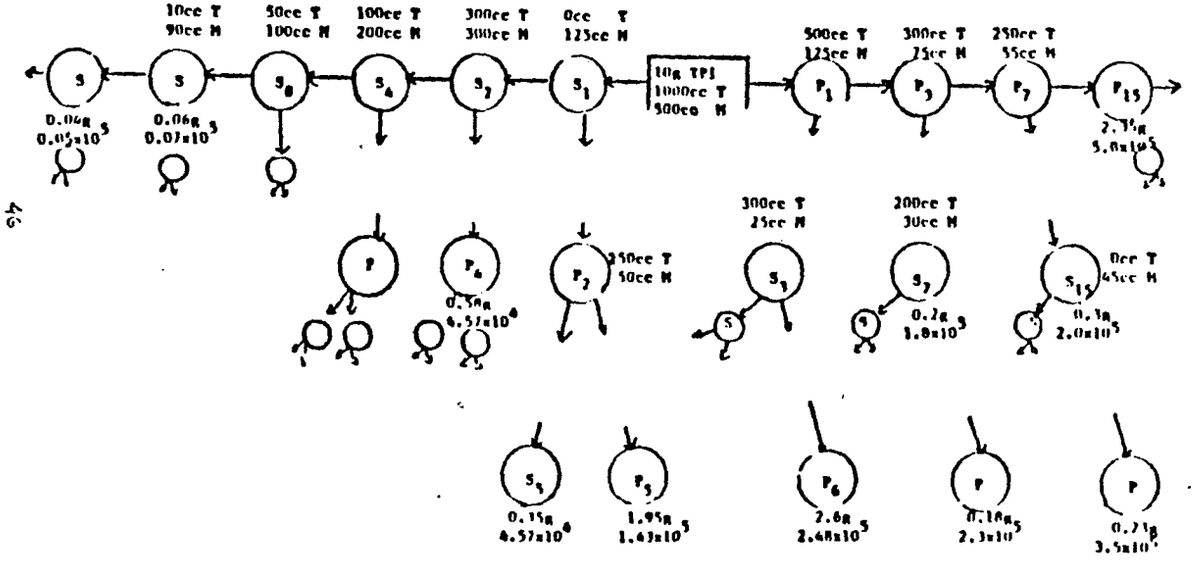

TABLE I

Values of $M_v x 10^5$ of TPI fractions

SOLVENT/ NONSOLVENT RATIO (v/v)	WEIGHT OF FRACTION(g)	% OF TOTAL	M_v X 10-5
46/81	0.04	0.4	0.05
45/72	0.06	0.6	0.07
30/41	0.58	5.8	0.45
25/17	0.35	3.5	0.67
25/17	1.95	19.5	1.43
80/20	0.2	2.0	1.8
100/23	0.18	1.8	2.3
80/15	2.6	26.0	2.48
105/25	0.3	3.0	2.9
105/30	0.23	2.3	3.5
105/25	2.35	23.5	5.8

M_v is the viscosity weight average

TABLE II

Weight average as determined from solution viscosity for TPI grown at various crystallization temperatures

Form[a]	T_c(C)[b]	M_v[c]
TPI pellet	-	1.6×10^5
TPI lamellas	10	1.6×10^5
TPI lamellas	20	1.6×10^5
TPI lamellas	30	2.0×10^5

a. Unfractionated with $M_v=1.55 \times 10^5$ from a 0.1% hexane solution

b. Crystallization temperature

c. The solution viscosity weight average

weights appear well defined and ellipsoidal (or oval) in shape, as shown in Figs. 7-9. When viewed under the optical microscope in suspension, the overgrown lamellas were curved. Therefore, due to drying on a flat substrate, these crystals collapsed and formed creases and ridges and were sometimes hard to observe under the electron microscope due to aggregation.

With regards to the choice of hexane as a solvent for crystallization, it should be pointed out that TPI dissolves readily at a relatively high temperature, but is only sparingly, or not at all soluble at the crystallization temperature used. A few experiments were carried out using crystallization liquids other than hexane. Precooled crystallization from amyl acetate or from dibutylether with synthetic TPI in 0.1% (w/v) at T_c= 20 C yielded oval shaped structures for amyl acetate as shown in Fig.10. When a poor solvent such as n-butyl acetate was used for unfractionated TPI at 20 C, lamellar aggregates alone or with some single crystals were found.

3. LAMELLAR THICKNESS MEASUREMENTS

Measurements of lamellar thickness from the shadow lengths were carried out for samples crystallized at 10 C, 20 C and 30 C. The values obtained in different fields for two sets of crystal preparations are given in table III where they

Fig. 7. Electron micrograph of highly overgrown TPI single crystal grown from a hexane solution. T_r=34 C, T_c=10 C

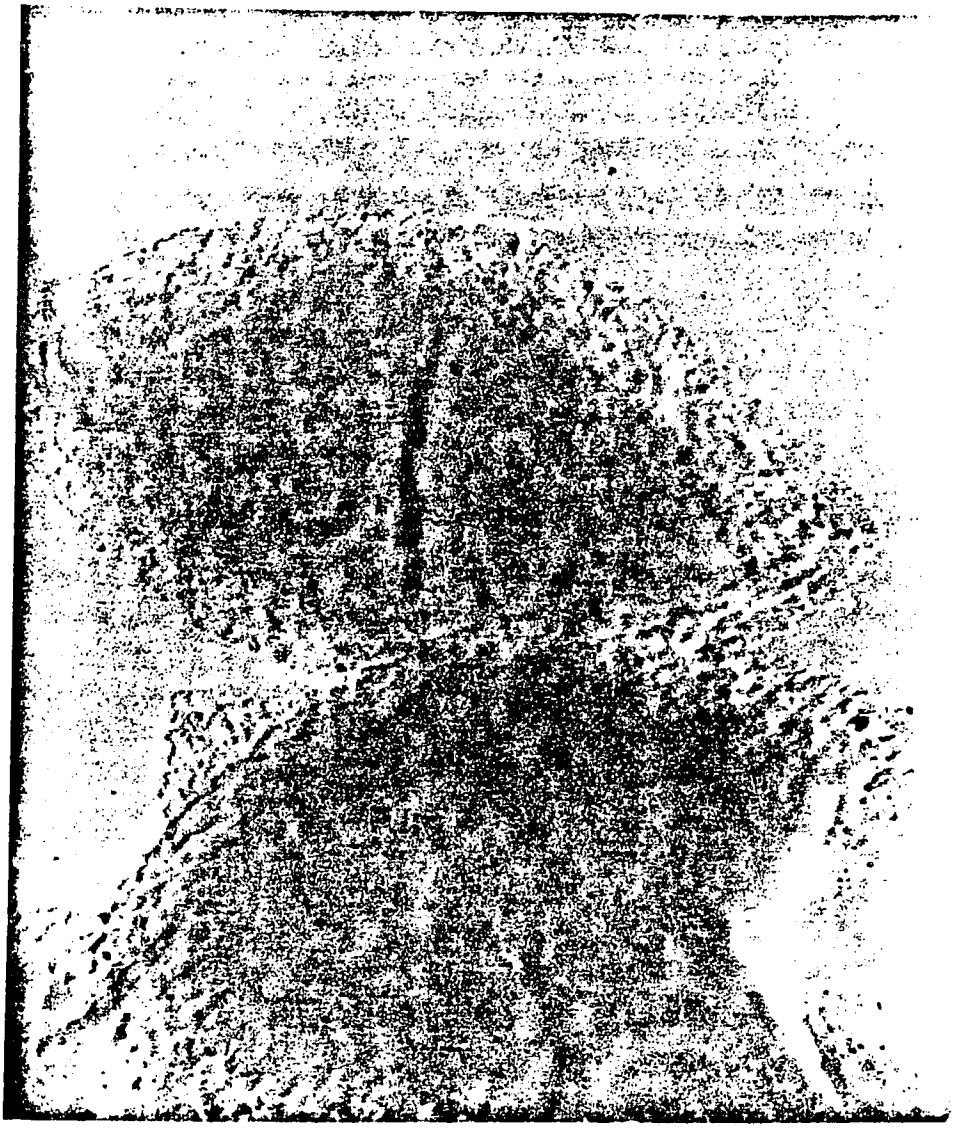

Fig. 8 . Electron micrograph of TPI single crystal grown from a dilute hexane solution. T_r=34 C, T_c=20 C

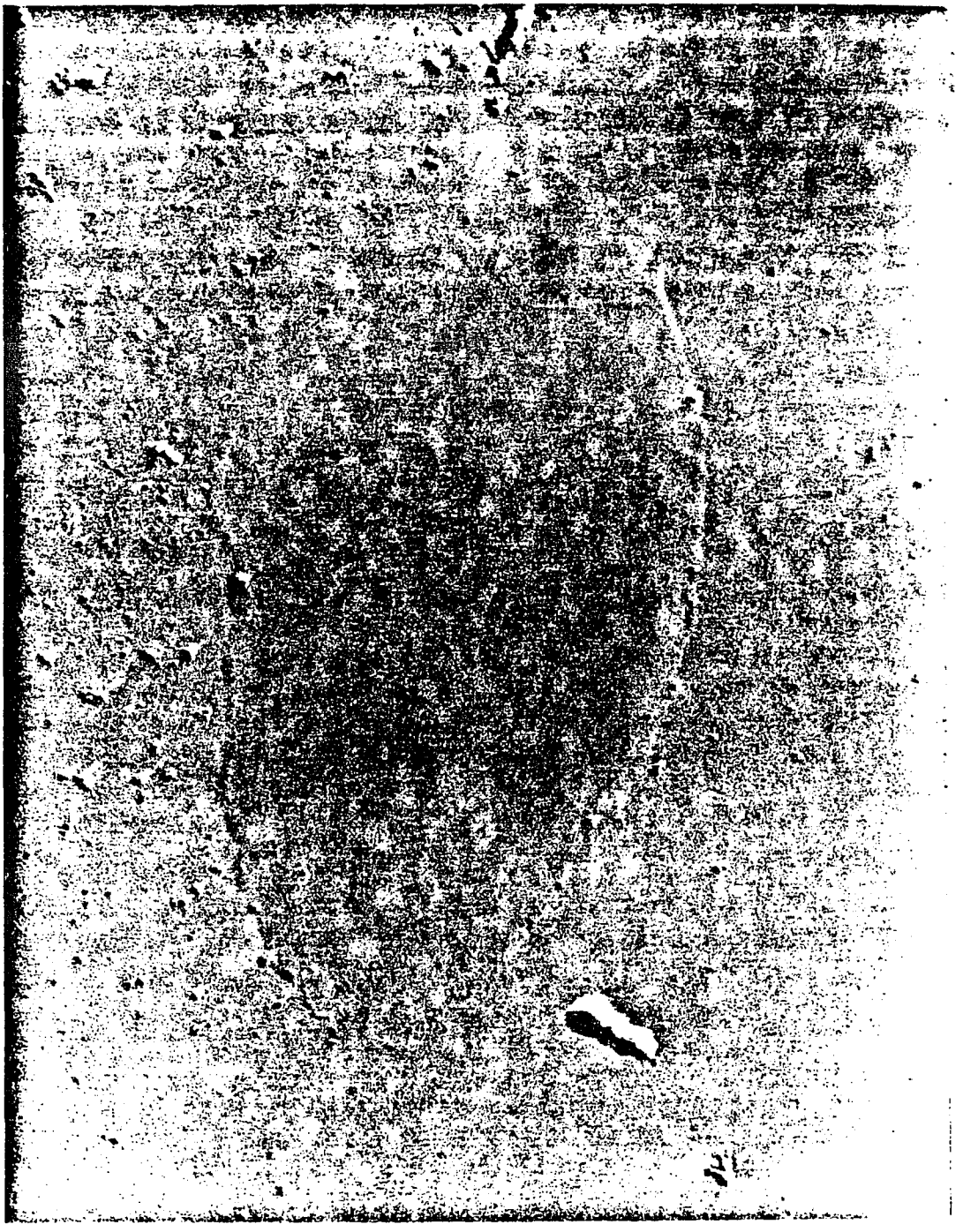

Fig. 9 . Electron micrograph of TPI single crystal grown from a dilute hexane solution. T_c=34 C, T_c=30 C

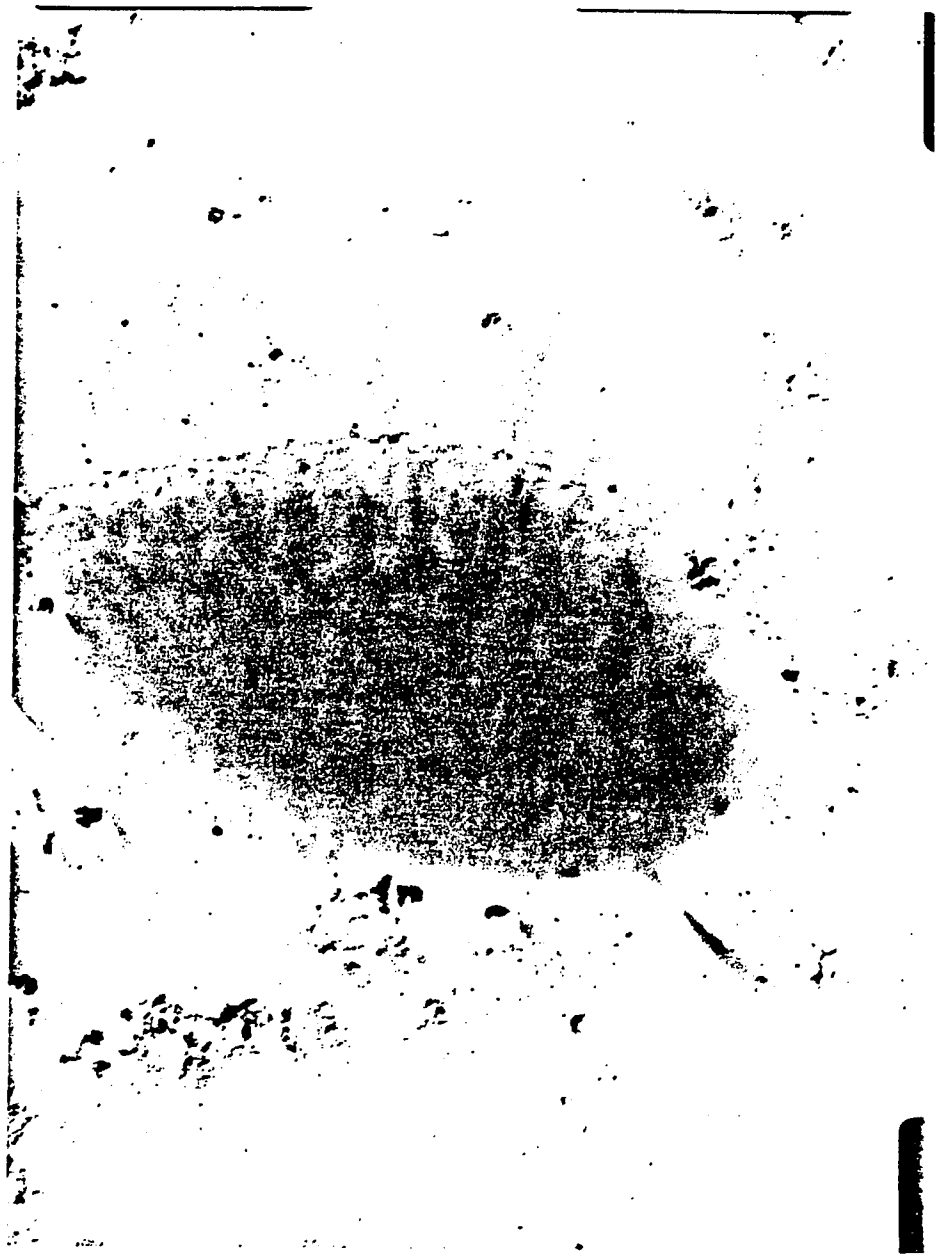

Fig. 10. Electron micrograph of TPI single crystal grown from an amyl acetate solution at 20 C

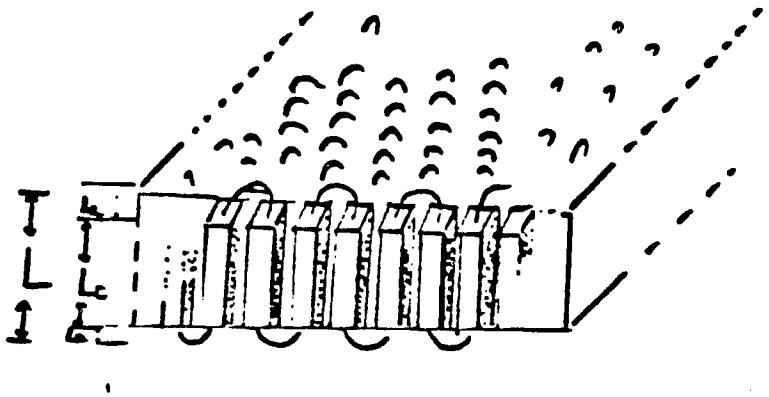

Fig. 11. Schematic representation of TPI crystals with surface folds. L_c- crystal thickness. L_a- amorphous thickness. L- total lamellar thickness.

TABLE III

Lamellar Thickness of α-TPI Crystals Grown from Dilute Hexane solutios; obtained by Electron Microscopy and C-13 NMR for $M_v=2.3x10^5$

T_r	T_c	Electron Microscopy				Average	C-13 NMR
34	10	78	80	79	79	79	80
34	20	80	71	104	85	85	83
34	30	96	89	94	93	93	91

are compared with those calculated from ^{13}C NMR studies on epoxidized lamellas. This latter calculation is discussed in Section 10 below.

4.DIFFERENTIAL SCANNING CALORIMETRY (DSC)

The hexane grown single crystals are in the α modification, as evidenced by the appearance of a single DSC endotherm. TPI crystals do not seem to undergo thermal rearrangements and lamellar thickening during the scans through the transition. The evidence for this is that the peaks obtained are regular, sharp and similar in shape to peaks identified previously (98, 99). This may be due to the fact that the samples were heated at the scan rate of 10 C/minute, which may not have allowed the crystals to recrystallize.

For samples of TPI obtained from hexane solutions after dissolution at 61 C and cooling to 0 C (T_p) followed by slow heating to 34 C (T_r) and crystallization at constant temperature (T_c) from 10 to 30 C, yielded one crystal form only. This is evidenced by the single DSC endotherm as seen in Fig. 12 in the 58 C region. Endotherms in the 58 to 69 C region have been previously identified (98, 99) with α-TPI. This finding has been confirmed in this work by carrying out wide angle X-ray diffraction on samples having T_c's of 10 and 20 C, as reported in the next section.

Surface epoxidized α-TPI lamellas grown at 20 C showed a single endotherm at approximately 62 C. A 4 C shift from that was found for unreacted α lamellas.

5.X-RAY DIFFRACTION MEASUREMENTS OF TPI

A typical x-ray diffraction diagram of TPI crystals in the α modification is shown in fig.13-14.The figure shows clear evidence for the presence of both sharp and diffuse diffraction. The sharp diffraction spots can clearly be linked to crystalline order, while the diffused lines are linked to the disorder in the crystal structure, or the amorphous region, since disordering results in broadening of the diffraction maxima. The x-ray technique used in this study provides primarily one method to determine the crystal modification, either α or β .

A comparison of d - spacings with those reported in the literature by Takahashi et al (106) for the α value, is shown in table X.The unit cell parameters are: a=7.98A , b=6.29A , c=8.77A , α and γ =90 and β =102 (96). Surface epoxidized TPI crystals in a 2-ethoxyethanol (cellosolve) suspension (see below) produced the same x-ray pattern as the α-TPI crystals.This indicates that only the amorphous surface regions of the crystal,

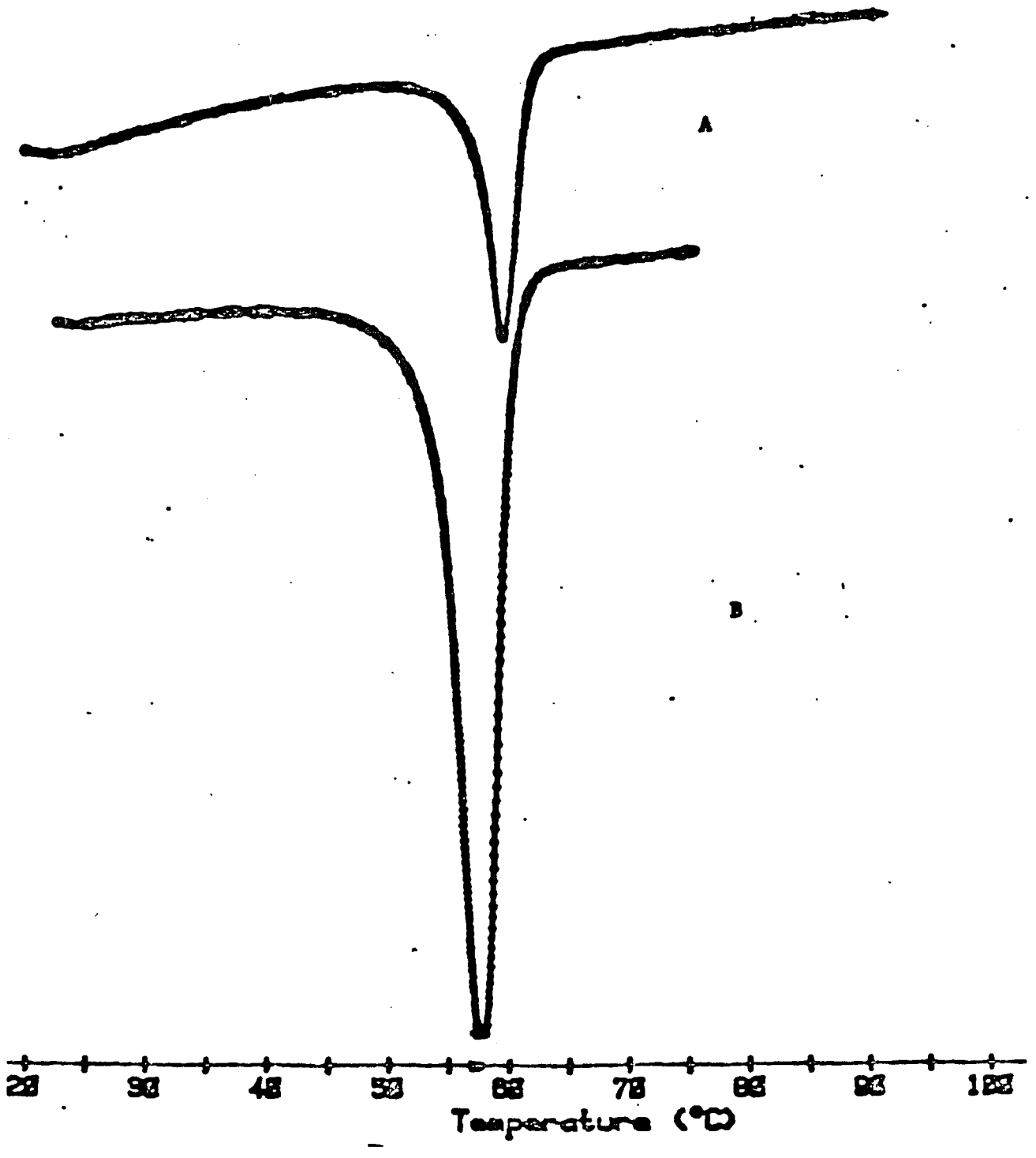

Fig. 12. DSC endotherms of α-TPI crystals, grown from a dilute hexane solution. $M_v=1.55\times10^5$, $T_c=$ 20 C. a. epoxidized. b. unepoxidized.

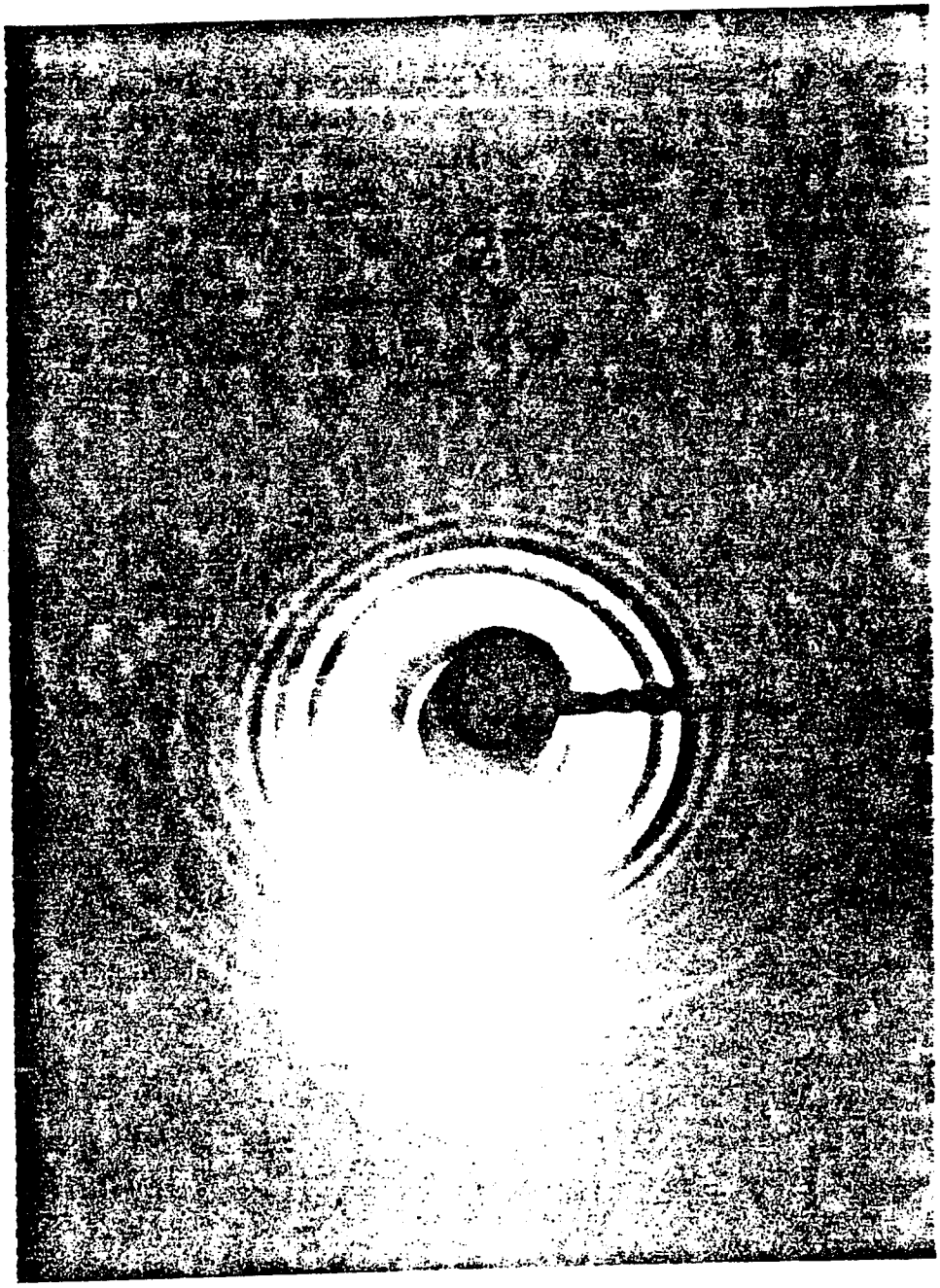

Fig. 13. Selected area diffraction pattern of a single crystal of the α-form of TPI grown from a hexane solution at T_c=20 C. The irradiation time was 18 hours with a voltage of 35 KV and a 15 mA filament current.

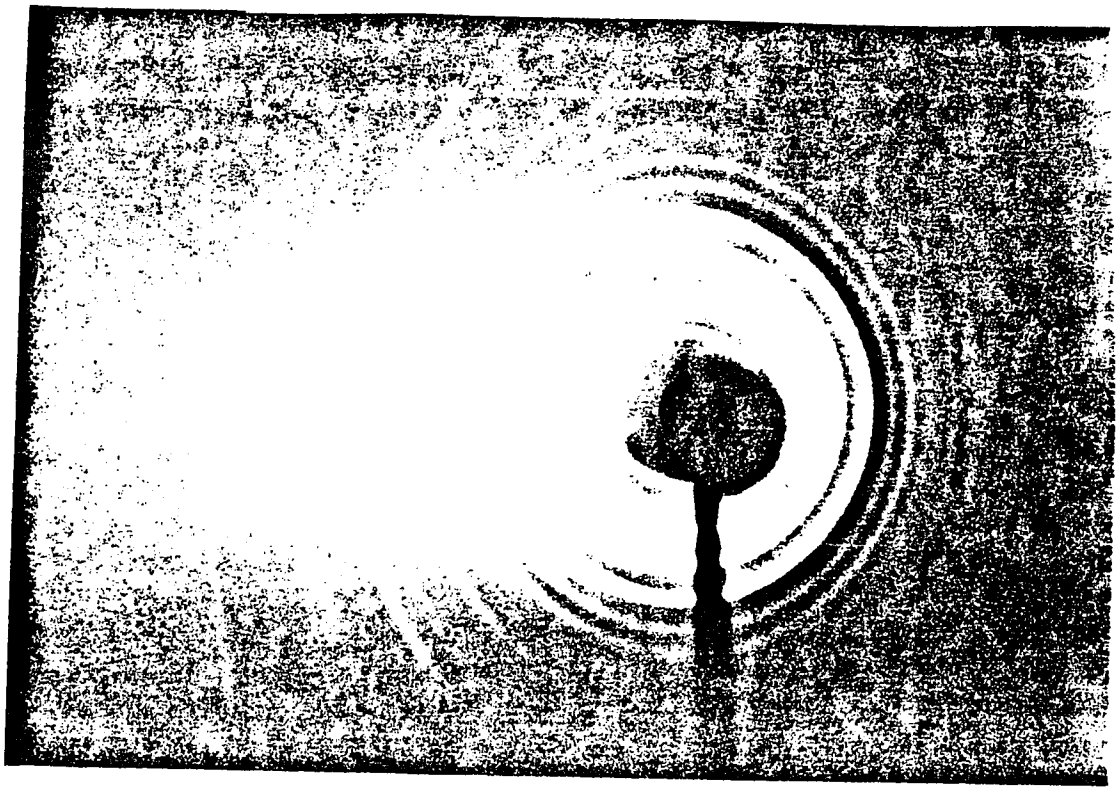

Fig. 14. Wide angle x-ray pattern of partially epoxidized TPI in 2-ethoxy ethanol. T_c=20 C, M_v= 1.55x10^5. The irradiation time was 18 hours, with a 35 KV voltage and a 15 mA filament current.

TABLE IV

Comparison of Observed d-Spacings with literature (106) Values for α Forms

d-observed A	Intensity	d-literature A
7.82	m	7.91
4.90	vs	4.95
3.94	vs	3.95
3.26	vs	3.36
3.02	mw	2.95
2.78	mw	2.73
2.30	vw	2.40
2.08	w	2.29
1.92	vw	2.03

w-weak, m-medium, s-strong.

Lamellas were grown in a 0.1% (w/v) hexane solution with T_d=61 C, T_r=34 C, and T_c=20. d spacings were calculated using Bragg's equation.

which do not give a sharp x-ray pattern have reacted, having, thus, no effect on the x-ray pattern of the crystalline core. The Bragg equation is

$$d = \lambda / 2\mathrm{Sin}[\arctan(z/d)/2]$$

where z is the experimental diameter of each line 1.2, 2.0, 2.5, 3.05, 3.85, 4.9, 7.8 cm; d is the diameter of the camera (5.72 cm) is 1.54A .

6.DENSITY

Density is a basic microscopic quantity of a polymer lamella. It is linked directly to the unit cell parameters and the amorphous content (104 - 106). Density determinations of either solution or melt crystallized polymer by any method such as dilatometry (107), pycnometry (6) or density gradient as used here, show immediately that the experimental values do not reach the densities for perfect crystals, computed from unit cell parameters. The data obtained lie somewhere between the crystalline and amorphous density, e.g. for TPI the pure crystalline density of the form at 25 C is 1.05 g/cm^3(104-105). The amorphous density at 25 C is extrapolated from the melt and is 0.905 g/cm^3, as established by dilatometry(104-105).

One experimental variable that has influence on the sample density is the crystallization temperature. The average

density value is found to increase with increasing T_c in the 20 to 30 range. This increase in density is caused mainly by the decrease in the amount of surface area (noncrystalline region) on the lamella, due to an increase in the crystal thickness. Based on these experiments, a fractional crystallinity is usually calculated, based on the assumption that the sample may consist of relatively perfect crystals and unaffected amorphous regions. The common crystallinity calculated from density data is the weight fraction crystallinity W^c derived as follows:

$$\text{Total Volume} = W/\rho = W_a/\rho_a + W_c/\rho_c$$

$$\text{so that} \quad 1/\rho = 1 - W^c/\rho_a + W^c/\rho_c$$

where $W^c = W_c/W$, the weight fraction crystallinity

$$\text{and finally} \quad W^c = (\rho_c/\rho_s)\{(\rho_s - \rho_a)/(\rho_c - \rho_a)\}$$

The quantities W, W_a and W_c represent the total amorphous and crystalline weights of the samples. ρ_s is the density of the sample obtained experimentally.

The seemingly perfect folded chain TPI single crystals are shown to deviate from perfect crystalline density. Special difficulties were found to exist for the measurement of density of the solution- grown folded chain single crystals. Kawai and Keller (108) have found that a typical folded chain single crystal weighs only 10^{-11}g and has such

a large specific surface area ($\sim 10^6$ cm^2/g) that on floatation experiments interaction of the solvent with the disordered surface layer may influence the flotation equilibrium. Once the folded chain lamellas are sedimented and dried, the thin lamellas may trap air in spaces between the lamellar surfaces. Although the dried crystals are pressed at 3.4×10^7 Pa to eliminate air. The flotation data may be somewhat too high due to solvent surface interaction. The sedimented (dry mats) data, however, are often too low. In any case, the measured values do show a systematic density defect, which is attributed to the noncrystalline region, even for the externally perfect looking single crystals, which is dependent on the crystallization temperature.

The densities obtained for mats of α-TPI crystals grown at various crystallization temperatures T_c, from 0.1% hexane solutions, are given in table V as a function of number average molecular weight, M_v, as determined from viscosity. The number of separate samples studied is indicated in parenthesis, if more than one sample was used. The largest number of measurements were made on the samples crystallized at a T_c of 20 C. At a T_c of 20 C, no systematic change in the density occurs with molecular weight from 0.22×10^5 to 5.8×10^5. An increase in density is observed for T_c=20 C, when the molecular weight is

decreased to 0.07×10^5. If all determinations at a particular T_c are averaged, the values found are those given in the last row of table V . The average deviation of these was within 0.003. The average density value is found to increase with increasing T_c in the 10 to 30 range. The effect on the density by keeping TPI crystals in contact with 2-ethoxyethanol at T_c for 65 days was monitored for the unfractionated TPI with $M_v = 1.6 \times 10^5$. Densities of 0.969 and 0.968 were obtained.

A total noncrystalline content, $1-W_c$, at each T_c used was obtained from the density values in table V and are given in table VI. The average deviation for this quantity is 0.02.

7. EPOXIDATION OF LAMELLAS

The following reaction preserves the stereochemistry of the double bonds producing only the trans oxirane rings, as demonstrated by the work of Schilling, Bovey and Woodward (54, 57) and again in the present work.

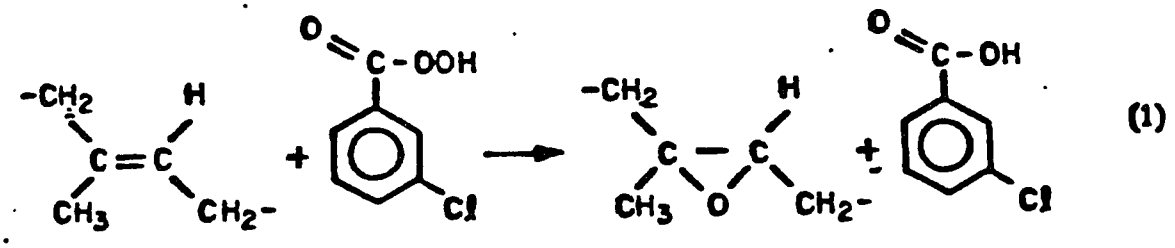

(1)

Selective epoxidation of the double bonds in the surface folds of TPI structure was carried out in a suspension

TABLE V

Densities (g/cm^{-3}) of TPI Crystals* Grown from a Dilute Hexane Solution (T_r=34 C)

$M_v x10^5$	10	20	26	30
0.05	0.975(3)	0.983(6)		
0.07	0.973	0.976(5)		
0.22	0.971	0.974(2)		
0.67		0.971		
2.3	0.967(2)	0.970(2)	0.975	0.979(3)
3.5		0.970	0.975	0.982
5.8	0.965	0.971	0.976	0.983
1.6**	0.963(3)	0.969(5)	0.975(3)	0.978(2)
AVE:	0.969	0.973	0.975	0.981

*

**X-ray diffraction and DSC show predominantly form unfractionated TPI

TABLE VI

Noncrystalline Content for Different Crystallization Temperatures at Various M_v

$M_v \times 10^5$	T_c	$1-W_c$
0.05	20	0.40
0.07	20	0.45
0.67	20	0.49
2.3	10	0.50
	20	0.50
	30	0.44
2.9	10	0.50
	20	0.47
3.5	20	0.50
5.8	10	0.53
	20	0.49
	30	0.40

in 2-ethoxy ethanol at 0 C in order to study the crystalline and non crystalline fractions of solution-grown crystals of TPI. The amorphous fraction is considered to be at the surface of the crystal and contains two components, the chain folds and the noncrystalline chain ends or cilia. The selective epoxidation of the double bonds in the fold region is carried out using metachloroperbenzoic acid, MCPBA, a mild, quantitative, but highly selective reagent, using in preliminary studies for most cases a molar ratio of MCPBA to unfractionated TPI repeat units of 1.6. For a few runs this ratio was set at 0.78 or 4.8. The molar ratios to double bonds were calculated assuming complete precipitation of the polymer during crystallization. Therefore, these values represent the lower limit. The actual ratio at the start of the epoxidation will be higher. Further, on analysing the extent of the reactions, it is clear that the amount of MCPBA initially present is in excess to that needed to react with the available double bonds.Duplicate determinations agreed within +0.02.

8.^{1}H NMR SPECTROSCOPY

^{1}H NMR spectroscopy was used to quantitatively determine the epoxidation of TPI with various amounts of epoxide

content. The ^1H NMR spectra of partly epoxidized TPI crystals, as shown in Figs. 15-16, indicate that the signals are assignable to the protons of the unmodified monomer unit and the epoxidized unit produced in the reaction. The degree of epoxidation is obtained from the relative integral intensity of ^1H NMR spectrum in the $CDCl_3$ solution by cutting out the spectral peaks and weighing. The ratio of the areas under each NMR resonance peak is proportional to the number of similar hydrogens persent in the compound. The chemical shift of the CH, CH_2 and CH_3 resonances for TPI are found at 5.14, 2.0 and 1.6 ppm and for epoxidized units they are at 5.14, 2.7 and 1.3 ppm(94), relative to TMS.

The epoxidized fraction was generally determined from the areas under both the CH and the CH_3 resonance peaks, although in a few cases only the first was used. For the latter calculation, the following equation was employed

$$F_s = 3Z_5/(3Z_4-Z_5)$$

Z_5 is the area under the resonance at 1.3 ppm and Z_4 is the area under the resonance at 1.6 ppm. The above standard method of calculating the amount of epoxidation was confirmed by quantitatively epoxidizing TPI in 2-ethoxy ethanol to various amounts of epoxide content and analysing the product by NMR using the above equation.

The relative composition of peroxidation reaction mixtures and % epoxidized obtained from ^1H NMR analysis for

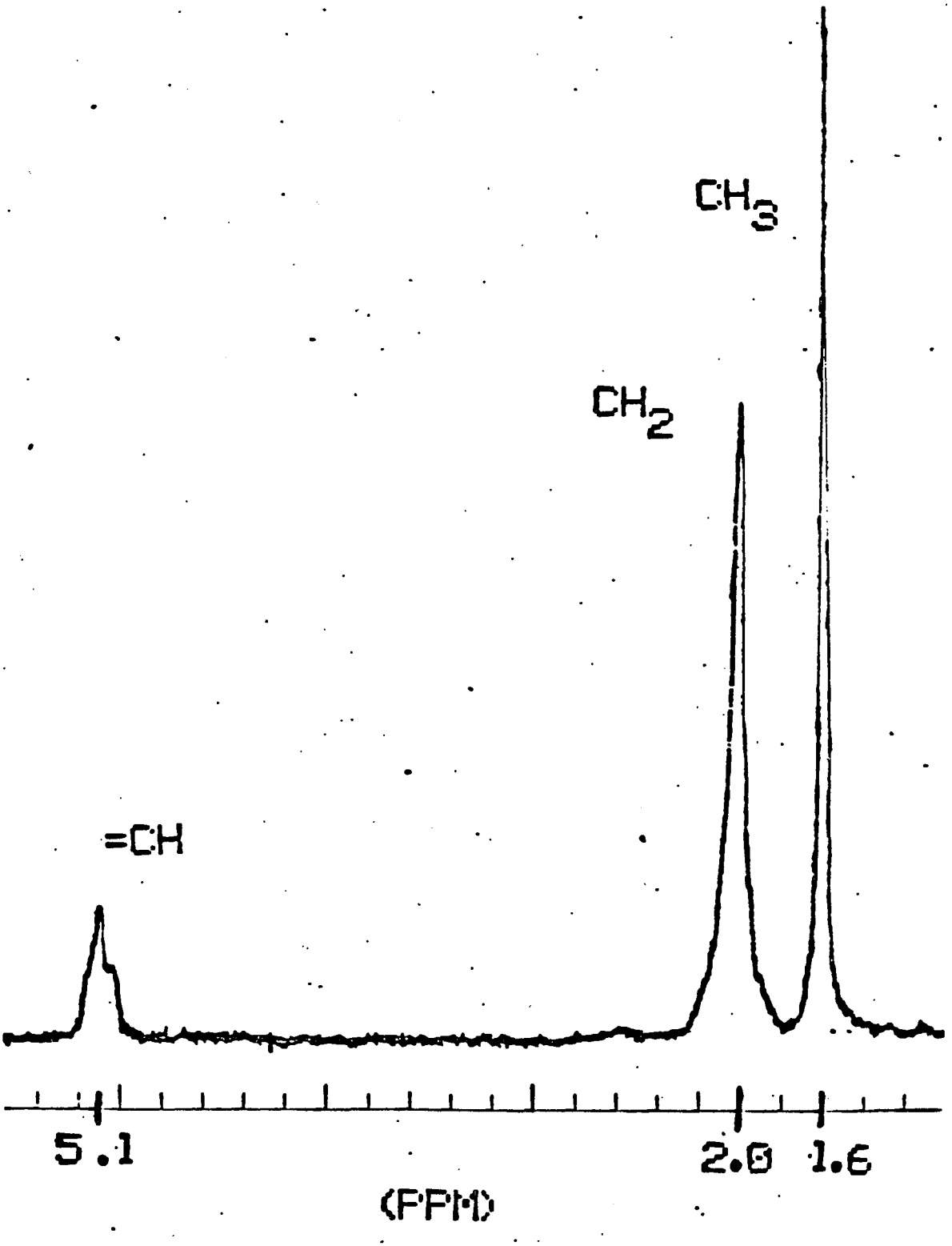

Fig. 15. 100 MHz proton NMR spectrum of unfractionated synthetic TPI dissolved in $CDCl_3$ (1% W/V)

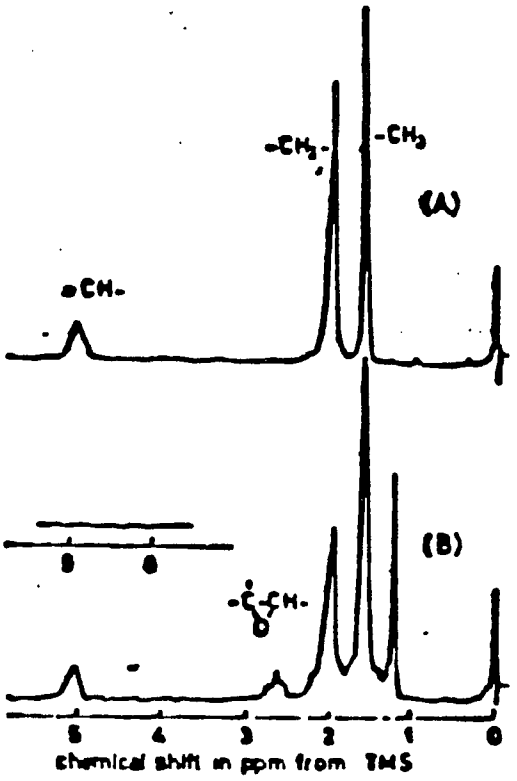

Fig. 16. ^{1}H NMR spectra of (A) unfractionated TPI and (B) PARTLY EPOXIDIZID TPI.

unfractionated TPI epoxidized at 20 C is shown in tableVII. The ^{1}H NMR spectra (Figs. 15-16) indicate that the reaction is a simple addition uncomplicated by side reactions and alternative routes, such as ring opening, hydroperoxide formation, isomerization or degradation. Thus, the only reaction that occurs yields only trans oxirane rings. An overestimation in the epoxidation values from ^{1}H NMR could possibly occur on the account of lesser peak separation. This is less likely in the C-13 NMR measurements due to an enhanced effective resolution. Therefore, the C-13 NMR is considered to be the most accurate method.

9.C-13 NMR SPECTROSCOPY

The C-13 NMR results were used quantitatively to obtain information on surface reactions of TP such as the fraction reacted and the average reacted and unreacted block lengths resulting from epoxidation of α -TPI preparations. This would lead to the determination of the crystalline stem length and the amorphous surface fold length of TPI crystals grown in solution. The 50.32 MHz C-13 NMR spectra of a representative sample of suspension epoxidized TPI lamellas dissolved in deuterated chloroform is shown in Fig.17.The C-13 NMR measurements were made with both PGD or with IGD NOE. Most data was collected with IGD.

TABLE VII

The % Double Bonds Reacted obtained from ^{1}H NMR Analysis for TPI Epoxidized in 2-Ethoxy Ethanol at O C

Wt. of TPI(g)	Wt. of MCPBA(g)	Mole Ratio MCPBA/DB	% DB Reacted CH	CH_3
0.5	1.6	1.3	26	27
0.5	1.8	1.4	26	28
0.5	2.0	1.6	33	35

The fraction of double bonds reacted as assessed from the CH and CH_3 NMR shifts are given in the last two columns of this table.

The unfractionated samples were used at $M_n=3.5x10^4$ and $M_w/M_n=4.8$. TPI is insoluble in 2-ethoxy ethanol. The values of ‹A› and ‹B› are given in monomer units, while L_s is given in nanometers. In all cases the calculations based on carbon #1 and #4 are averaged in the final result. The pertinent C-13 NMR assignments for TPI-epoxidized TPI copolymer, as made earlier by Schilling, Bovey, Anandakumaran and Woodward (54) and used in this work, are given in table VIII. Many of the assignments are in agreement with those made previously on solution epoxidized TPI(109-110).The original assignment of resonances 10 and 14(appendix 4) did not take into consideration the sensitivity of the C3 oxirane carbon to the chirality of neighboring units in both directions along the chain. This resonance is split into four lines produced by the four possible enantiomers in which all R and S designations in the four sequences are interchanged. Therefore, the assignment of the resonances by Hayashi et al(110) to oxirane carbons (10 and 14) that showed sensitivity to chirality was made erroneously. This was corrected later by Schilling, Bovey, Anandakumaran and Woodward (54). These assignments are given in appendices 2-4 along with spectra for TPI epoxidized in a homogeneous solution in chloroform to a level of 25% (spectrum a) and 90% (spectrum b) of completion and epoxidized as crystals

suspended in amyl acetate at 0 C (spectrum c). The designations shown are based on D for double bond and O for oxirane ring (epoxy unit).

The numbering of the carbon atoms in the repeat unit used in Fig. 17 is as follows:

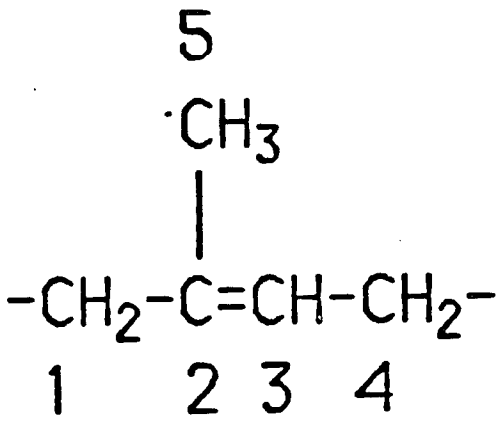

In the sequences referred to below I represents an isoprene unit and E an epoxidized isoprene unit. Some sequences of interest are given below:

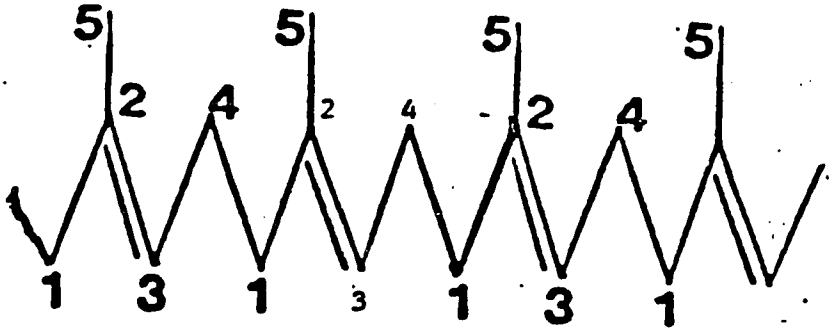

III

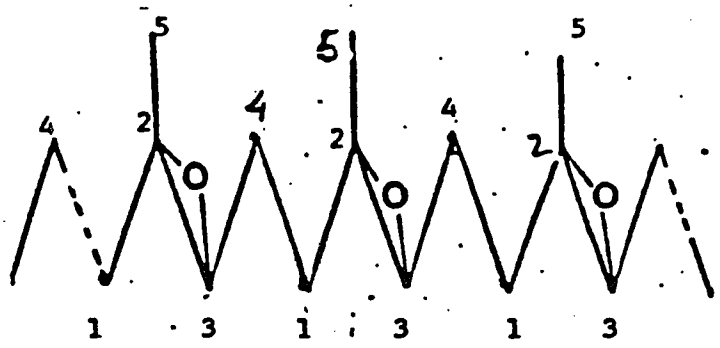

EEE

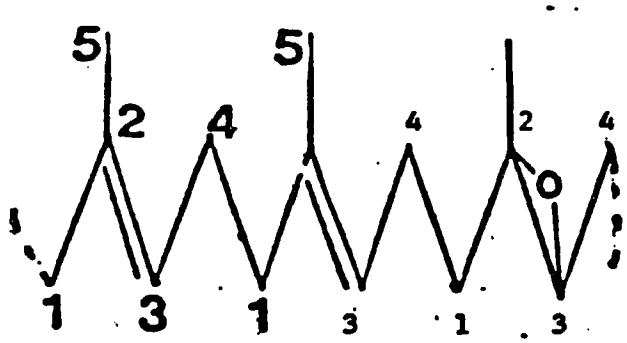

IIE

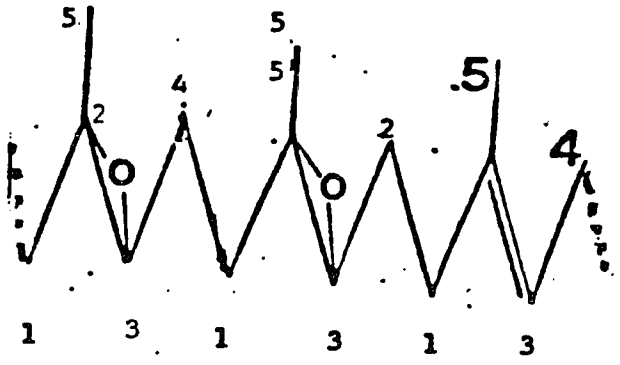

EEI

A number following the sequence designation gives the carbon atom referred to. As an example, the region of absorption in the spectrum denoted III-5 refers to the methyl group in a TPI sequence.

10.CALCULATION OF FOLD LENGTH, STEM LENGTH AND EPOXIDATION LEVEL

Epoxidation of TPI lamellas produces an ABAB... block copolymer, where A represents a sequence of TPI units originally in the crystalline stem and B represents a sequence of epoxidized TPI originally in chain folds. the extent of epoxidation can be established for each sample by a comparison of the graphical integration of the unepoxidized resonance with the epoxidized ones. A quantitative comparison of the unreacted block ‹A›, and the reacted block ‹B›, gives a measure of the average length in monomer units of the crystal stem and the

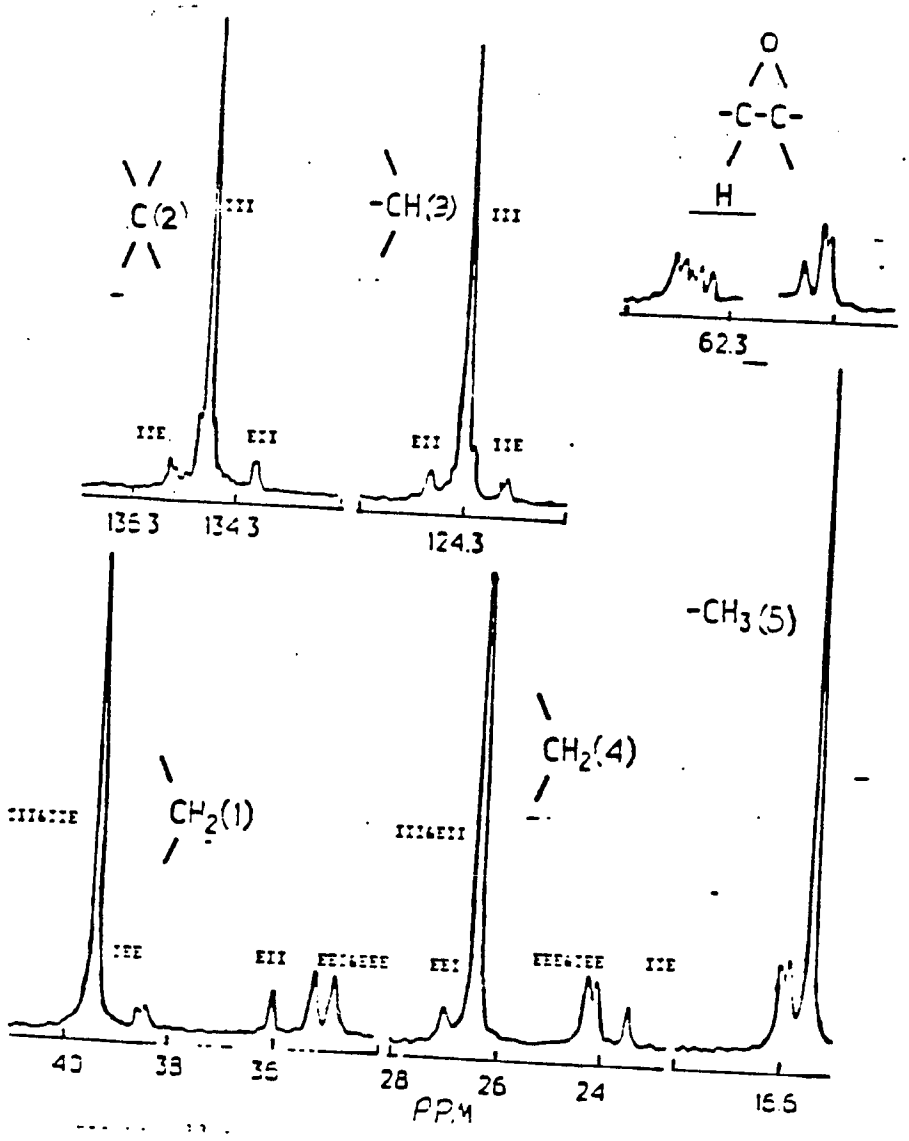

FIG 17. ^{13}C NMR-EPOXIDIZED TPI LAMELLAS

TABLE VIII

C-13 NMR Assignments Used for Analysis of TPI-Epoxidized TPI Block Copolymers[a]

Assignment[b]	Chemical Shift ppm vs. TMS
IIE-C4	23.76
III-&EII-C4	26.77
IEE-&EEE-C4	24.42, 24.57
EEI-C4	27.47
EII-&EEE-C1(m,r)	35.17, 35.54
EII-C1	36.33
IEE-C1	38.78
III-&IIE-C1	39.75
IIE-C3	123.53
III-C3	124.33
EII-C3	125.00

a.assignments as given in ref.54.
b.represents an isoprene unit and an E an epoxidized isoprene unit

surface fold, respectively. Each resonance area represents the total number of equivalent carbon atoms present in the sample. In the equations given below, [III-4] represents the area under the resonance of the methylene carbon atom #4 in an unreacted TPI unit. [EEE-4] represents the area under the resonance for atom #4 in an epoxidized block.[J-4] is the resonance area of junction carbon #4 between the reacted and the unreacted blocks.The formation of segmented block copolymers, upon reaction of the lamellar surfaces, yields original unreacted blocks and newly formed reacted sections, represented by A and B, respectively. ‹A› is the average number of unreacted units per block which includes any irregularities in the crystalline stems or lack of completion of the epoxidation in the surface; ‹B› represents an average number of monomer units in the reacted block which includes any variation in the fold length, significant amounts of unreacted chain ends and reacted lateral surfaces or even epoxidizing agent [MCPBA] penetration into the crystal core. The given values are an average of those obtained from the C-1 and C-4 C-13 NMR resonances. ‹A›, ‹B› and F_e are calculated from the resonance area expressed as a ratio of reacted or unreacted or unreacted areas , a carbon unit neighboring an unreacted block on one end and a reacted one on the other, or vice versa. The completely epoxidized sample is expected

to show four regions of absorption for the junction peaks present: IIE and EEI for carbon unit #4; EII and IEE for carbon unit #1. These are found at 23.76, 27.47, 36.33, 38.78 respectively. The equations are as follows:

$$\langle A\rangle=\{2[II(I \text{ or } E)-C1]/[IEE-C1]+[EII-C1])\}+1$$

$$\langle B\rangle=\{2[EE(E \text{ or } I)-C1]/([IEE-C1]+[EII-C1])\}+1$$

The epoxidized fraction, F_e, can be expressed as the ratio of the epoxidized carbon resonance area plus its junction over the sum of all resonances reacted plus junction and unreacted plus junction.

$$F_e = \frac{[EE(E \text{ or } I)]+[IEE-C1]}{[II(I \text{ or } E)-C1]+[IEE-C1]+[EII-C1]+[EE(E \text{ or } I)C1]}$$

where the brackets[ ] represent relative amounts for the resonance given therein, signifying areas under the particular resonance. For the calculations from the C-4 resonances, the equations used for ‹A› and ‹B› differ from the above, because the EEI and (E or I) II resonances are not completely separable. The equations used are as follows

$$\langle A\rangle=\{[(E \text{ or } I)II-C4]+[EEI-C4]\}/[IIE-C4]$$

or $$\langle A\rangle=([III]+[J])/[J]$$

$$\langle B\rangle=\{[(I \text{ or } E)EE-C4]/[IIE-C4]\}+1$$

or $$\langle B\rangle=[EEE]/[J]+1$$

The C-1 and C-4 resonances were used in all the cases to calculate ‹A›, ‹B› and F_e from the above equations. In a few cases, ‹A› was also calculated from the C-3 resonances

with IGD only by

$$\langle A\rangle = \frac{\{[III-C3]+[IIE-C3]+[EII-C3]\}}{[IIE-C3]}$$

The values obtained for ‹B› from the C-1 and C-4 resonances agreed within 17% and for 90% of the determination, the agreement was within 10%; the values obtained for ‹A› agreed within 19% and for 85% of these, the agreement was within 10%. Reaction times from 30 minutes to 38 days were used for various samples.

The calculations are done using the computer's graphical integration of the resonance areas, as shown in Fig.18 for methylene carbon #1.

Assuming that none of the double bonds in the crystalline region have been reacted, that complete surface reaction has occurred and that the number of noncrystalline chain ends and lateral surfaces are small compared to the folds and taking the chain repeat distance, R, of an isoprene unit as 0.4339nm,(96), then

$$L_s = \langle A\rangle xR$$

where L_s, the average stem length, is the crystallite thickness along the chain direction. Similarly,

$$U = \langle B\rangle_f$$

where U is the average number of monomer units per fold. Turning back to the subject of the olefinic A block, we can use III-C1 or C4 and for the oxirane B block- EEE,

C2 or C4, as shown below:

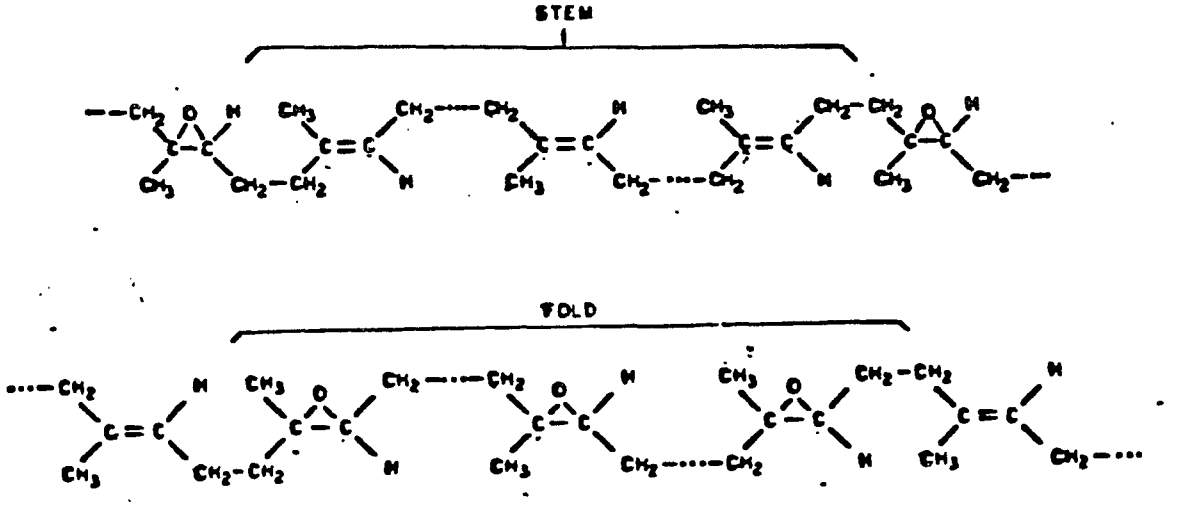

The IEE-C1 and EII-C1 are measures of the stem fold junction, as are IIE-C4 and EEI-C4. If [J] is the resonance area of a junction carbon and [D] is the resonance area of a carbon in the oxirane fold, and we let U represent the average fold length in monomer units, then the number of J carbons per fold is 1, the number of D carbons per fold is U-1 and

$$[D]/[J]=(U-1)/1 \quad \text{or} \quad U=([D]/[J])+1$$

The stem length , L_s, can be determined as follows:

$$L_s(nm)=\{([A]/[J])+1\}xR$$

Fig.18. Computer integration of the resonance area for carbon #1 of TPI block copolymer and block length

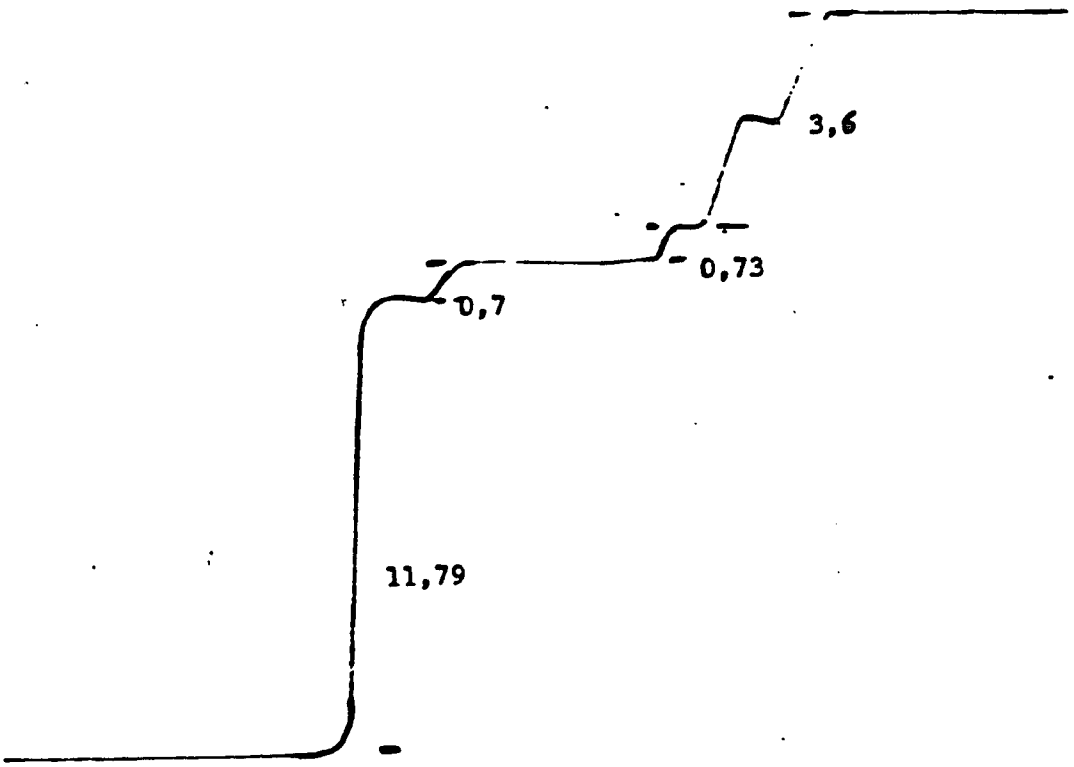

$$A=(11.79+0.715)/0.715=17.5$$

$$B=(3.6+0.715)/0.715=6$$

$$L_s=(11.79/0.715+1)0.439=7.68$$

$$F_e=(3.6+0.715)/(3.6+11.79+2(0.715))=0.26$$

Scale: 2:1. The TPI crystals were grown in hexane solutions of 0.1%(w/v) by self seeding methods at T_c= 30 C and epoxidized in 2-ethoxyethanol at 0 C.

For comparison, the average stem may also be determined from the following expression, assuming a large M_n and complete epoxidation of the fold material:

$$L_s(nm)=[(U/F_e)-U]R$$

The quantity F_e is the fractional extent of epoxidation, as determined by C-13 NMR.

The crystal thickness, L_c, of amylacetate grown TPI crystals was calculated earlier by Woodward et al (53), using electron microscopy measurements of the lamellar thickness, L, and the following relationship:

$$L_c=\{(1-F_s)\ _aL\}/\{(1-F_s)\ _a+F_s\ _c\}$$

where F_s is the fraction of monomer units at the crystal surface, as determined by ^1H NMR . Generally speaking, the general thickness can be estimated from the value of the stem length by multiplying L_s and the Sine of the inclination angle for the crystalline stem. If we assume the fold surface to be in the 001 plane, the chain tilt will equal the angle in the unit cell(102) for the form(105). The lamellar thickness, L,(Fig.11, Table III) was calculated for lamellas prepared from hexane at T_c's 10, 20 and 30 C with a $M_v=2.3x10^5$(T_r=34 C), using C-13 NMR and the following relationship:

Amorphous thickness $L_a = L_c\ (B/A)\ (\rho_c/\rho_a)$

Crystalline thickness $L_c = AR$

Total thickness $L = L_a + L_c$

where A is the average number of monomer units in the unreacted block, B is the average number in the reacted block, ρ_a is the amorphous density (95) and ρ_c is the crystalline density(96). The L was assumed to be independent of M_v and only to depend on T_c. The R value employed (0.439 nm) is that given by Takahashi et al (96). The C-13 NMR results were compared with those values obtained with electron microscopy measurements and found to be in excellent agreement.

11. EFFECT OF SUSPENDING LIQUID ON SURFACE REACTION OF CRYSTALS

When a single lamella is brought in contact with a liquid, the following can occur: 1) penetration of the fold surface 2) penetration of both the fold surface and the crystal interior, usually accompanied by dissolution and possibly recrystallization or 3) no penetration. If the polymer contains chemically reactive groups, such as double bonds, then in the first two cases above, a chemical reaction can take place. If only surface penetration occurs, then the crystal core should remain unreacted and only the chain folds, the chain ends and the chains on the lateral crystal surfaces would be involved in the chemical reaction. Such being the case, a suspending liquid had to be carefully

chosen, to ascertain that the reaction take place preferentially at the folds and may be physically confined to this region. The epoxidation in suspension of TPI in the β form was carried out by J.Xu in 14 different liquids at 0 C, leading to the formation of segmented block copolymers with an average unreacted sequence of monomer units ‹A› characteristic of the average number of monomer units in the crystal traverses and an average reacted sequence of monomer units ‹B› characteristic of the number of monomer units in the folds, noncrystallizing chain ends and interlamellar traverses. The results for the epoxidation in suspension of β-TPI structures, prepared as given above, are found in table IX in terms of ‹A›, ‹B› and the fraction of the double bonds reacting, F_e as a function of the epoxidizing liquid medium and the time. The values given are an average of those obtained from the C-1 and C-4 C-13 NMR resonances separately using gated decoupling with NOE (see table VIII for the NMR assignments). Equations for the calculation of ‹A›, ‹B› and F_e using the C-1 resonances are given above.

It is observed (Table IX) that ‹B› changes four-fold (from 4.3 to 16) and F_e doubles in value (from 0.25 to 0.50) with change in the reaction medium, keeping the reaction time constant, whereas ‹A› fluctuates by 12%. The dissolution temperatures in eight of the liquids listed in table X of portions of a β-TPI crystal mat and of a TPI lamellar

sample epoxidized in suspension to 35% were measured using a heating rate of 1 C/hour. The results obtained are given in table X. It is seen that as the dissolution temperature for the epoxidized lamellas decreases the ‹B› and F_e obtained by reaction carried out in that liquid (table IX) increases.

12.EFFECTS OF TIME & REACTANT CONCENTRATION ON EPOXIDATION

For α-TPI lamellas grown from hexane, the epoxidation medium chosen was 2-ethoxyethanol, a poor solvent for both the reacted and the unreacted blocks. While TPI pellets are insoluble in 2-ethoxyethanol, the epoxidized TPI lamellas have a high dissolution temperature. When this liquid was employed in the study described above, the ‹B› and Fe values were low. The C-13 NMR measurements on these samples were made without the NOE. The values given are an average of those obtained from the C-1 and C-4 carbon- 13 NMR resonances and were used in all cases to calculate ‹A›, ‹B›. In a few cases, ‹A› was also calculated from C- 3 resonances.

Reaction times from one day to 38 days for unfractionated TPI crystallized at 20 C and epoxidized at a molar ratio for MCPBA to TPI units of 1.6 were used, Table XI, Fig. 19. The ‹A› and ‹B› values showed no change within experimental fluctuation (+0.3 for ‹B› and +1 for ‹A› from 4 to 18 days).

When a ratio of 0.78 was used for unfractionated

TABLE IX

Average Number of Monomer Units in Reacted and Unreacted Sections of Epoxidized β-TPI Lamellar Structures[a]

Reaction Medium	Time-Da.	F_e	⟨B⟩	⟨A⟩
2-ethoxyethanol	10	0.24	3.9	12
	10	0.23	3.6	12
	12	0.23	4.0	13
	14	0.23	4.7	13
	28	0.23	3.6	12
average		0.23	4.0 0.3	12
methanol	14	0.25	5.4	17
	21	0.25	5.0	15
octanol	28	0.26	4.3	13
3-pentanone	14	0.26	4.6	14
ethanol	14	0.30	7.0	16
methyl-ethyl ketone	14	0.30	7.2	17
2-pentanone	14	0.32	6.8	15
acetone	14	0.34	7.2	14
4-methyl-2-pentanone	14	0.35	7.5	14
ethyl acetate	14	0.38	8.2	14
	21	0.42	9.5	15
methyl acetate	14	0.39	8.7	12
	21	0.43	9.4	13

Table IX continued

	Time-Da.	F_e	‹B›	‹A›
propyl acetate	14	0.40	8.7	13
	21	0.41	11	14
amyl acetate	14	0.45	13	16
	21	0.49	13	14
	28	0.53	16	14
average		0.49+0.3	14+1	15
butyl acetate	14	0.50	16	16

[a] crystallized from amyl acetate at 0 C and heated to 30 C in the suspension liquid using unfractionated TPI followed by epoxidation at 0 C and determination of fraction epoxidized (F_e), reacted ‹B› and unreacted block length ‹A› by C-13 NMR.

* Results by Xu and Woodward

*Table X

Dissolution temperatures for β-TPI Lamellar Mats and for a 65% TPI-35% Epoxidized TPI Block Copolymer[a]

Liquid	Dissolution Temperature- C[b]	
	β -TPI	TPI-Epoxidized TPI
2-ethoxyethanol	insoluble	64
methanol	insoluble	insoluble
acetone	insoluble	48-58
methyl acetate	insoluble	45
ethyl acetate	insoluble	32
propyl acetate	50	27
butyl acetate	48	25
amyl acetate	47	25

[a]the β-TPI lamellas were crystallized from amyl acetate at O C and slowly heated in suspension to 30 C; the block copolymer was prepared in acetone at O C using lamellas grown at O C in amyl acetate and heated in suspension to 30 C; the heating rate for the dissolution studies was 1 C per hour, starting from 25 C for 2-ethoxyethanol, methanol and acetone and from O C for the others.

*Results bu Xu and Woodward

TPI, the ‹B› value at 5 days reaction was 30% below that found for a ratio of 1.6:1 (Fig. 19, Table XII). The ‹B› values obtained for a 0.78 ratio show a large deviation between different preparations but show an apparent increase with time. Furthermore, the increase in the ‹B› value at the 0.78 ratio continued even after 27 days. A shorter time is necessary to reach equilibrium at a higher concentration (for a few runs this ratio was set at 2.4, 3.9, Table XIII). As shown above from unfractionated TPI it is clear from Figs. 20-21 that for a fractionated TPI the ‹A› value reaches equilibrium after 0.5 days and stays constant , while the level of epoxidation, F_e, changes with time the same way as ‹B› (Fig. 22). Fig. 23 suggests a mechanism of random distribution of epoxidized units spread along the folds till they are fully reacted and an equilibrium value of ‹A› is reached reflecting the actual value for the crystalline core of the lamellas. Since an increase in the available double bonds with higher molecular ratio of the epoxidizing agent could not be observed (Tables XII-XIII, Fig.24), regions of reaction of double bond in the crystalline regions were ruled out. A limiting value for the amount of reaction is always reached with time at a constant concentration of MCPBA without it being completely consumed. Furthermore, for a molar ratio of MCPBA to TPI units of 1.6 and epoxidation at 10, 20 or 30 C (Figs. 25-36, Tables XIV-

XXV), the values of ‹A› and ‹B› showed no change with time within experimental uncertainty after 1 day.

Table XXVI compares lamellas grown at T_c=20 C and epoxidized with MCPBA to lamellas grown at T_c=20 C and hydrochlorinated in acetone (106). The results agree, within experimental error.

Experiments using a TPI fraction with $M_v=3.5x10^5$ (Table XXIII) and a reactant ratio of 4.8 were run for 4, 8 and 14 days and the ‹A› and ‹B› values found to agree within experimental error with those run at a ratio of 1.6:1.

13. EFFECT OF MOLECULAR WEIGHT AND CRYSTALLIZATION TEMPERATURE ON ‹A› AND ‹B› VALUES

A study of the effect of molecular weight on the ‹A› and ‹B› values for α-TPI lamellas crystallized at 20 C from hexane was carried out using fractions with M_v=5,000 to $5.8x10^5$ and a reactant ratio of 1.6:1 (See page 90). (F_e) and ‹B› are found to be essentially constant from $M_v=5.8x10^5$ down to and including $M_v=6.7x10^4$. ‹A› remains constant within +1 over the complete molecular weight range studied.

An increase in the averages of ‹B› and F_e with decreasing molecular weight commences at an M_v value between 22,000 and 67,000 (Tables XIV-XVII, Figs. 25-28) and is attributed to noncrystallizing chain ends . The ‹A› value increases with increasing T_c.

The results of seven fractions crystallized at 20 C are summarized in Table XXIX in terms of the values of $(F_e)_f$, $\langle B \rangle_f$ and $\langle A \rangle_f$, which are the averages of the results obtained from a 4 to 31 days reaction; the number of determinations used in obtaining these values varied from 4 to 12 (see column 3). For TPI with $M_v=0.67x10^5$, however, the $\langle B \rangle_f$ and $(F_e)_f$ values reflect the lower molecular weight tail of the distribution curve, since they are larger than the corresponding values found for the fractions with $M_v=2.3x10^4$.

The $\langle A \rangle$ values for epoxidized lamellas grown at 10 C increase from 10 to 12 monomer units(Table XXVII-XVIII, Fig. 29-30). These values are, however, less reliable, since the lamellar thickness is smaller and therefore the lamellas can contain more defects which lead to an easier destruction of the lamellas.

Samples of the TPI fraction with $M_v=2.3x10^5$ crystallized from hexane at 10 and 30 C were epoxidized in suspension. These results along with those for $T_c=20$ C from Table XXIX are included in Table XXX. It can be seen in the latter Table that with an increase in the crystallization temperature from 10 to 30 C, $\langle B \rangle_f$ fluctuates around a value of 5 and $\langle A \rangle_f$ increases.

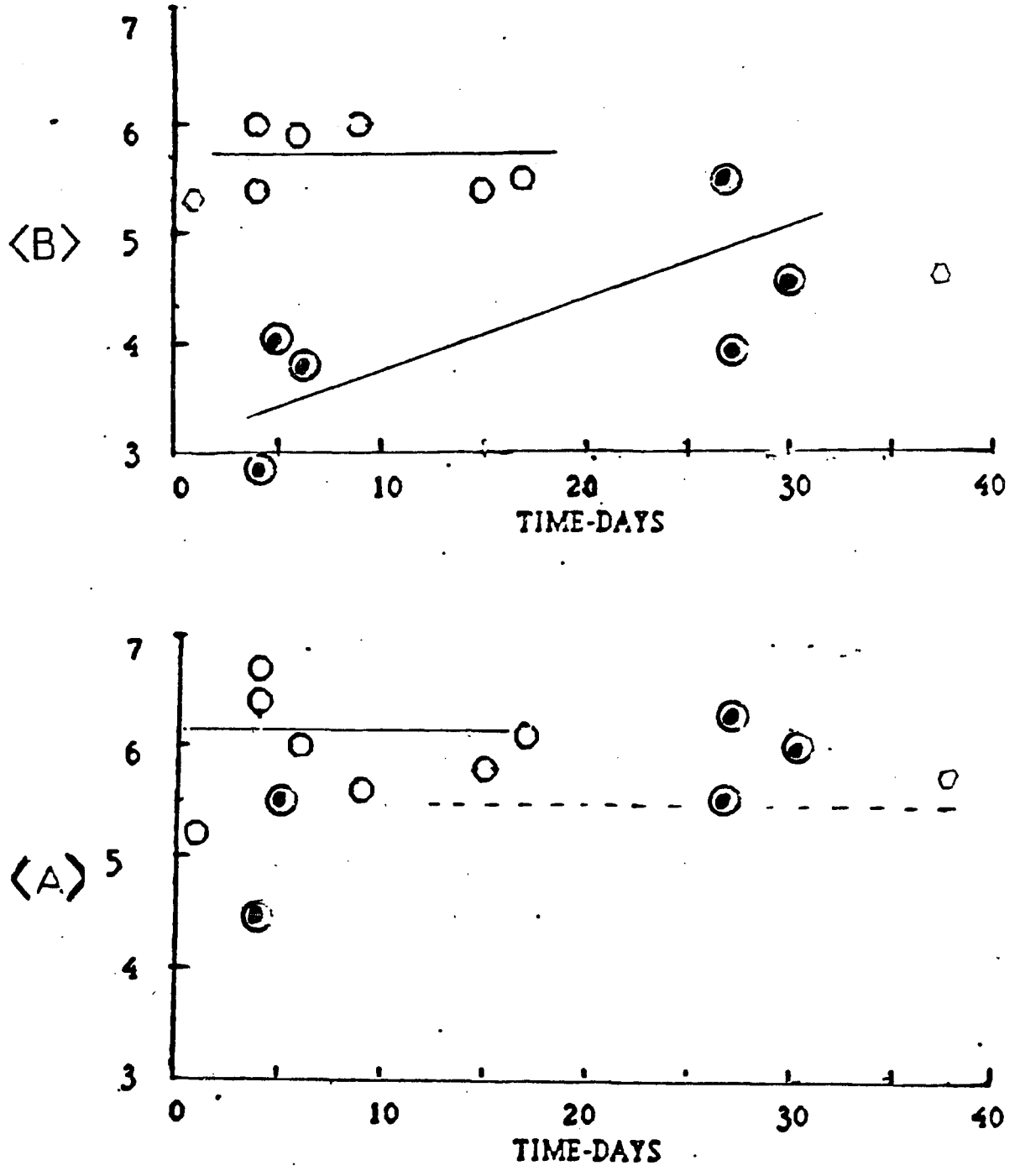

Fig.19. The average block length reacted, U, (monomer units per fold(and unreacted, L_s (crystalline stem length in nm) for unfractionated TPI lamellas grown from a hexane solution at T_c=20 C, M/D=0.78, 1.6.

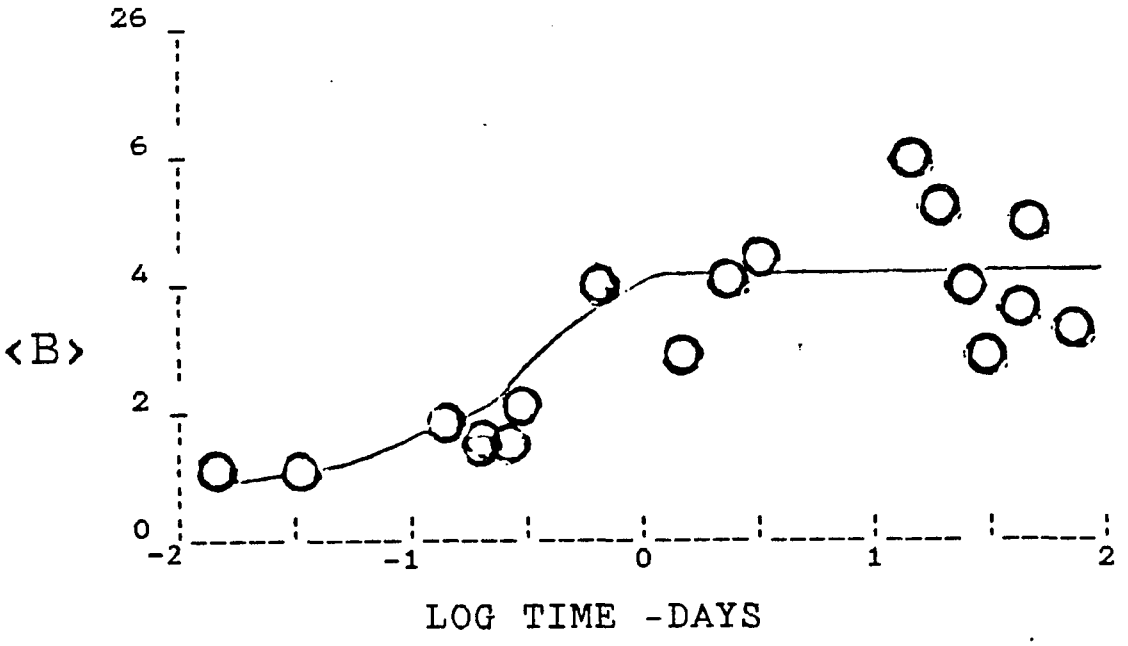

Fig. 20 ‹B› vs. log time for TPI lamellas epoxidized in 2-ethoxy ethanol at 0 C and grown in a hexane solution. M_v=2.9x10^5, M/D=1.6.

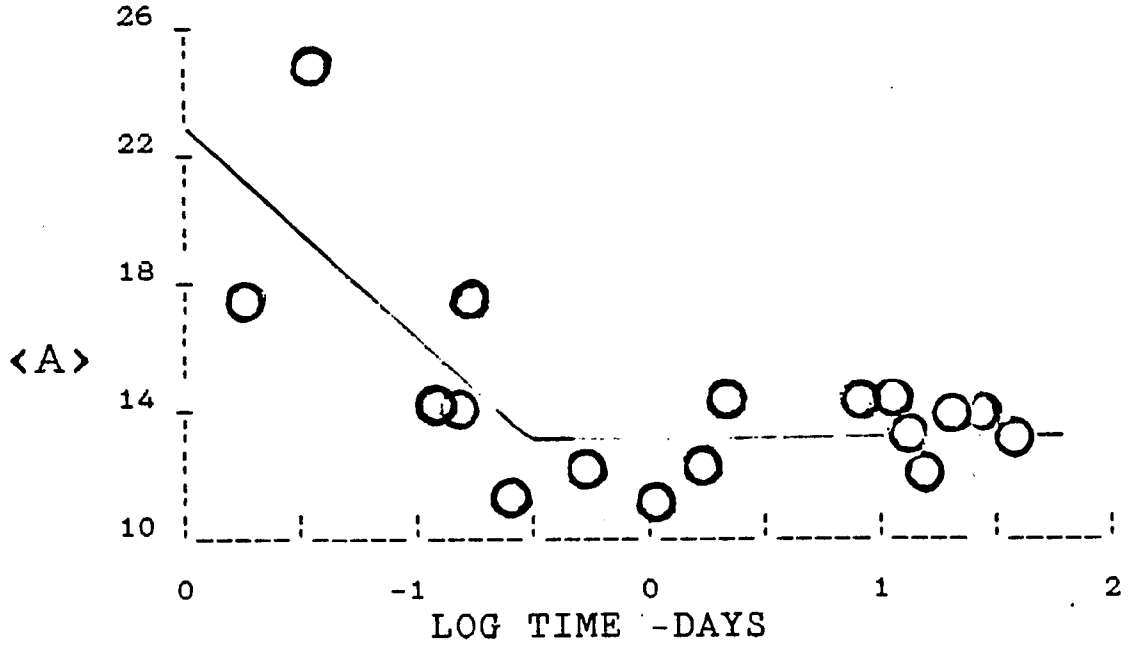

Fig.21. ‹A› vs. log time for TPI lamellas, epoxidized in a 2 ethoxy ethanol suspension at O C and grown in a hexane solution at T_c=20 C, M_v=2.9x10^5 and M/D=1.6.

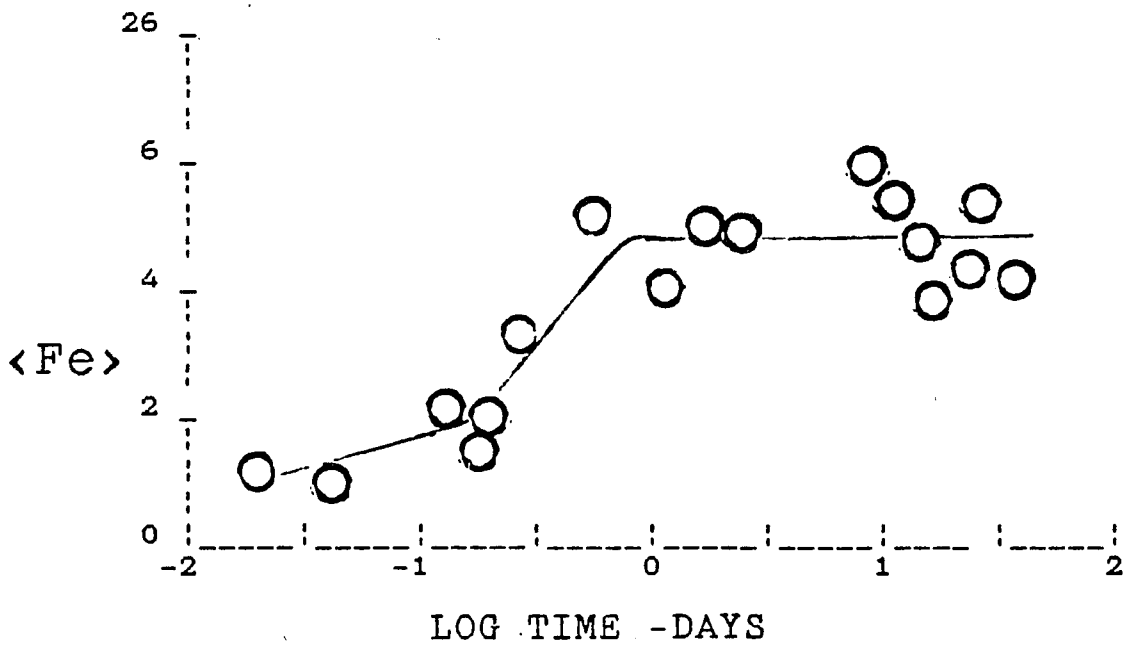

Fig.22. Epoxidation fraction F_e vs. log time for TPI lamellas in a 2-ethoxy ethanol suspension, prepared from a dilute hexane solution at T_c=20 C and M_v=2.9x10^5.

This suggests that the nature of the fold is similar for crystals grown at different T_c giving a mean value of 4.9 monomer units. The lamellar crystalline stem increases from 12 to 17 monomer units as the crystallization temperature increases from 20 to 30 C. This trend has been noted previously (13, 86) using microscopy and small angle diffraction. ‹A› values for epoxidized lamellas grown at 10 C also show the same trend ranging from 10 to 12 monomer units.These values are, however, less reliable since the lamellar thickness is smaller and therefore the lamellas can contain more defects which lead to an easier destruction of the lamellas.

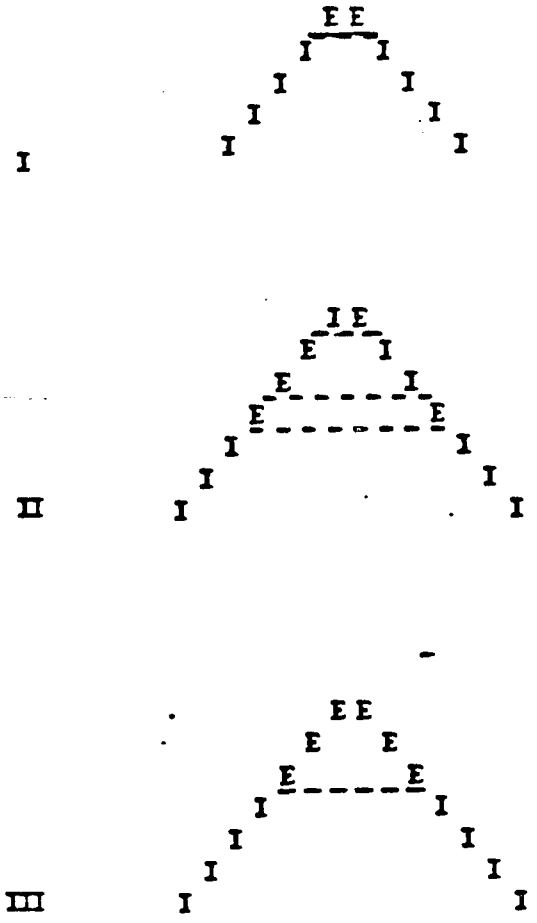

Fig. 23. I: unreacted fold or fold in process of being reacted. Large ‹A›. II: Random distribution of epoxidized units in the fold. Small ‹A› values. III: fully reacted surface, represents the actual value of the stem length of the crystalline region.
---- represents a junction.

TABLE XI

Results of Epoxidation of Unfractionated TPI in Cellosolve at O C from a Dilute Hexane Solution at 20 C. M_v=1.6x10^5. C-13 NMR Done both with NOE(Power Gated Decoupling) or without NOE(Inverse Gated Decoupling)

M/D	Time-Da	U	Ls(nm)	‹A›	F_e	Comment
1.6	1	5.2±0.1	5.8±0.1	12	0.29±0.01	PGD
		4.6±0.1	5.2±0.2	10	0.27	IGD
1.6	4	5.1±0.1	6.4±0.3	12	0.26	PGD
		5.4±0.1	6.7	12	0.26	IGD
1.6	4	6.2±0.3	6.3±0.2	14	0.30	PGD
		6.0±0.1	6.4±0.1	14	0.29	IGD
1.6	6	5.9±0.3	6.0±0.2	14	0.30	IGD
1.6	9	5.3±0.3	5.4±0.6	12	0.32±0.01	PGD
		6.0	5.6±0.2	14	0.32±0.01	IGD
1.6	15	5.9	6.3±0.3	14	0.30	PGD
		5.4	5.8	12	0.29	IGD
1.6	17	4.9±0.2	5.2±0.2	12	0.29	PGD
		5.5±0.2	6.1±0.3	13	0.29±0.01	IGD
1.6	38	4.5±0.1	5.6±0.1	10	0.26	PGD
Average		5.7±0.3	6.1±0.3	13	0.29±0.01	

TABLE XII

Results of Epoxidation of Unfractionated TPI in 2-Ethoxy Ethanol at O C prepared from a Dilute Hexane Solution at T_c=20, M_v=1.6x10^5 and M/D=0.78

M/D	Time-Da	U	Ls(nm)	‹A›	F_e
0.78	4	(I)2.9±0.2	4.5±0.3	7	0.22±0.01
0.78	5	(I)4.0±0.1	5.5±0.2	9	0.24
0.78	6	(P)3.9±0.1	5.1±0.1	9	0.25
0.78	27	(I)5.5±0.1	6.3	13	0.27±0.01
		(P)5.7±0.2	6.3±0.1	13	0.27
0.78	27	(I)3.9±0.2	5.5±0.4	9	0.25±0.01
0.78	30	(I)4.6±0.1	6.0±0.1	10	0.25

I= IGD -- Inverse Gated Decoupling

P= PGD -- Power Gated Decoupling

TABLE XIII

Results of Epoxidation of Unfractionated TPI in Cellusolve at O C, M_v=1.6x10^5; Prepared in Amyl Acetate at 20 C.

M/D	Time-Da	U	Ls-nm	‹A›	Fe
2.4	2	5.8	5.3	13.2	0.31
2.4	4	5.8±0.2	5.5±0.3	13.2	0.32
2.4	6	7.9±0.1	5.4±0.1	17.9	0.40±0.01
2.4	8	6.3±0.4	5.4±0.2	14.3	0.32
2.4	16	6.1	5.3±0.1	13.8	0.34±0.01
3.9	20	4.0±0.3	4.7±0.2	9.1	0.27
2.4	20	4.0±0.1	5.2±0.1	9.1	0.26±0.01
2.4	28	6.1	6.2	13.8	0.30
Average		5.4±0.8	5.4±0.3	12.3	0.30±0.02

TABLE XIV

Results of Epoxidation of TPI Lamellas (T_c=20, M/D=1.6) in a Cellosolve Suspension at 0 C. Grown from a Hexane Solution. M_v=0.05x10^5, M/D=1.6

Time-Da	‹A›	‹B›	Ls(nm)	F_e
5	14	7.2±0.2	6.3±0.1	0.34±0.01
8	14	6.8±0.4	6.0±0.3	0.33
9	13±1	7.2±0.4	5.8±0.2	0.35
11	16±2	7.4±0.6	6.9±0.6	0.32±0.01
13	15	6.2±0.2	6.6±0.2	0.31±0.01
Average	14±1	7.0±0.4	6.3±0.3	0.33±0.01

TABLE XV

Results of Epoxidation of Lamellas in 2-Ethoxy Ethanol at 0 C. M_v=7,000, M/D=1.6 and T_c=20 C. Grown from dilute hexane solution.

Time-Da	‹A›	‹B›	Ls(nm)	F_e
4	14±1	6.0±0.1	6.4±0.4	0.30±0.01
6	16	6.2	7.2±0.1	0.28±0.01
8	14±1	5.8±0.1	6.2±0.4	0.29±0.01
10	16	5.8	7.0±0.1	0.27±0.01
12	14±1	5.9±0.3	6.3±0.4	0.29
14	14±1	6.0±0.1	6.3±0.4	0.29
Average	15±1	6.0±0.1	6.6±0.3	0.29±0.01

TABLE XVI

Results of Epoxidation of TPI Lamellas in a 2-Ethoxy Ethanol Suspension at 0 C. Grown from a Hexane Solution. T_c=20 C, M/D=1.6 and M_v=0.22x10^5.

Days	‹B›	‹A›	F_e
8	5.3±0.2	14	0.28
12	4.8±0.3	14±1	0.26
28	4.9±0.2	12	0.29
18	5.0	12	0.29*
18	5.0	12	0.30*
7	4.7	14	0.26
24	4.3	12	0.27
27	5.4±0.4	13±2	0.30
Average	4.9±0.3	13±1	0.28+0.01

* C-1 only, NS 10,000 PGD

TABLE XVII

Results of Epoxidation of TPI Lamellas in a 2-Ethoxy Ethanol suspension at O C. Grown from a Hexane Solution at T_c=20 C, M_v=0.67x10^5 and M/D=1.6.

Sample	Days	‹A›	‹B›	Ls(nm)	F_e
122	5	14	5.0±0.2	6.0±0.2	0.27
81	6	15	5.9±0.1	6.7	0.28±0.01*
120	7	14	4.8	6.1±0.1	0.26
88	9	12	3.9±0.1	5.2	0.25±0.01*
121	11	13	4.7±0.2	5.9±0.2	0.26±0.01
90	13	13	4.7±0.1	5.7±0.2	0.27±0.01
85	16	14±1	4.8±0.2	6.1±0.3	0.26±0.01
Average		14±1	4.8±0.3	6.0±0.4	0.26±0.01

* Poor graphical integration

TABLE XVIII

Results of Epoxidation of TPI Lamellas in a Cellusolve Suspension at O C. Prepared from a Dilute Hexane Solution at T_c=20 C, M_v=2.3x10^5 and M/D=1.6

TIME-da	‹A›	‹B›	Ls(nm)	F_e
7	16±2	4.7±0.4	7.0±0.9	0.24±0.01
9	15±1	4.7	6.4±0.2	0.24
11	15	4.8±0.2	6.6	0.25
13	14	4.5±0.1	6.1	0.24
15	14±1	4.6±0.2	6.5±0.2	0.24
Average	15±1	4.7	6.4±0.2	0.24

TABLE XIX

Results of Epoxidation of TPI lamellae in a 2-Ethoxy Ethanol Suspension at 0 C. T_c=30, M_v=2.3x10^5. Grown in a Hexane Solution.

Days	‹B›	‹A›	F_e
8	5.6	17±1	0.26
16	5.8±0.1	16±1	0.29±0.01
24	5.6±0.5	16±2	0.28±0.01
4	5.5±0.1	17±2	0.26
12	5.7±0.1	16	0.26
Average	5.6±0.1	16	0.27±0.01

TABLE XX

Results of Epoxidation of TPI Lamellas in Cellusolve at O C Prepared in a Hexane Solution. C-13 NMR done with both NOE(Power Gated Decoupling, PGD) or witheot NOE (Inverse Gated Decoupling, IGD). M_v=2.9x10^5, T_c=20 C and M/D=1.6

	Days	‹A›	‹B›	Ls(nm)	F_e
IGD	0.02	17	1.1	7.6±0.1	0.06
PGD	0.04	24	1.0	10	0.05
PGD	0.13	14	1.7	6.3±0.3	0.11±0.01
PGD	0.17	14	1.6±0.1	6.0	0.10
IGD		17	1.4	7.5	0.08
PGD	0.25	11	2.1	4.9	0.16
IGD	0.50	12	3.8±0.1	5.1	0.25±0.01
IGD	1	11	2.8±0.1	4.8	0.20
IGD	1.5	12	3.8±0.1	5.3	0.24
IGD	2	14±1	4.2±0.1	6.1±0.3	0.24±0.01
IGD	7	14	5.7±0.3	6.2±0.1	0.29±0.01
IGD	9	14	5.0±0.2	6.2±0.1	0.26
IGD	11	13	3.8±0.2	5.6±0.3	0.23
IGD	13	12	2.7±0.1	5.0±0.3	0.19
IGD	17	13	3.4±0.1	5.7±0.3	0.21±0.01
IGD	19	13	4.7±0.1	5.8±0.1	0.26
IGD	27	13	3.1±0.3	5.6±0.4	0.20±0.01
Average(0.5-27 Da)		13	3.9±0.7	5.6±0.4	0.23±0.02

TABLE XXI

Results of Epoxidation of TPI Lamellas in a Cellosolve Solution at O C, Grown in a Dilute Hexane Solution at T_c=10 C and M_v=2.9x105 (IGD)

Days	‹B›	‹A›	Ls(nm)	F_e
11	4.7	11	4.9±0.1	0.29±0.01
16	4.7±0.1	11	4.8±0.1	0.30
21	3.9±0.2	12	5.4±0.2	0.23±0.02
26	5.0±0.1	12	5.4±0.1	0.29
28	4.5±0.1	11	5.0±0.1	0.29±0.01
29	4.1±0.1	11	5.0	0.27±0.01
30	5.3±0.03	12	5.3±0.3	0.30
Average	4.6±0.3	11	5.2±0.2	0.28±0.02

TABLE XXII

TPI Lamellas Epoxidized in Cellusolve at 0 C, Prepared in a Hexane Solution at 20 C. M/D=1.6, M_v=3.5x10^5 (IGD)

Days	‹A›	‹B›	Ls(nm)	F_e
5	12	4.3±0.1	5.4±0.1	0.27±0.01
7	13	4.8±0.2	5.9±0.1	0.26
8	14	4.3±0.1	6.1±0.1	0.24±0.01
9	12	4.2±0.1	5.3±0.2	0.26
10	13	5.4±0.2	5.8±0.2	0.30±0.01
11	12	5.3	5.4±0.1	0.31±0.01
12	15	5.2±0.1	6.7±0.1	0.25
12	16	4.7±0.1	6.9±0.5	0.23±0.01
14	13	3.8±0.1	5.7±0.4	0.22
14	14	5.8±0.3	6.3±0.6	0.29±0.01
15	12	4.7	5.5±0.1	0.28±0.01
Average	13+1	4.8±0.5	5.9±0.4	0.26±0.02

TABLE XXIII

Results of Epoxidation of Fractionated TPI in 2-Ethoxy Ethanol at O C from a Hexane Dilute Solution at T_c=20 C, M_v=3.5x105 and M/D=4.8

M/D	Days	‹A›	‹B›	Ls(nm)	F_e
4.8	4	14	6±0.1	6.4±0.1	0.29
4.8	8	12	3.8±0.2	5.4±0.3	0.23
4.8	12	13	4.5	5.6±0.1	0.26

TABLE XXIV

Results of Lamellas Epoxidized in a Cellusolve Suspension at 0 C, M/D=1.6, Prepared in a Dilute Hexane Solution at T_c=20 C, M_v=5.8x10^5 (IGD)

Sample	Days	‹A›	‹B›	Ls(nm)	F_e
164	5	12	4.6±0.2	5.4±0.2	0.27
165	7	13	4.7	5.8±0.2	0.26±0.01
166	9	12	4.6±0.1	5.4±0.2	0.27±0.01
167	11	13	4.7±0.1	5.6±0.2	0.27
Average		13±1	4.7±0.1	5.6±0.2	0.27

TABLE XXV

Results of Unfractionated TPI Lamellas Epoxidized in a 2-Ethoxy Ethanol Suspension at O C. T_c=10. Prepared from a dilute Hexane Solution. M/D=1.6.

Time-Days	U	Ls(nm)	F_e
9	4.3±0.1	5.1±0.2	0.27±0.01
13	3.3	4.9±0.3	0.22
15	4.5±0.1	5.1±0.1	0.27±0.01

TABLE XXVI

Epoxidation and Hydrochlorination results for TPI Lamellas Grown from an Amyl Acetate Solution at 20 C, using Unfractionated TPI

	U	‹A›	L_s	F_e
Epoxidized Lamellas	5.4±0.8	12±1	5.4±0.3	0.3±0.02
* Hydro-chlorinated Lamellas	4.8±0.5	11±2	5.0±0.9	0.29±0.01

* Woodward and Tischler

TABLE XXVII

Results of Epoxidation of TPI Lamellas in a 2-Ethoxy Ethanol Suspension at 0 C. T_c=10 C, M/D=1.6 and M_v=2.3x10^5. Grown in an amyl acetate solution.

Days	‹B›	‹A›	Ls(nm)	F_e
10	4.6	14±1	6.1±0.5	0.27
4	5±0.4	14±1	6.1±0.5	0.27
12	5.6±0.1	14	6.1±0.5	0.27
0.3	2.5±1	15±1	6.6±0.5	0.15
0.5	2.5	15±1	6.6±0.5	0.15
Average	4±0.1	14±1	6.3±0.5	0.22

TABLE XXVIII

Results of Epoxidation of TPI Lamellas in Cellusolve at 50 C, Grown from a Hexane Solution at 10 C. $M_v=2.3x10^5$, M/D=1.6

Days	‹B›	‹A›	F_e
4	5.7±0.6	14±1	0.28±0.01
6	4.7±0.3	13±1	0.28±0.01
6	5.0	13	0.27
8	7.3±0.2	13	0.37±0.01
8	7.2±0.3	13	0.36±0.01
10	7.3±0.3	13±1	0.37±0.01
12	6.7±0.2	11	0.37
12	5.2±0.2	15±1	0.27
12	3.3±0.2	12	0.22
16	7.8±0.2	12	0.36
Average	6.0±0.2	13±1	0.31±0.05

TABLE XXIX

Effect of Molecular Weight on Density and Epoxidation Results for TPI Lamellas[a]

$M_v \times 10^5$	$1-W_c$[c]	No. Epox.	$(F_e)_f$[d]	$\langle B \rangle_f$[e]	$\langle A \rangle_f$[f]
0.05	0.40	5	0.33±.01	7.0±.4	14±1
0.07	0.45	8	0.29	6.0	15±1
0.22	0.47	7	0.28±.01	4.0±.3	13±1
0.67	0.49	7	0.26±.01	4.8±.3	14±1
2.3	0.50	6	0.24	4.6±.1	15±1
3.5	0.50	11	0.26±.02	4.8±.5	13±1
5.8	0.49	4	0.27	4.7±.1	13±1
1.6[b]	0.50	12	0.29±.01	5.7±.3	14±1

a. Grown by seeded crystallization from 0.1%(w/v) hexane solution at T_c=20 C epoxidized in 2-ethoxyethanol at 0 C.

b. Unfractionated TPI

c. Noncrystalline fraction from density measurements

d. Fraction of TPI units epoxidized in suspension

e. Average number of TPI units in the epoxidized block

f. Average number of TPI units in the unepoxidized block

TABLE XXX

Effect of Crystallization Temperature(T_c) on Density and Epoxidation Results for TPI Lamellas[a]

Tc (C)	1-Wc[b]	No. Epox. Detms.	$(Fe)_f$[c]	$\langle B \rangle_f$[d]	$\langle A \rangle_f$[e]	Ls[f]
10	0.50	10	0.31±.05	6.0±1	13±1	5±0.7
20	0.50	6	0.24	4.6±.1	15±1	6±0.5
30	0.44	5	0.27±.01	5.6±.1	16	7±0.1

a. Grown by seeded crystallization from 0.1%(w/v) hexane solution using a TPI fraction with $M_v=2.4x10^5$ and epoxidized in 2-ethoxyethanol at 0 C.

b. Noncrystalline fraction from density measurements

c. Fraction available for epoxidation

d. Average number of monomer units per fold

e. Average number of monomer units in crystalline traverse

f. Average crystalline thickness along chain direction

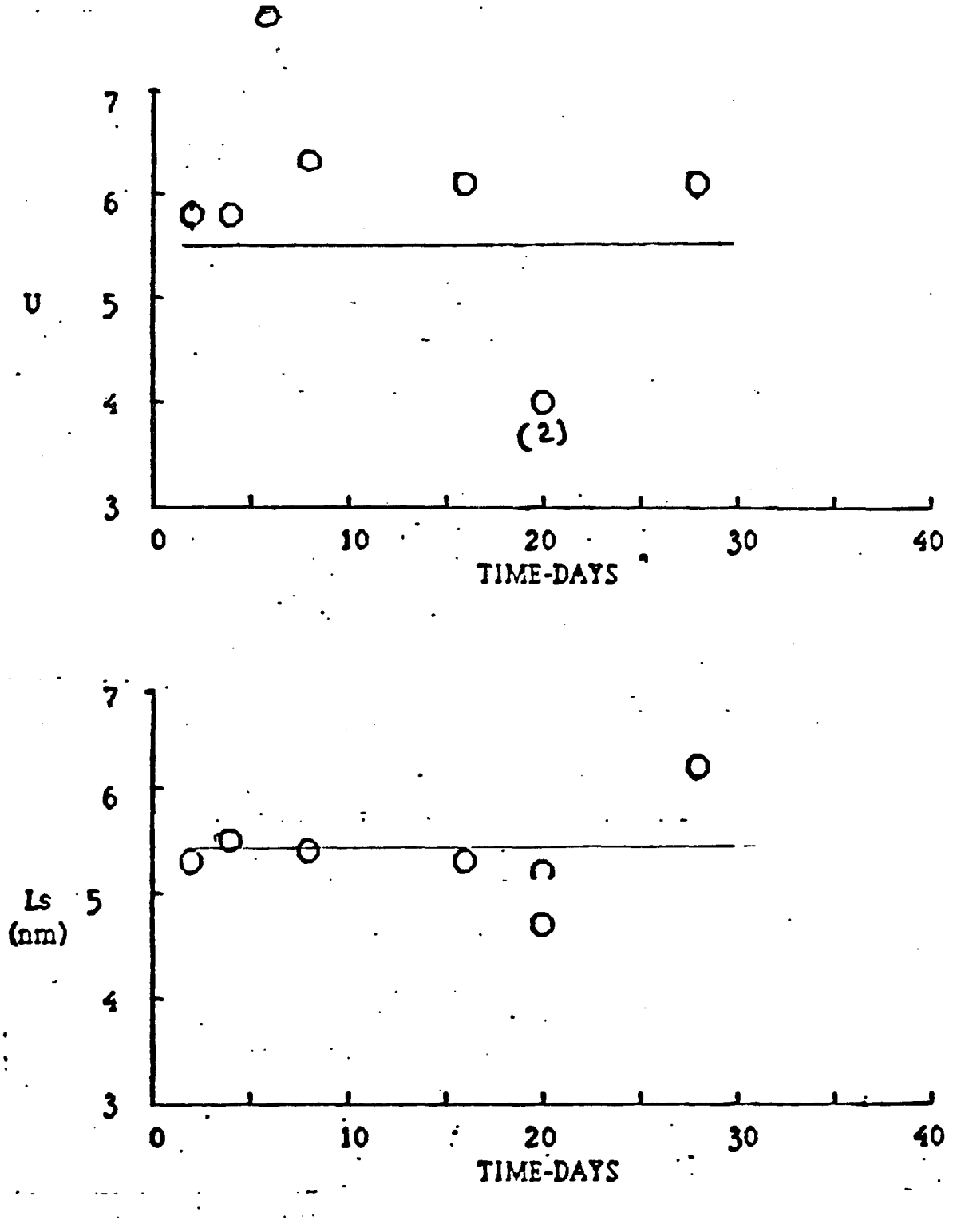

Fig.24. U and L_s vs. time for epoxidized, unfractionated TPI in 2-ethoxy ethanol at O C. M/D=2.4, 3.9. Grown from an amyl acetate solution at T_c=20 C.

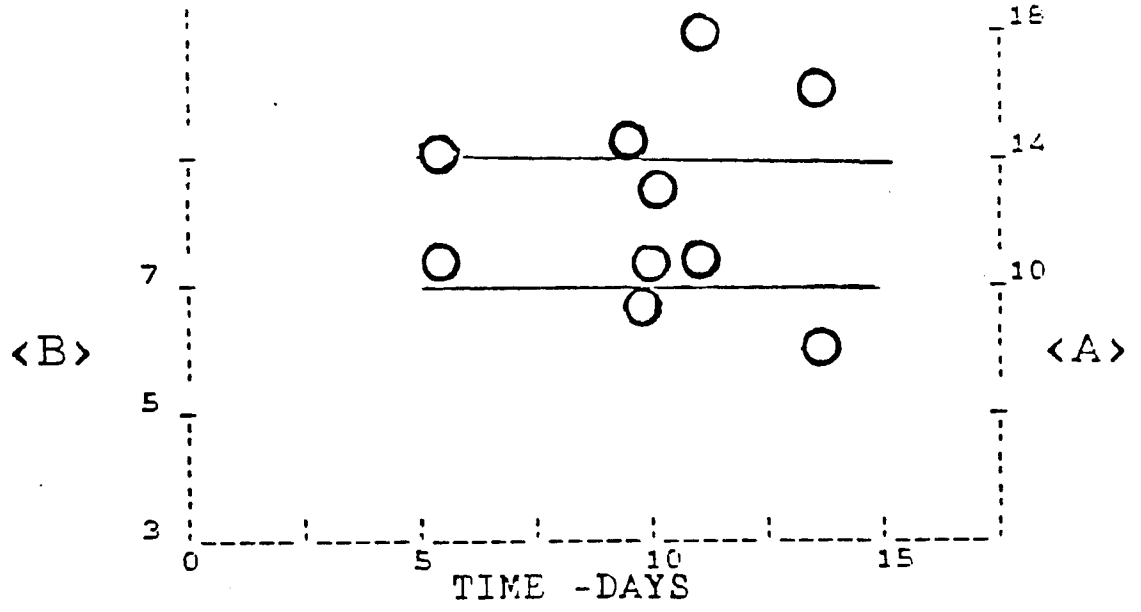

Fig. 25. Representative of ‹A› and ‹B› vs. time for TPI lamellas(T_c=20, M/D=1.6) in a cellosolve suspension at 0 C. Grown from a hexane solution. M_v=5000.

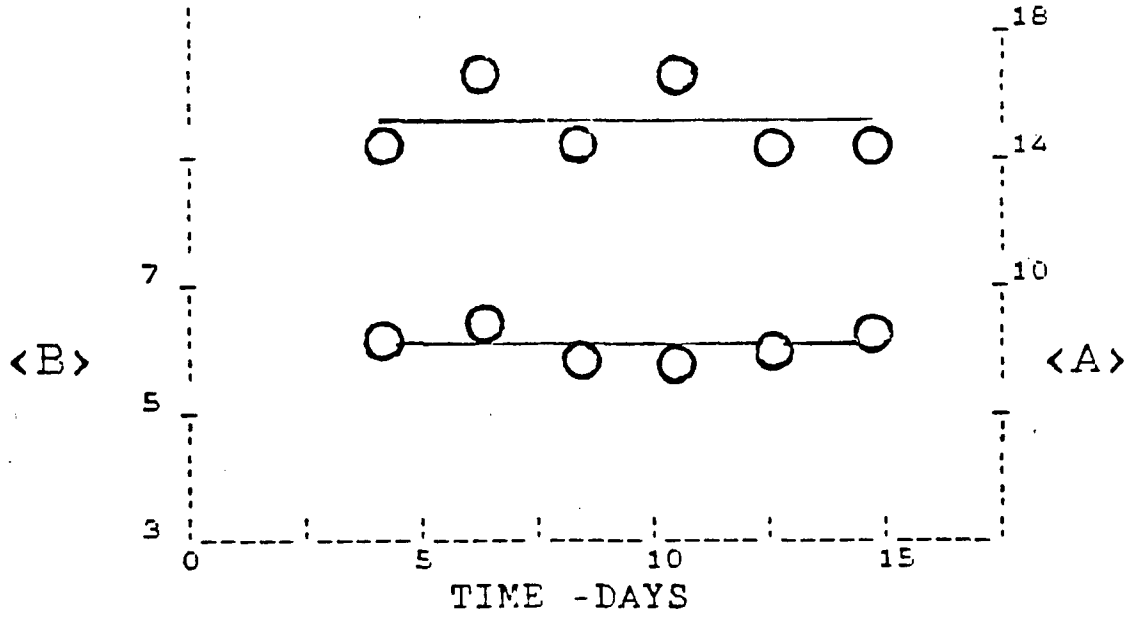

Fig. 26. ‹B› and ‹A› vs. epoxidation time in cellusolve suspension at 0 C.
Average block length, ‹A› (unreacted) and ‹B› reacted for TPI lamellas grown from dilute hexane solution at T_c=20 C and M_v=0.07x105

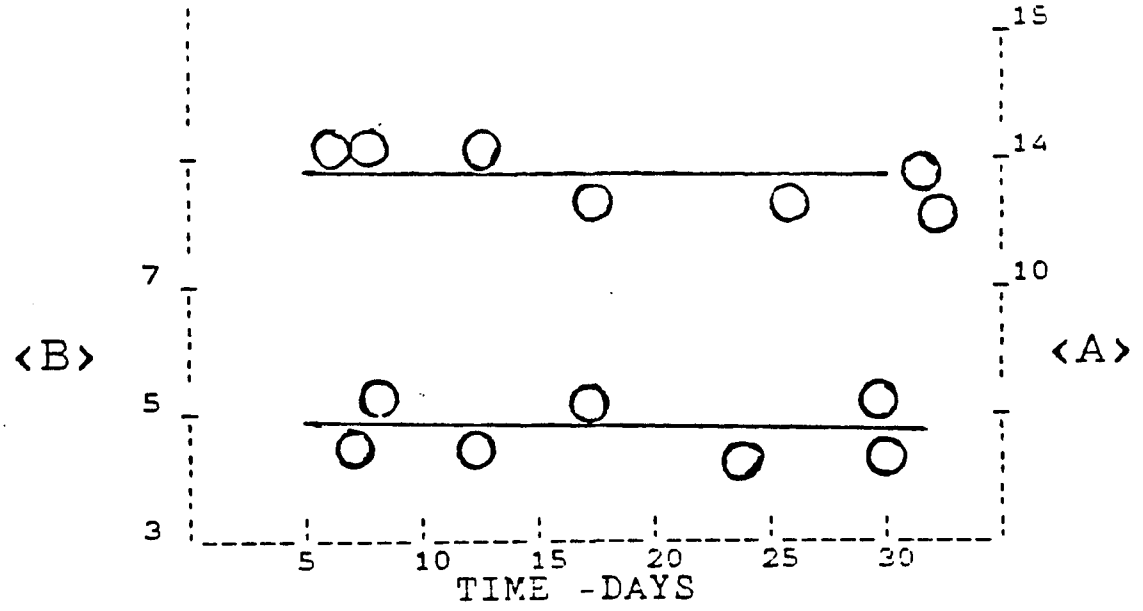

Fig.27. ⟨B⟩ and ⟨A⟩ vs. epoxidation time in cellusolve at 0 C. Average block length, ⟨A⟩ and ⟨B⟩ for TPI lamellas crystallized from dilute hexane solution at T_c=20 C and M_v=0.22x105

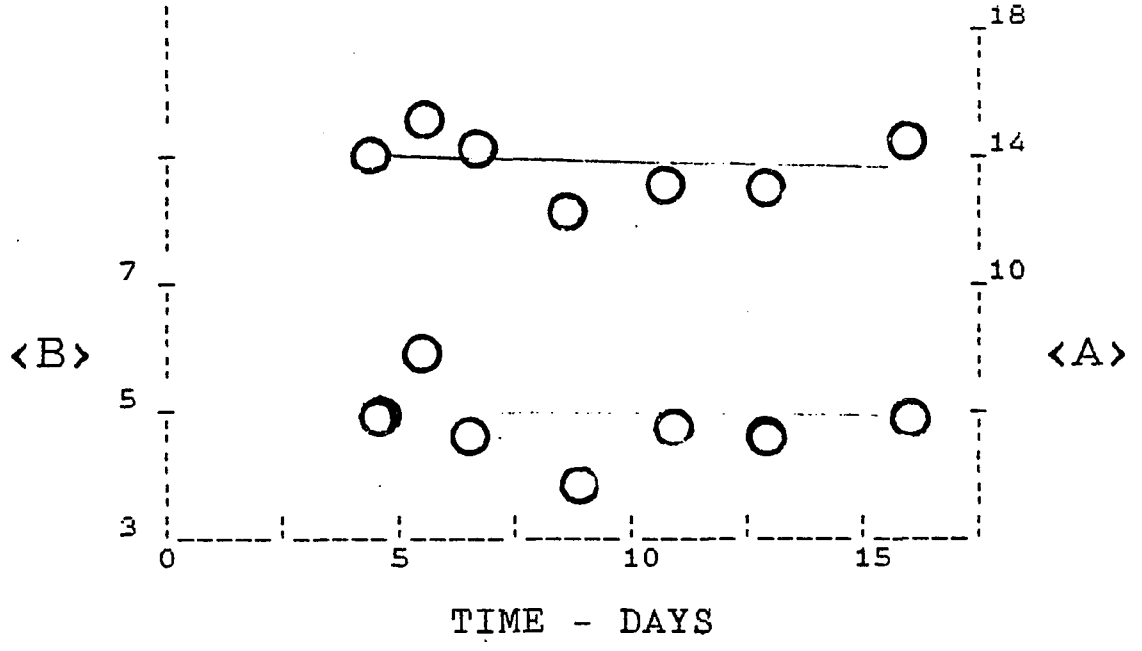

Fig.28. Representatives of ‹A› and ‹B› vs. time for TPI lamellas in a cellusolve suspension at 0 C. Grown in a hexane solution at T_c=20 C, M/D=1.6 and M_v=0.67x10^5

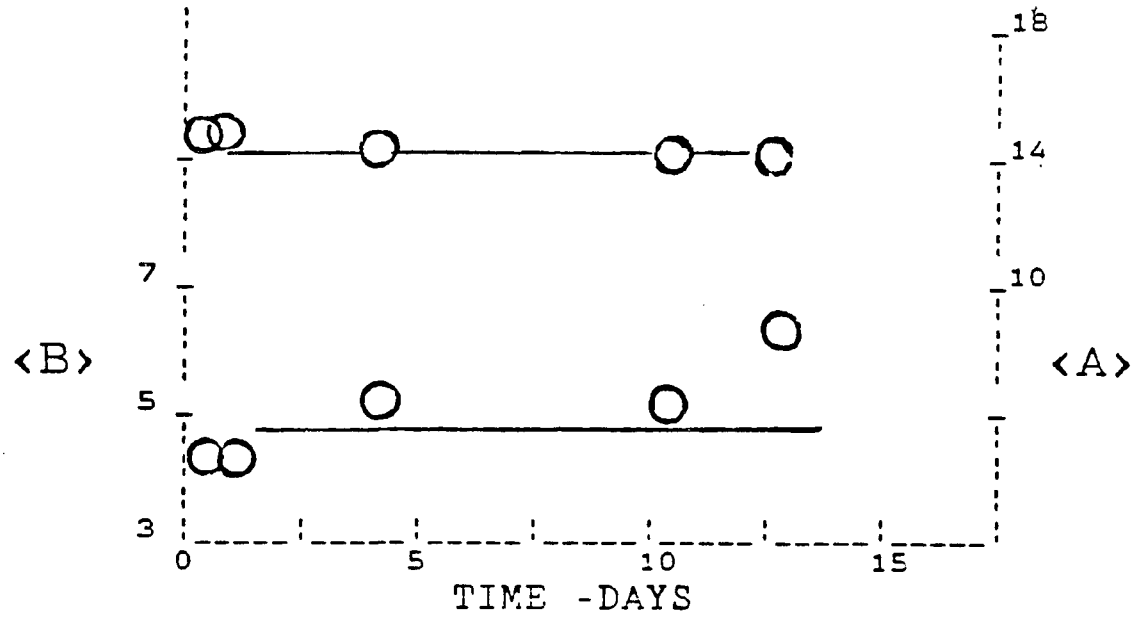

Fig. 29. ‹A› and ‹B› vs. epoxidation time. Average block length , ‹A› and ‹B› for TPI lamellas at T_c=10 C, M_v=2.3x105.Grown from dilute amyl acetate solution.

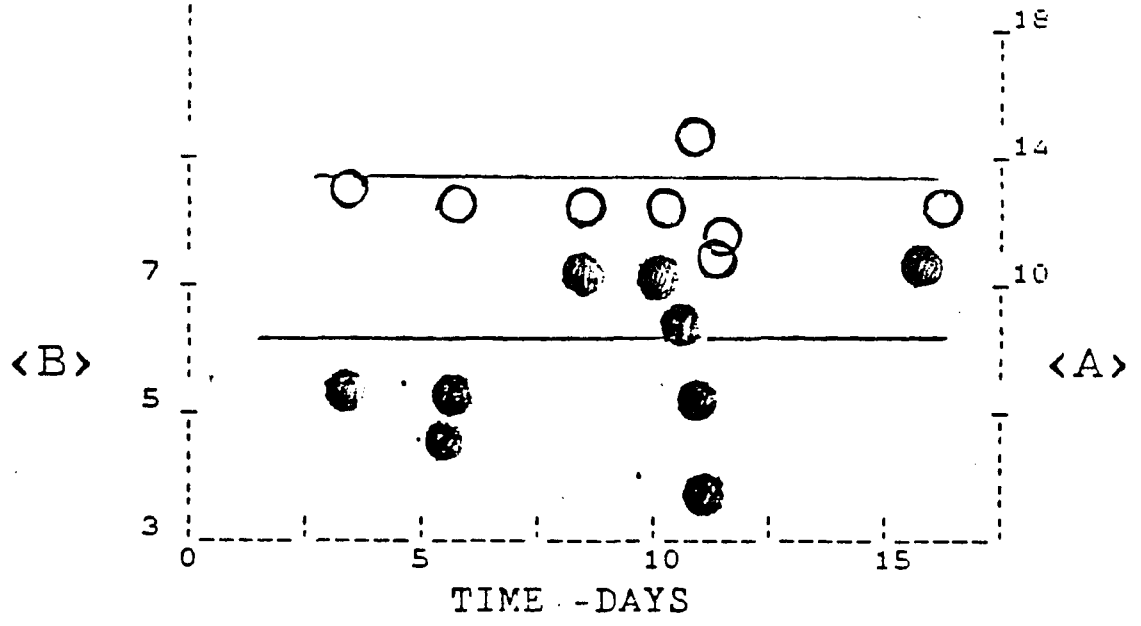

Fig. 30. ‹A› and ‹B› vs. epoxidation time. Average block length, ‹A› and ‹B› for TPI lamellas. T_c=10 C, M_v=2.3x10^5 Grown from dilute hexane solution.

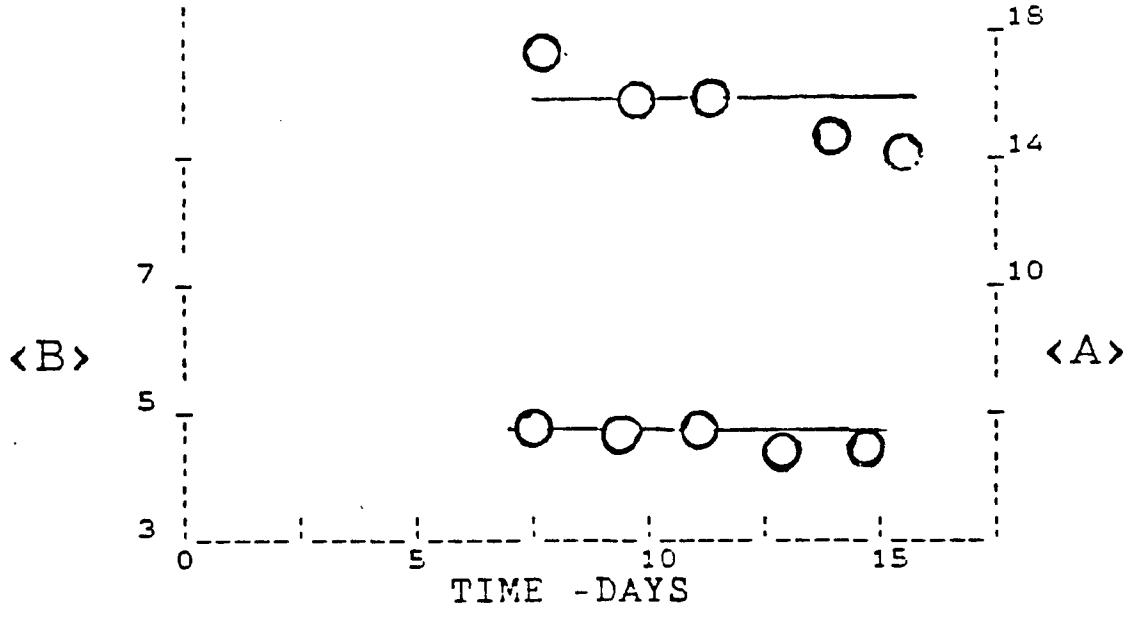

Fig.31. ‹A› and ‹B› vs. epoxidation time. Average block length, ‹A› and ‹B› for TPI lamellas. T_c 20 C, M_v=2.3x10^5 Grown from dilute hexane solution.

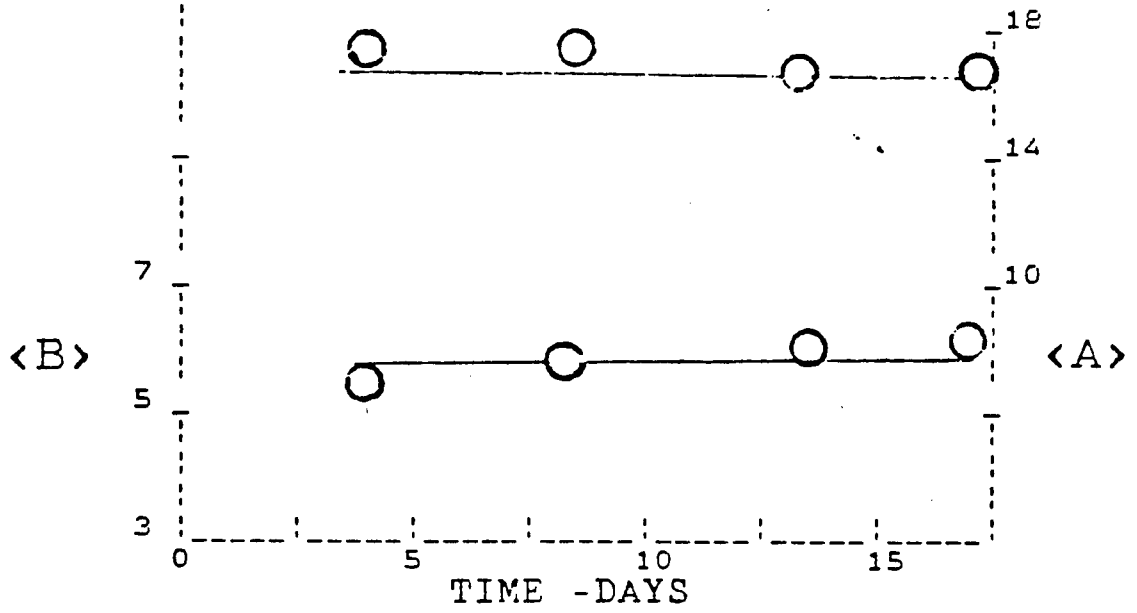

Fig. 32. ‹A› and ‹B› vs. epoxidation time. Average block length, ‹A› and ‹B› for TPI lamellas at T_c=30 C, M_v=2.3x10^5 Grown from dilute hexane solution.

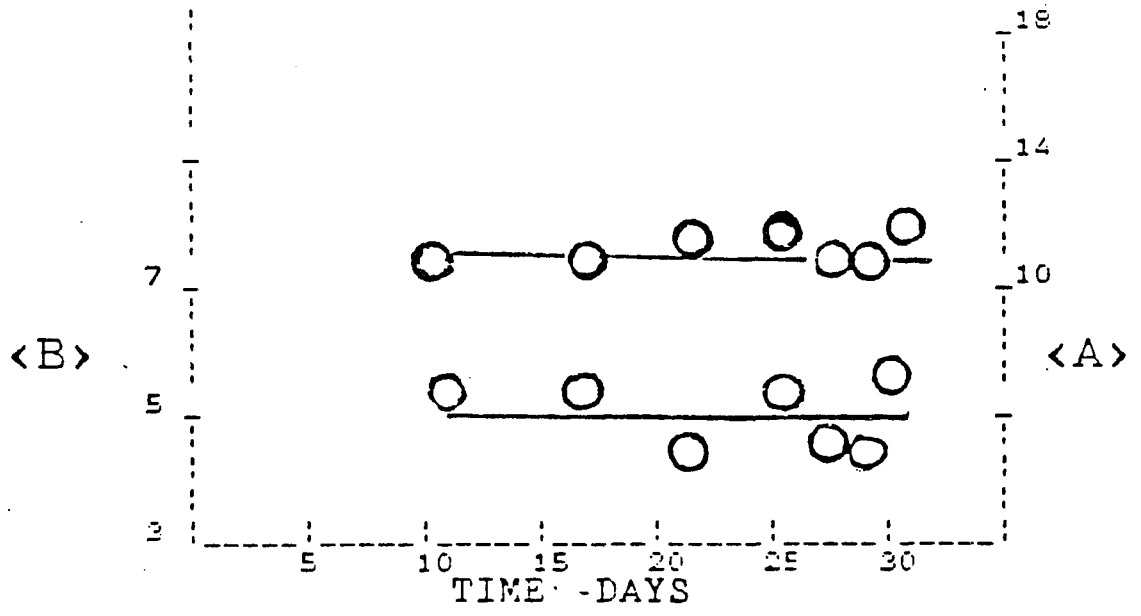

Fig. 33. ‹A› and ‹B› vs. epoxidation time in cellusolve at 0 C. Average block length, ‹A› and ‹B› for TPI lamellas grown from dilute hexane solution at T_c=10 C, M_v=2.9x10^5

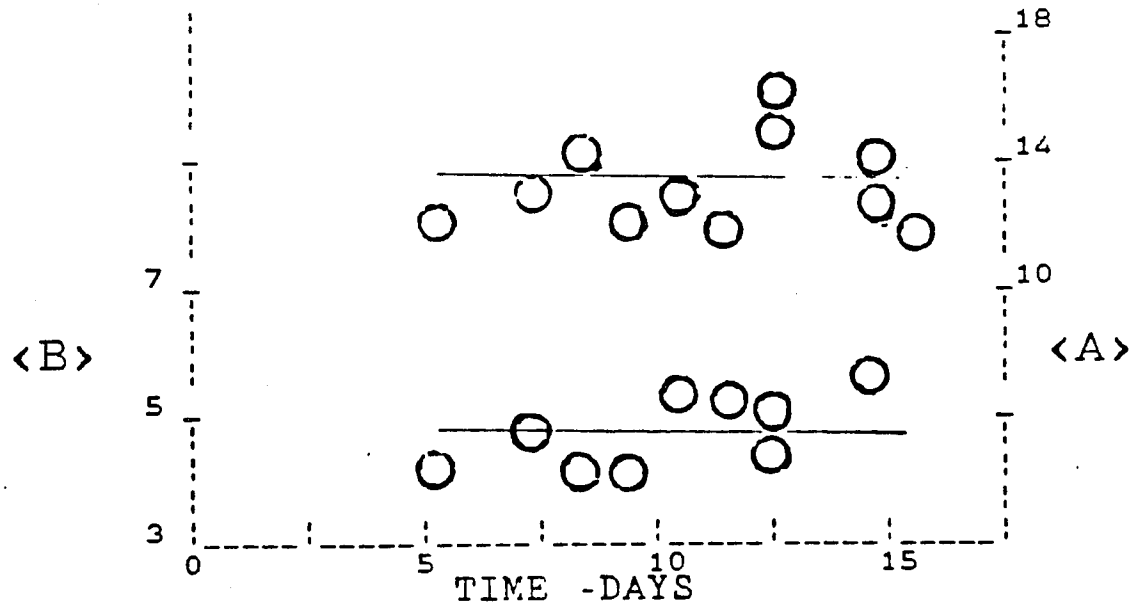

Fig.34. Epoxidized TPI lamellas in a cellusolve suspension at 0 C. Crystals grown from a hexane solution at T_c=20 C and M_v=3.5x105. ‹A› and ‹B› vs. time (days) at M/D=1.6.

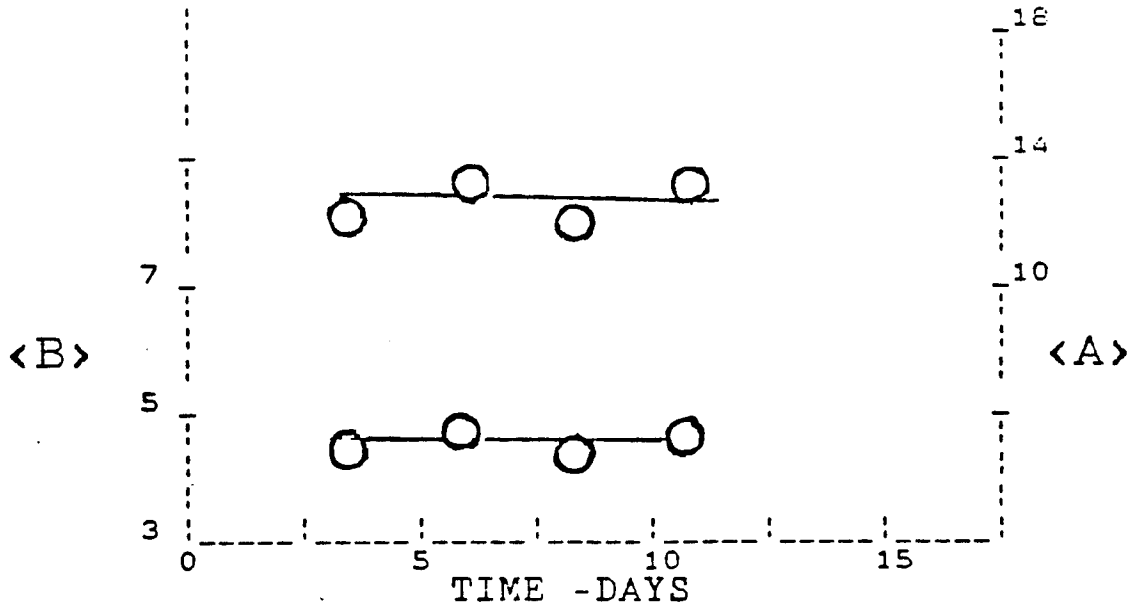

Fig. 35. ‹A› and ‹B› vs. epoxidation time. Average block length, ‹A› and ‹B› for TPI lamellas. T_c=20, M_v=5.8x10

IV. DISCUSSION

TPI crystals are assumed to be composed of chain folding lamellas with crystalline and amorphous noncrystalline components. The latter consists of, mainly, these chain folds which appear at the surfaces of the crystal. Thus, the surface epoxidation of the crystal results in regular block copolymers that may be schematically represented, as shown in Fig. 36.

Information about the distribution of molecular weights in a polymer is often the goal of a fractionation experiment. Such information requires the measurement of weight and molecular weight of each fraction. One requirement of successful fractionation is that the sum of the weight and the fractions should be equal to that of the original weight of the polymer (111). Some possible explanations for the loss of polymer during the fractionation could be - (1) poor coagulation of the lower molecular weight fractions;(2) adsorption of the polymer on the glass walls of the beaker; (3) cross linking of higher molecular weight fractions, which could not be used for further fractionation. The lower molecular weight fractions were recovered in this fractionation, hence the loss of polymer was caused mainly by (2) and (3).

When single lamellas are grown by the precooling method the initial dissolution temperature(T_d) is not important if the

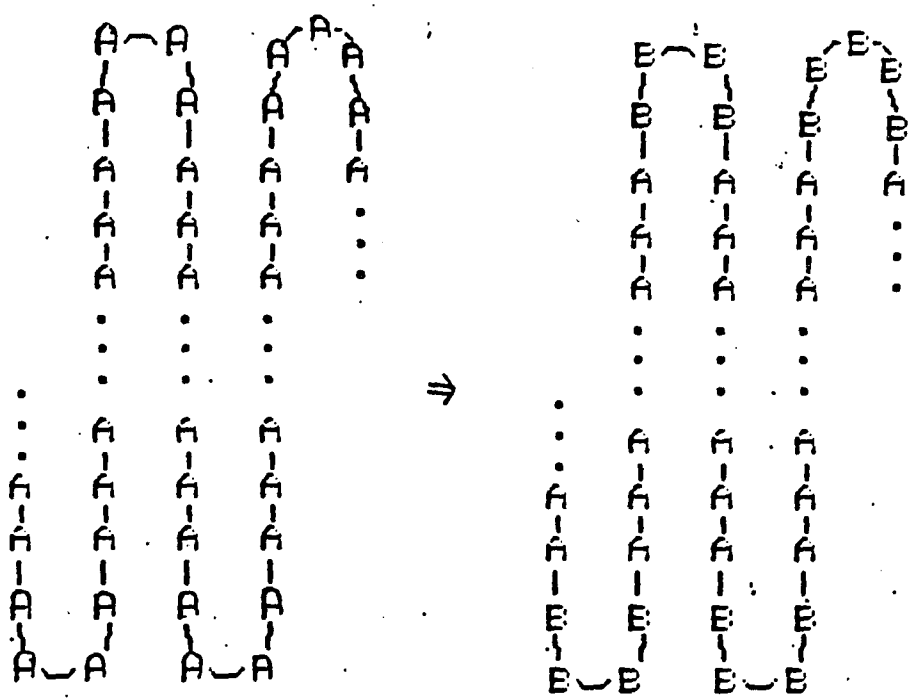

Fig. 36. Schematic representation of ‹A› and ‹B› in a folded crystal. ‹A›= Ave.# of A units/stem. ‹B›= Ave.# of B units/fold.

sample is dissolved completely. The unfractionated TPI was crystallized with T_d=50, 60 or 70 C and with T_c=20 C in 0.1%(w/v) hexane solution and the same type of lamellas were formed. The precipitation temperature T_p is also not important as far as the morphology is concerned. Whether the fraction was precipitated at T_p=-6 or 0 with constant crystallization temperature (T_c=10, 20), the single lamella formed had the same oval shape as it was seen under the electron microscope and the same endotherm from DSC measurements (58c). Previous studies by both Kuo (74) and Anandakumaran (84) show that the form begins to appear only at crystallization temperatures of 15 C and under. More specifically, high molecular weight TPI lamellas grown by a direct method at T_c=20-30 C showed only the form. The same lamellas grown at T_c=10 C showed the form. Low molecular weight crystals grown by the direct method at T_c=0 C were collected 15 minutes after crystallization commenced. Only the form was found. The same sample collected after one day of crystallization produced both and forms. In the present work it is obvious that the nuclei necessary to bring about crystallization have been transformed from the to form in the heating procedure, which is not reversible, hence leaving only nuclei. This transformation is probably induced by the lower stability of the form and a swelling effect at elevated temperatures.

Heating well above the redissolution temperature leads to the destruction of all the existing nuclei. The number of nuclei is also dependent on the rate of heating to T_r after an initial crystallization at T_p. Normally, the number of nuclei per gram of polymer increases with decreasing the heating rate and is mainly controlled by T_r, hence regulating the shape and size of the crystals (97). Generally, in this work, T_r was at the clearing temperature of the suspension or 1-2 degrees higher. A molecular weight effect on T_r was found in this work. The clearing temperature of aggregates initially crystallized at 0 C at a heating rate of 0.3 C/min increased from 34 C to 37 C when the molecular weight was increased from $M_v=1.6x10^5$ to $3.5x10^5$.

The lamellar thickness for various polymers such as polyethylene(6), TPBD(119) and 1,4 trans polyisoprene(120) decreases with decreasing T_c at high temperatures and then becomes invariant. A similar effect was observed in this study for TPI also. An increase in the lamellar crystalline length along the chain direction from 5.7 to 6.5 to 7 nm with increase in the crystallization temperature from 10 to 20 to 30 C respectively was observed. When the crystallization temperature decreases and therefore the supercooling increases, the lamellas also become more susceptible to defects, penetration, reaction and destruction. Another variable is the crystallization time.

The increase in the DSC endotherm temperature with increasing T_c, reported by Woodward et al (87), is characteristic of lamellar crystals. This is due to an increase in the lamellar thickness with an increase in the crystallization temperature. A similar effect has been reported (95, 99) for melt crystallized TPI. The DSC endotherms did not show any observable changes with M_n. A small decrease in density was found on changing the M_n from 0.26×10^5 to 2.9×10^5. An increase in crystallinity with decreasing M_n down to about M_n of 10^4 was reported for polyethylene (75-76) and for various polyalkene oxides (77-80) crystallized from the melt. However at M_n below 10^4 a decrease in crystallinity occurs for a number of these polymers, including polyethylene(PE), (76) polyethylene oxide(PEO), (78) and polyhexanemethyleneoxyde (PHO), (79). For melt crystallized PE(79), PHO(79) and POM(80) a dramatic decrease in the basal surface free energy with decreasing molecular weight has been shown. The density variation observed in bulk crystallized polyethylene is explained (113) in terms of the presence of tie molecules or reduced mobility in high molecular weight fractions. In this study an increase in density of dried mats of TPI crystals is observed (Table XXX) with an increase in the crystallization temperature. This is due to an increase in the crystalline /amorphous ratio as T_c increases. A large discrepancy exists,

however, between F_e, as obtained for crystals in suspension from C-13 NMR analysis, and the noncrystalline fraction, $(1-W_c)$, as obtained by density measurements on dried mats (tables 29-30). A density variation and a decrease in crystallinity with decreasing M_n in the 5,000-30,000 range was reported (44, 57) for solution crystallized TPDB lamellas epoxidized in suspension. The reacted fraction is usually smaller than $(1-W_c)$. Possible explanations for this discrepancy are the following:

(1) An introduction of disorder upon drying the lamellas. Density measurements may show a higher ratio of the noncrystalline component due to lamellar collapse and rearrangement upon drying. (2) The failure of the two component model in obtaining the crystallinity from density measurements . The total noncrystalline fraction calculated from density measurements assumes that the crystals contain a component with a density the same as that of the unit cell obtained by x-ray diffraction and a component that is completely amorphous as found in the melt but corrected to room temperature. (The difference between mat and suspension crystals is not resolved at present and it is seemingly dependent on the technique of measurement or may have to do with the detailed surface structure) and (3) Incomplete reaction of the noncrystalline component due to a significant fraction of noncrystalline material not

available for chemical reaction. Evidence for (1) and (2) (114) has been shown for polyethylene lamellas. Experimental results(115) and calculations using space filling models for polyethylene (116) suggest that ρ_a, as extrapolated from the melt, is larger than the fold surface density. However, solid state C-13 NMR results for TPBT lamellas (65) agree with those from density measurements. These results(65) also suggest that complete reaction does occur in the noncrystalline component. Therefore ruling out possibilities(2) and (3), the only viable explanation is possibility (1), where lamellar collapse occurs during the drying process, increasing the noncrystalline component present during density measurements. Evidence for molecular collapse has been found in this work. F_e that was obtained from surface epoxidized low molecular weight TPI lamellas, using C-13 NMR, show a better agreement with $(1-W_c)$ values than similar experiments on higher molecular weight samples. Due to changes in both (F_e) and $(1-W_c)$ for α-TPI, the discrepancy between them decreases as the molecular weight is decreased below 67,000.(table XXIX). As the molecular weight is decreased the number of chain ends increases and any fold crowding that would occur in TPI lamellas should be diminished if these chain ends are noncrystallizing. A decrease in fold crowding would be expected to reduce the amount of disorder introduced in TPI

lamellas on drying, to increase the penetration of the surface or to do both. However, the increase in $(F_e)_f$ is accompanied by an increase in $\langle B \rangle_f$ with $\langle A \rangle_f$ remaining constant suggesting that further penetration is not the process occurring. In earlier work (53, 74) a decrease in $(1-W_c)$ with decreasing molecular weight at small values of M for amyl acetate grown lamellar structure was found. The results are similar to those reported in this work for hexane grown lamellas; however, this change was attributed (74) to the presence of very short cilia, using an analysis similar to that discussed below. The value for $\langle A \rangle_f$ is equal to the average number of monomer units in a chain traverse through the crystal core, if the epoxidation reaction is confined to the surface regions. Measurements of lamellar thickness for dilute solution grown lamellas of polyethylene using low angle x-ray measurements and electron microscopy show that this parameter stays constant with decreasing molecular weight when the crystallization temperature and the solvent are kept constant and increases with increasing T_c(6). Kern et al (117) found on solution crystallization that there is a broad range of molecular weights where the effects on thickening are negligible. Arlie et al(118) found that seven fractions of molecular weight between 1,000 and 3,500 always crystallized from the melt fully extended. At higher

molecular weights up to 25,000 folded crystals resulted but the number of folds depended critically on the crystallization temperature. Therefore the constancy of $\langle A \rangle_f$ for α-TPI vs. molecular weight and the change with T_c is in agreement with that work. $\langle B \rangle_f$ appears to remain constant at 5 with an increase in crystallization temperature, although considerable fluctuation occurs. The results are in agreement with those found for hydrochlorinated TPI lamellas carreid out by Woodward and Tischler(106). The value of $\langle B \rangle_f$ is related to the average number of monomer units per fold and the average number per crystallizing chain end combined. The effect of chain ends should diminish with increasing molecular weight and, as observed, $\langle B \rangle_f$ should become constant and equal to the average number of monomer units per fold assuming full penetration of the fold surface, and a small lateral surface contribution. The lateral surface area has been previously estimated (53) to be approximately 2% or less, depending on the preparation, and can, therefore, be neglected. From moleculer models, a tight 110 adjacent reentrant folds can be made with three TPI repeat units. Therefore, the experimental value suggests adjacent reentry with some fold looseness or a mixture of tight adjacent reentrant folds with some nonadjacent reentrant ones(53). A quantitative relationship between the surface fraction, F_s,

the number of monomer units per fold, U, the number average degree of polymerization, N_n, the average number of monomer units in two chain ends, C, and $\langle A \rangle_f$ is (44, 74)

$$1-F_s=\langle A \rangle_f\{1+(U-C)/N_n\}/\{U+\langle A \rangle_f\} \qquad \text{Eq.7}$$

Calculation of C from eq. 7 with the data in table 29 was carried out for the α-TPI lamellas prepared at 20 C with M_v of 7,000 and 5,000; values used in the calculations were: $\langle A \rangle_f=14$, an average of values found over the complete molecular weight range, U=4.7, an average of the $\langle B \rangle_f$ values for the fractions with M_v of 22,000 or greater, $N_n=N_v/1.2$ and $F_s=F_eC$ is found to be 8 and 10 for M_v of 7,000 and 5,000, respectively. If F_s is set equal to $1-W_c$, the calculated value of C would be smaller than U due to the decrease in $1-W_c$ with decreasing molecular weight; in fact, previously, using density results a C of zero was obtained(74). This is not believed to be correct, as discussed above. An equation relating $\langle B \rangle_f$ at any molecular weight to U and C can be obtained by extension of a treatment given by Schilling, Bovey and Woodward(57). In here C is believed to be a linear function of L, and is represented as C=aL/R. The total number of isoprene units per number average chain at the lamellar surface is given by $\langle B \rangle_f(F_n+1)$ where F_n is the number of folds per chain. In terms of U and C

$$\langle B \rangle_f(F_n+1)=UF_n+C-2 \qquad \text{Eq. 8}$$

since the carbon atoms in two units, one in each chain end, will not contribute to the some resonances as the carbon in the rest of the noncrystallizing reacted chain end due to a different chemical shift. The total number of isoprene units per number average chain is (44):

$$N_n=\langle A\rangle_f(F_n+1)+UF_n+C \qquad \text{Eq. 9}$$

Combining eqs. 8 and 9 to eliminate F_n gives

$$C=\{N_n\langle B\rangle_f+2\langle A\rangle_f+U(\langle A\rangle_f+\langle B\rangle_f+2-N_n)\}/\{\langle A\rangle_f+\langle B\rangle_f\} \qquad \text{Eq. 10}$$

Using the some $\langle A\rangle_f$ and U values as in the calculations above gives C of 12 and 14 for M_v of 7,000 and 5,000, respectively. An average value of C found from this work is therefore 11+2. In using eqs. 7 and 10 to calculate C it was assumed that the contribution of the lateral surfaces to F_e and $\langle B\rangle_f$ is negligible and that all of the chain ends are noncrystallizing. The value for C agrees with that for $\langle A\rangle_f$ within experimental error ane therefore the average length of noncrystallizing chain ends is about one half of the crystallite thickness.

The kinetics of the epoxidation of peracids with TPI has been shown to be first order with respect to the peracid and also first order with respect to the double bond concentrations(94). It was found in the present study also, that the rate of the reaction of TPI single crystals at the surface depend on both the number of double bonds available for reaction and peracid. It is evident that the peracid

will react first with the accessible double bonds at the folds and then will react with the less accessible inner bonds. This result is consistent with data given by Schilling, Bovey and Woodward(54, 57) on epoxidation with peracid. While suspended in the solvent the lamellas are separated from each other except in the vicinity of the screw dislocation(121). There is little cohesion between the faces of adjacent lamellas.

It was found in a study by J.Xu that when β-TPI lamellar structures in suspension are epoxidized the amount of reaction taking place depends on the liquid medium used. Since the larger F_e values found exceed the noncrystalline fraction calculated from density measurements, it appears that penetration of the crystalline core of the lamellas occurs. As F_e increases, ‹B› increases and ‹A› fluctuates which suggests that the penetration occurring takes place principally from the lateral surfaces but not from the fold surfaces. The double bonds on the chains at the lateral surfaces are expected to react immediately. If the attractive forces between the epoxidized chains and the liquid medium exceed those between epoxidized TPI and TPI units and if the folding is reentrant along an exposed fold plane, the reacted lateral chains could separate from the rest of the crystal and allow reaction of the next row of chains formerly inside the core. This would give a mixture

of block copolymer and completely epoxidized TPI. As the amount of completely reacted chains increase, ‹B› would increase but ‹A› would not change. The decrease in dissolution temperature for a 65/35 TPI-epoxidized TPI block copolymer with the increase in F_e for various liquids (see tables IX and X) supports this mechanism. Some of the results from a study of the chlorination of polyethylene lamellas were explained in terms of penetration from the lateral surfaces (112). In another investigation the amount of reaction taking place during hydrochlorination of TPI lamellas and lamellar structures is also found to depend on the reaction medium used (106). That study was carried out on α -TPI lamellar structures prepared at various temperatures; the hydrochlorination was done in two different liquids as a function of time. The differences in ‹A› and ‹B› with time for the reaction products from the two liquids are explainable in terms of penetration. The electron microscopy studies carried out earlier on α -TPI lamellas. TPI lamellas epoxidized in amyl acetate showed considerable erosion at the sides as well as holes through the interior parts after reaction even to short times for the higher molecular weight fractions(53). In the present work very little if any discernible change in the appearance of the lamellas was found after reaction in 2-ethoxyethanol. Also, the F_e values reported in the earlier epoxidation

study were 0.33 and 0.43 for molecular weights of $2.6x10^4$ and $6.9x10^4$ and a 20 C crystallization temperature in amyl acetate. Comparison with values of F_e from the present work obtained at the some crystallization conditions for α -TPI lamellas show that when amyl acetate is used F_e is larger than when 2-ethoxy ethanol is employed; the difference decreases with decreasing molecular weight suggesting that penetration of reacted lamellas by amyl acetate decreases with molecular weight, as found earlier from electron microscopy studies. 2-ethoxy ethanol is a nonsolvent for both TPI and epoxidized TPI.The ‹A› and ‹B› values obtained remain constant after an initial period for crystals grown at 20 C and 30 C. This indicates that penetration of the epoxidizing agent into the crystal core does not occur or that completely reacted chains are washed away. The crystalline stem length along the chain direction, L_s, can be calculated from the average number of unreacted monomer units ‹A›, by multiplying ‹A› by the chain repeat distance, R(96). The average number of reacted monomer units, ‹B›, is equated to the average number of monomer units in the chain fold, U. This assumes that not only is the reaction in the crystal core negligible, but also lateral surfaces are small compared to the folds.

The observation of chain folding of linear macromolecules on crystallization immediately raised a number of questions

fundamental to the understanding of crystalline polymers. Three types of folds have been proposed for polymer single crystals: (I) Irregular adjacent re-entry (loose folds). (II) Regular adjacent re-entry (tight folds). (III) Switch board or non adjacent re-entry folds. In deciding on the appropriateness of a model it is instructive to calculate the average number of monomer units per fold from the fold regions amorphous content, as done for TPI copolymers in the last section (page 81), When a copolymer is prepared it consists of blocks of unreacted polymer units alternating with blocks of reacted units. The number of repeat units in the unreacted blocks will depend on the crystal thickness along the chain direction, as determined by the crystallization temperature and solvent. The average size of the reacted blocks is dictated by the average number of monomer units per fold. The average size will be smallest and the width of the size distribution sharpest for the reacted blocks if only adjacent reentry, using the minimum number of chain units occurs. If fold looseness is present due to noncrystallizing chain ends then a distribution of fold lengths, ranging from tight to loose, is expected and a big value of F_e, the extent of epoxidation, will be obtained. The largest values for the average fold length and the broadest size distributions are expected if a significant amount of nonadjacent reentry

takes place. For TPI the number of monomer units per fold, B, increases with T_c and is higher at low molecular weights (M_v=0.05x10^5 and 0.07x10^5). U values for surface epoxidized TPBD lamellas with a M_n of 1.7x10^4 and 4.4x10^4 have been found by Schilling, Bovey and Woodward using C-13 NMR to be 2.4, 3.0 and 4.9. Therefore at comparable molecular weights, the number of monomer units per fold for TPI lamellas is about 0-2 fold larger than that for TPDB lamellas. U values for TPBD fractions were reported (44) to increase with the crystallization temperature, the same effect in the same direction as for TPI.

When models of the fold surfaces for α-TPI have been constructed by Mukherji and Woodward (123) using the crystal structures given by Takahashi et al (96) and by Fisher(105) a tight adjacent reentrant fold is found to contain 3 or 4 monomer units, respectively, assuming 110 folding(122). These values are not much smaller than the values obtained in this work at medium or high molecular weights (4.7+0.1). This is evidence for a predominance of adjacent reentry folding. When calculations for these molecular weights were made it was assumed that contribution of the lateral surfaces to F_e and $\langle B \rangle_f$ is negligible and does not exceed more than 2% and all of the chain ends are noncrystallizing. The average value of C found is 12 and 14 respectively which agree with that for

$\langle A \rangle_f$ within experimental error and therefore the average length of a noncrystallizing chain end is about one half of the crystallite thickness.

CONCLUSIONS

The results of this study lead to the following conclusions:

(I) Segmented block copolymers containing unreacted TPI sections and epoxidized TPI sections can be prepared using 2-ethoxyethanol as the reaction medium. The unreacted block length can be increased by increasing T_c.

(II) Differences in values for the noncrystalline fraction in α-TPI lamellas, as found by density measurements and by chemical reaction, are believed to be due to changes taking place on drying; these changes become less apparent at molecular weights below a value in the 7,000-20,000 range as a consequence of the increasing number of chain ends.

(III) In α-TPI lamellas grown from hexane at 20 C, the average number of monomer units per fold is 4.7+0.1, suggesting nonadjacent reentry folding to be small in amount; the average number of monomer units in the two crystallizing chain ends is 11+2.

(IV) The fraction of amorphous material on the surface of TPI available for epoxidation and the number of monomer units per fold, U, increase with increasing T_c.

Appendix I

Molecular structures of TPI: (A) -structure from Bunn.
(B) -structure from Bunn.
(C) -structure from Takahashi et al.
The unit cell due to Fisher has a=5.9A , b=7.9A , c=9.2A , $\alpha=\beta=90$, $\gamma=94$. This cell corresponds to the -structure proposed by Bunn (71).
The unit cell proposed by Takahashi et al has(73) a=7.98A , b=6.29A , c=8.87A , $\alpha=\gamma=90$, $\beta=102.0$

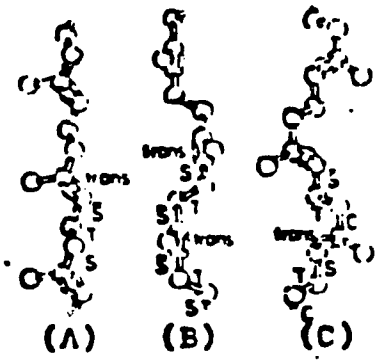

Appendix .2

Olefinic carbon region of the 50.3-MHz ^{13}C spectra of (a) 25% and (b) 90% solution-epoxidized and (c) crystal-epoxidized 1,4-*trans*-polyisoprene. Observed in $CDCl_3$ at 40 °C.

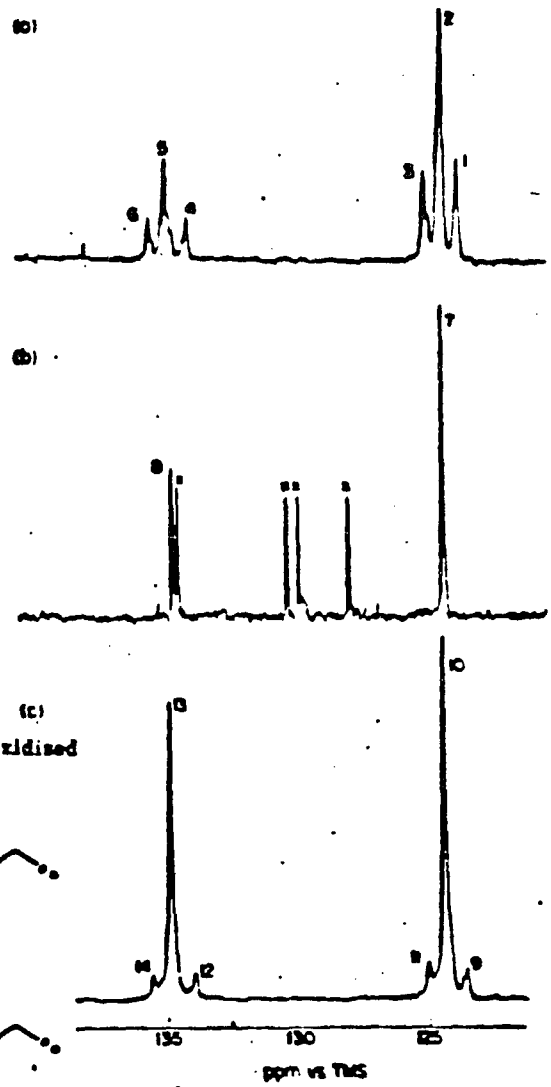

^{13}C Chemical Shifts of Olefinic Carbons in Epoxidized 1,4-*trans*-Polyisoprene (See Figure 4)*

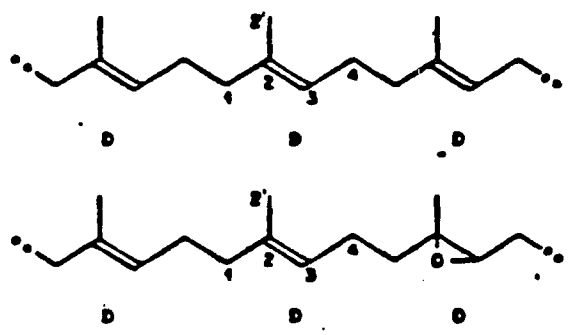

peak desig	assignment	chem shift: 25% solution-epoxidized TPI	chem shift: 90% solution-epoxidized TPI	chem shift: crystal-epoxidized TPI
1, 9	DDO-C3	123.75		123.53
2, 10	DDD-C3	124.43		124.33
3, 11	ODD-C3	125.01		125.00
4, 12	ODD-C2	134.09		133.93
5, 13	DDD-C2	134.95		134.87
6, 14	DDO-C2	135.55		135.58
7	ODO-C3		124.29	
8	ODO-C2		134.72	

*Structural formulas of two representative sequences are shown.

The peaks labeled "a" result from an apparent side reaction in TPI epoxidized to 90% at 20 °C. It is probable that the MCBA is reacting with oxirane to form an ester linkage and a secondary alcohol.

Appendix 3.

Figure 5. Oxirane carbon region of the 50.3-MHz ^{13}C spectra of (a) 25% and (b) 90% solution-epoxidized and (c) crystal-epoxidized 1,4-*trans*-polyisoprene. Observed at $CDCl_3$ at 40 °C. ("a" indicates residual amyl acetate.)

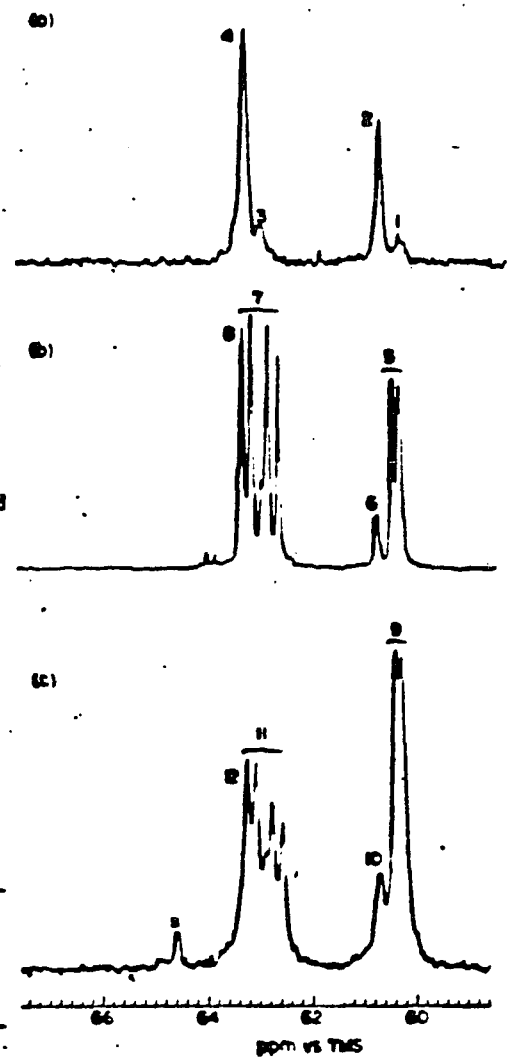

^{13}C Chemical Shifts of Oxirane Ring Carbons in Epoxidized 1,4-*trans*-Polyisoprene[a]

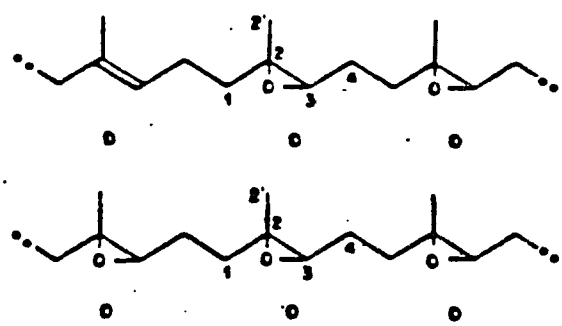

peak desig	assignment	chem shift: 25% solution-epoxidized TPI	chem shift: 90% solution-epoxidized TPI	chem shift: crystal-epoxidized TPI
1, 5, 9	OOD-C2 (m,r)	60.22	60.32	60.21
		60.31	60.44	60.33
2	DOD-C2	60.69		
2, 6, 10	DOO-C2	60.69	60.70	60.66
			60.76	
3, 7, 11	DOO-C3	62.94	62.63–63.31	62.53–63.20
		62.99		
4	DOD-C3	63.09		
4, 8, 12	OOD-C3	63.09	63.31	63.20
5, 9	DOO-C2 (m,r)		60.32	60.21
			60.44	60.33
7, 11	OOO-C3 (mm, mr,rm,rr)		62.63	62.53
			62.82	62.74
			63.14	63.05
			63.31	63.20

[a]Structural formulas of two representative sequences are shown.

Appendix 4.

Alkyl carbon region of the 50.3-MHz ^{13}C spectra of (a) 25% and (b) 90% solution-epoxidized and (c) crystal-epoxidized 1,4-*trans*-polyisoprene. Observed in $CDCl_3$ at 40 °C. ("x" indicates residual amyl acetate.)

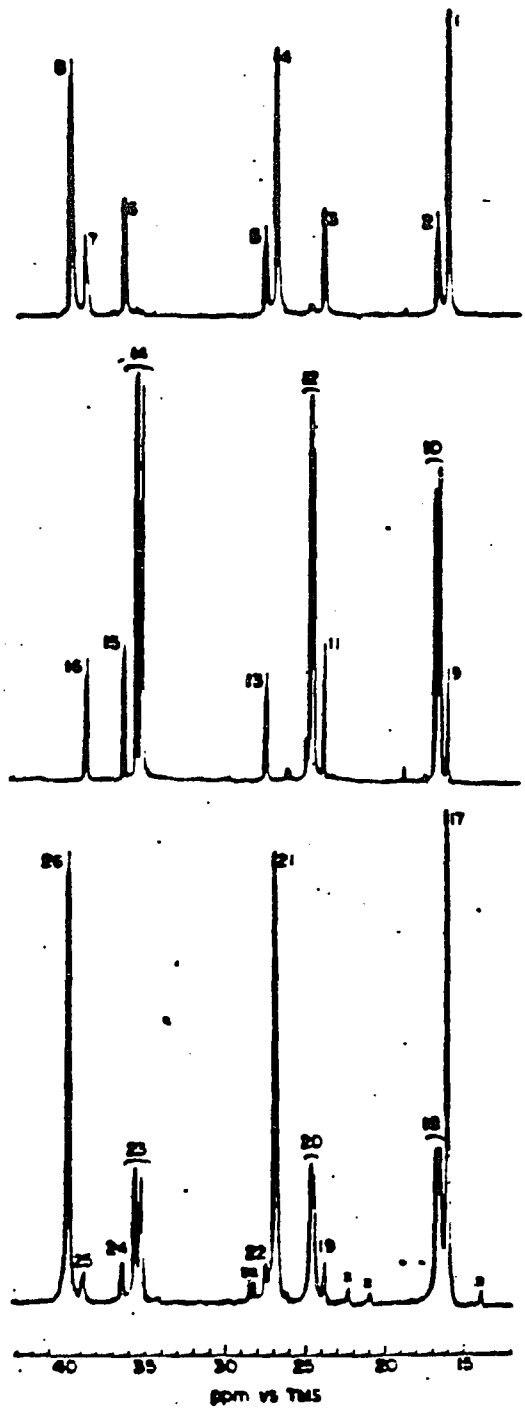

^{13}C Chemical Shifts of Alkyl Carbons in Epoxidized 1,4-*trans*-Polyisoprene[a]

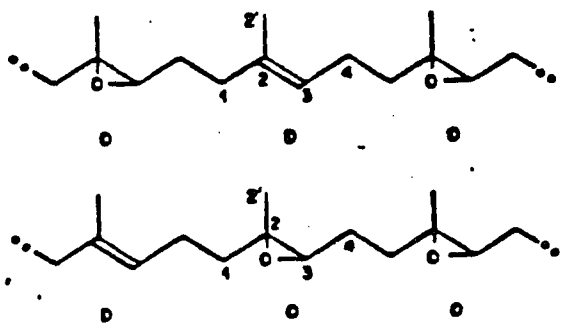

peak desig	assignment	chem shift: 25% solution-epoxidized TPI	90% solution-epoxidized TPI	crystal-epoxidized TPI
1, 17	DDD-C2'	16.10		16.03
	ODD-C2'			
	DDO-C2'			
2	DOD-C2'	16.72		
3, 19	DDO-C4	23.86		23.76
4, 21	DDD-C4	26.88		26.77
	ODD-C4			
5	DOD-C4	27.57		
6, 24	ODD-C1	36.46		36.33
7	DOD-C1	38.98		
8, 26	DDD-C1	39.85		39.75
	DDO-C1			
9	ODO-C2'		16.06	
10, 18	OOD-C2'		16.56	16.47
	DOO-C2'		16.78	16.69
	OOO-C2' (m,r)			
11	ODO-C4		23.80	
12, 20	DOO-C4		24.49	24.42
	OOO-C4 (m,r)		24.66	24.57
13, 22	OOD-C4		27.44	27.48
14, 23	OOD-C1		35.24	35.17
	OOO-C1 (m,r)		35.61	35.54
15	ODO-C1		36.40	
16, 25	DOO-C1		38.74	38.78

[a] Structural formulas of two representative sequences are shown.

REFERENCES

1. Keller, A. Phill.Mag.1957, 8, 1171-1175.
2. Till, P.H. J.Polym.Sci.1957,24, 301.
3. Fischer, E.W. Z.Naturforsch, 1957, 12a, 753.
4. Jaccordine, R., Nature, 176, 305, 1955.
5. Geil, P.H.Polymer Single Crystals, Wiley, N.Y., 1963.
6. Wunderlich, B. Macromol.Phy., Vol.1, Academic press, 1963.
7. Bunn, C.W. Trans.Farad.Soc. 1939, 35, 482.
8. Voebel, R.; Sillescu, H. Macromol. 1979, 12, 162.
9. Ingram, P. and Peterlin, A. Morphology, pp.204-274 in H.F.Mark, N.G.Gaylord and N.M.Bikales Eds. Encyclopedia of Polymer Science and Technology, Vol. 9, Wiley-Interscience, N.Y., 1968.
10. Smets, G.; Hart, R. Adv.Polym.Sci. 1960, 2, 173.
11. Keith, H.D. J.Polym.Sci.1964, A2, 4339.
12. Geil, P.H. Growth and perfection of crystals, pp.579-582.
13. Kuo, C.C. Doctoral Dissertation, C.U.N.Y., 1983.
14. Bassett, D.C.; Hodge, A.M., Polym. 1978, 19, 469.
15. Bassett, D.C.; Hodge, A.M.Proc.Roy.Soc.1978, A359, 121
16. Bassett, D.C.; Hodge, A.M.; Olley, R.H. Disc. Farad. Soc. 1978, 68, 218.
17. Bassett, D.C.; Hodge, A.M. Proc.Roy.Soc.1981, A377, 25.
18. Bassett, D.C.; Hodge, A.M.Proc.Roy.Soc.1981, A377, 39.
19. Bassett, D.C.; Hodge, A.M.Proc.Roy.Soc.1981, A377, 61.
20. Keller, A. Farad.Dis.Chem.Soc.1980, 68, 145.
21. Wunderlich, B. Macromolecular Physics, Vol.1, Academic Press, New York, 1973, 208,454.
22. Keller, A.Polymer, 1962, 3, 393.
23. Lindenmeyer, P.H. Science,1965, 147, 1256.
24. Hoffman, J.D. Soc.Plas.Eng., 1964, 4, 315.
25. Geil, P.H. J.Polym.Sci, 1960, 47, 65.
26. Ng, S.B.; Stelman, J.M.; Woodward, A.E. J.Macromol.Sci.Phys., 1973, B7, 533.
27. Blundell, D.J.; Keller, A.; O'Connor, T. J.Polym.Sci., 1967, A2, 5, 991.
28. Keller, A. Macromol.Chem. 1959, 34, 1.
29. Fischer, E.W.; G.Schmidth. Angew.Chem. 1962, 74, 551.
30. Flory, P.J. J.Amer.Chem.Soc., 1962, 84, 2857.
31. Williams, T.; Blundell, D.J.; Keller, A.; Ward, I.M. J.Polym.Sci. 1968, A2, 6, 1613.
32. Williams, T.; Keller, A.; Ward, I.M. J.Polym.Sci. 1968, A2, 6, 162.
33. Keller, A.; Martuscelli, E.; Priest, D.J.; Udagawa, Y. J.Polym.Sci., 1971, A2, 9, 1807.

34. Keller, A.; Udagawa, Y. J.Polym.Sci., 1971, A2, 9, 1793; A2, 9, 437.
35. Priest, D.J. J.Polym.Sci., 1971, A2, 9, 1777.
36. Patel, G.N.; Keller, A. J.Polym,Sci.:Polym,Phys. 1975, 13, 2259.
37. Bank, M.I.; Krim, S. J.Appl.Phys. 1968, 39, 4951.
38. Schonhorn, H.; Luongo, J.P. Macromol. 1969, 2, 366.
39. Koenig, J.L.; Hannon, M.J. J.Macromol.Sci.Phys., 19967, B1, 19.
40. Koenig, J.L.; Agboatwalla, M.G. J.Macromol.Sci.Phys. 1968, B2, 391.
41. Stellman, J.M.; Woodward, A.E. J.Polym.Sci., 1969, B7, 755.
42. Stellman, J.M.; Woodward, A.E. J.Polym.Sci., 1971, A2, 9, 59.
43. Hendrix, C.; Whiting, D.A.; Woodward, A.E. Macromol. 1971, 4, 57.
44. Tseng, S.; Herman, W.; Woodward, A.E.; Newman, B.A. Macromol., 1982, 15, 338.
45. Ergoz, E.; Mandelkern, L. J.Polym.Sci.Polym.Phys., 1972, 10, 631.
46.Keller, A.; Matreyek, W.; Winslow, F.H..J.Polym.Sci., 1962, 62, 291.
47.Harrison, I.R.; Baer, E. J.Polym.Sci.,1971, A2, 9, 1305
48.Equiluz, M.; Ishida, H.;Hiltner, A. J.Polym.Sci.Polym.Phys. 1979, 17, 893; 1980, 18, 2295.
49. Harrison, I.R.; Butler, J,S.;Runt, J.P. Org.Coat. Plas. Chem. Rep.,1981, 44, 176.
50. Bassett, D.C. Polymer, 1964, 5, 457.
51. Tsuboi, K.J. Macromol. Sci.Phys. 1968, B2, 603.
52. Harrison, I.R.; Baer, E. J.Coll. and Interfac.Sci. 1983, 31, 176.
53. Anandakumaran, K.; Herman, W.; Woodward, A.E. Macromol.,1983, 16, 563.
54. Schilling, F.C.; Bovey, F.A.; Anandakumaran, K.; Woodward, A.E. Macromol., 1985, 18, 2688.
55. Elkayam, A.; Xu, J.; Woodward, A.E.. Submitted for publication.
56. Taylor, M.; Woodward, A.E., Unpublished results. See Woodward, A.E., "Modification of Polymers", J.A. Moore and C.E.Carraher, Jr. Eds., Plenum, 1983.
57. Schilling, F.C.; Bovey, F.A.; Tseng, S.; Woodward, A.E. Macromol., 1983,16, 808.; Poly. Preprints, 1983, 24-1,235.
58. Tseng, S.; Woodward, A.E. Macromol. 1982, 15, 343.
59. Wichachewa, P.; Woodward, A.E. J.Polym.Sci. Polym.Phys. 1978, 16, 1849.

60. Marchetti, A.; Martuscelli, E. J.Polym.Sci.Polym.Phys. 1976, 14, 151.
61. Guzman, J.; Fatou, J.G.; Parena, J.M. Makromol.Chem. 1980, 181, 1051.
62. Drefahl, C.; Horhold, H.-H.; Hesse, E. J.Polym.Sci. 1967, C16, 965.
63. Schultz, W.J.; Etter, M.C.;Pocius, A.V.; Smith, S. Polym. Preprints, 1981, 22, 1.
64. Pinazzi, C.; Broose, J.C.; Pleurdeau, A.; Reyx, D. Appl. Polym. Symp. 1975, 26, 73.
65. Schilling, F.C.; Bovey, F.A.; Tonelli, A.E.; Tseng, S; Woodward, A.E. Macromol. 1984, 17, 728.
66. Tutorskii, I.A.; Sokolova, L.V.; Dogaddin, B.A. Vysokomol.Soyed. 1971, A13, 952.
67. Lotz, B.; Kovacs, A.J.; Bassett, G.A.; Keller, A. Kolloid Z.Z. Polymer 1966, 209, 115.
68. Kay, H.F.; Newman, B.A. J.Appl.Phys. 1967, 38, 4105; Acta Crys. 1968, B24, 615.
69. Miyagi, A.; Wunderlich, B. IUPAC Int. Symp. Macromol.Abst.Leiden 1970, 2, 765.
70. Wunderlich, B.; Kashdan, W.H. J.Polym. Sci. 1961, 50, 71.
71. Davis, G.T.; Eby, R.K.; Marlin, G.M. J.Appl.Phys. 1968, 39, 4973.
72. Kitamaru, R.; Mandelkern, L. J.Polym. Sci. 1970, A2, 8, 2079.
73. Fischer, E.W.; Goddar, H.; Schmidt, G.F. J.Polym.Sci. B. 1967, 5, 619.
74. Kuo, C.C.; Woodward A.E. Macromol.1984, 17 1034.
75. Hamada, F.; Wunderlich, B.; Sumida, T.; Hayashi, S.; Makajuma, A. J.Phys.Chem. 1968, 72, 178.
76. Banks, W.; Gordon, M.; Roe, R.J.; Sharples, A. Polym. 1963, 4, 61.
77. Maclaine, J.Q.G.; Booth, C. Polymer, 1975, 16, 680.
78. Se, K.; Adachi, K.; Kolaba, T. Polym.J. 1981, 13, 1009.
79.Marco, C.; Fatou, J.G.; Bello, A.; Blanco, A. Polymer, 1977, 18, 1100.
80.Marco, C.; Fatou, J.G.; Bello,A.; Blanco, A. Polymer, 1980, 20, 1250.
81. Peterlin, A.; Meinel,G. J.Polym.Sci.Part B., 1965, 3, 783.
82. Glenz, W.; Morsoff, N.; Peterlin, A. J.Polym.Sci. PartB., 1971, 9, 211.
83. Illers, K.H.; Haberhorn, H. Makkkromol.Chem. 1971, 142, 31. Ibid.1971, 146, 267.

84.Xu, J.; Woodward,A.E. Macromol. 1986, 190, 000.
85. Schilling, F.C.; Bovey, F.A.; Tonelli, A.E.; Xu, J.; Woodward, A.E., Unpublished results.
86. Anandakumaran, K. C.U.N.Y. Doctoral dissertation, 1984.
87. Anandakumaran, K.; Kuo, C.C.; Mukerji, S.; Woodward, A.E. J.Polym.Sci.Polym. Phys., 1982, 20, 1669.
88. Xu, J.; Woodward, A.E. , Unpublished results.
89. Ann Marrie; Maffroy-Biget. Bull.Soc.Chim., France, 1958, 458.
90. Meyerhoff, G. J.Polym.Sci. 1958, 29, 399.
91.Flory, P.J. Principles of Polymer Chemistry, Cornell Press, Ithaca, New York, 1953, p.563.
92. Fernandy-Berridi, M.J.; Ansarena, F.J.; Iruin, J.J.; Guzman, G.M. Macromol. 1980, 13, 190.
93. Salzberg, H.M.; Morrow, J.I.; Cohen, S.R.; Green, M.E. Physical Chemistry Laboratory, Principles and Experiments MacMillan, 1978, p.118.
94. Tutorskii, I.A.; Khodzhaeva, I.D.; Dogadkin, B.A. Pol.Sci: U.S.S.R., 1974, 16, 186.
95. Cooper, W.; Vanghan, G. Polym., 1963, 4, 329.
96. Takahashi, Y.; Sato, T.; Tadokora, H.; Tanaka, Y. J.Polym.Sci.Poly. Phys., 1973, 11, 233.
97.Blundell, D.J.; Keller, A.; Kovacs, A.J. J.Polym.Sci., 1966, B4, 481.
98. Keller, A.; Matruscelli, E. Macromol.Chem., 1972, 151, 189.
99. Lovering, E.G.; Wooden, D.C. J.Polym.Sci.A-2, 1971, 9, 175.
100. Kawai, T; Keller, A. J.Polym.Sci.1964, B3, 333.
101. Sadler, D.M. J.Polym.Sci.A-2, 1971, 9, 779.
102. Sanchez, I.C.; Dinancio, E.A. J.Res.Nat.Bur.Std.(U.S.), 1972, 76A, 213.
103. Mandelkern, L.; Price, J.M.; Gopalan, M.;Falou, J.G. J.Polym.Sci. A2, 1966, 4, 385.
104. Bunn, C.W. Proc.Phys.Soc.,London, 1942, A180, 40.
105. Fischer, D, Proc.Phys.Soc., London, 1953, 66, 7.
106. Tischler, F.; Woodward, A.E. Macromol., 1986, 19, 000.
107. Mandelkern, L.; Quinn, J.A.; Roberts, D.E. J.Amer. Chem.Soc.1., 1956, 78, 926.
108. Kawai, T.; Keller, A. Phil.Mag., 1973, 82.
109.Gemmer, R.V.; Golub, M.A. J.Polym.Sci.Polym.Chem., 1978, 16, 2985.
110. Hayashi, D.; Takahashi, T.; Kurihara, H.; Veno, H. Polym.J., 1981, 13-3, 215.
111. Cantow, M.J.R. Ed. Polymer Fractionation, Academic Press, N.Y., 1966

112. Chang, B.H.; Siegmann, A.; Hiltner, A. J.Polym.Sci.Polym.Phys., 1984, 22, 255.
113. Hoffman, J.D.; Davis, G.T.; Lauritzen, J.I. Treatise on Solid State Chemistry, Vol. 3, Plenum Press, N.Y. Ed. Hannay, N.B., 1976.
114. Fanconi, B.; Sarazin, D. Polym.Preprints, 1984, 25(2), 173.
115. Harrison, I.R.; Runt, J.J. Macromol.Sci.Phys., 1980, B17, 83.
116. Harrison, I.R.; Juska, T. J.Polym. Sci. Polym. Phys., 1980, 17, 491.
117. Kern, W. Macromol.Chem., 1961, 43, 106.
118. Arlie, J.P. Macromol.Chem., 1966, 99, 170; Macromol. Chem., 1967, 104, 212.
119. Finter, J.; Wengner, G. Macromol.Chem., 1981, 182, 1859.
120. Jones, D.H.; Latham, A.J.; Keller, A.; Girolamo, M. J.Polym. Sci.Polym.Phys., 1973, 11, 1759.
121. Geil, P.H. Introduction to Polymer Science and Technology, Ed. H.S.Kaufman and J.J. Falcella, Interscience, N.Y. 1978.
122. Davies, C.K.L.; Long, O.E. J.Mat.Sci., 1977, 12, 2165.
123. Mukerji, S., C.U.N.Y. Doctoral Dissertation, 1984.